Faculty of Biological and Veterinary Sciences, Department of Microbiology, Nicolaus Copernicus University in Torun

Soil Science, Faculty for Agriculture, Civil and Environmental Engineering, University of Rostock

Matteo Marangi

Doctoral Thesis in Biological sciences,

PhD Degree

Potential of *Salicornia europaea* in decreasing colonization of plants by Human Pathogenic Microorganisms

Supervisors

Prof. dr hab. Katarzyna Hrynkiewicz, Nicolaus Copernicus University, Torun, Poland

Prof. Dr. hab. Christel Baum, University of Rostock, Rostock, Germany

Toruń, 2025

Oubaitori (n.): *the idea that people, like flowers, bloom in their own time and take their own individual journeys; the acceptance of not comparing oneself to others and focusing on one's own uniqueness*

Statements by the author of the dissertation

The dissertation is self-created, does not contain content obtained in a non-compliant manner, the dissertation has not previously been the subject of procedures in another unit, the version of the dissertation is identical to the attached electronic version**.**

Table of contents

Acknowledgments

To be international is to inhabit multiple cultural frameworks simultaneously, negotiating identity across shifting contexts of language, place, and belonging.

This PhD was far from a solo endeavour—it was a marathon built on collaboration between scientists, Co-Authors, and others at Nicolaus Copernicus University in Toruń and the University of Rostock, all working toward a shared goal.

Life, and particularly the pursuit of a PhD, is fundamentally a shared endeavour, where individuals engage with one another to find mutual understanding. The ability to reach agreement across different perspectives is not only a mark of true education but also one of the highest expressions of what it means to be human. Undertaking this PhD has been a truly transformative journey—intellectually, emotionally, and personally. It would not have been possible without the support, guidance, and encouragement of many individuals, to whom I owe my deepest gratitude.

First and foremost, I would like to express my sincere appreciation to my supervisors, Prof. Katarzyna Hrynkiewicz and Prof. Christel Baum, for their unwavering guidance, thoughtful criticism, and patient mentorship. Your insights have shaped my thinking and your encouragement has helped me persevere through the most challenging moments of this research. I also deeply appreciate Prof. Peter Leinweber and his colleagues, who taught me extensively about the scientific world and guided me through the process of submitting and publishing my first paper.

I am sincerely grateful to Dr. Sonia Szymańska for her continuous availability and insightful discussions that helped me navigate all the technical and scientific aspects of my experiments.

To the administrative and technical staff, especially Ms. Justyna Trawicka, thank you for ensuring that everything ran smoothly and for always being ready to help, since the first day of this journey.

To my parents, sisters and my cousin Michele, who have always stood by me and instilled in me a love for learning while reaching resilience. Your sacrifices have not gone unnoticed.

Finally, I want to sincerely thank my friends, Dr. Grande and Dr. Rajabi Dehnavi, for the unforgettable time we have spent together and for their constant support through all my ups and downs.

Abbreviations

µL – microliter

16S – bacterial 16S ribosomal RNA

ANOVA – analysis of variance

AT – annealing temperature

atm – atmosphere

B&W – Binding and Washing Buffer

bp – base pairs

Br^- – Bromide ion

Ca – Calcium

CAS – Chemical Abstracts Service

CFU – colony forming units

Cl^- – Chloride ion

cm – centimetre

cpm – counts per minute

Ct – Control

ddH_20 – double distilled water

DMDS – dimethyl disulfide

DNA – deoxyribonucleic acid

dsDNA – double stranded deoxyribonucleic acid

***E. coli* (Ec)** – *Escherichia coli*

EC – electrical conductivity

EDTA – ethylenediaminetetraacetic acid

F1 – old sandy marsh at site 1 in France

F2 – young muddy marsh at site 2 in France

GC-MS – Gas Chromatography – Mass Spectrometry

H_2O_2 – hydrogen peroxide

HCl – hydrochloric acid

HCO_3^- – Bicarbonate ion

HPMOs – Human Pathogenic Microorganisms

HS-SPME-GC-MS – Head Space – Solid Phase Microextraction – Gas Chromatography – Mass Spectrometry

K – Potassium

***L. monocytogenes* (Lm)** – *Listeria monocytogenes*

M – molar

m/z – ion mass to charge ratio (mass spectrometry)

meq/L – milliequivalents per Liter

Mg – Magnesium

MIC – minimum inhibitory concentrations

mL – millilitre

mm – millimetre

mM – millimolar

mS – milli siemens

mVOCs – microbial Volatile Organic Compounds

Na – Sodium

NaCl – Sodium Chloride

PCM – Polish Collection of Microorganisms

PCR – Polymerase Chain Reaction

PGPB – Plant Growth-Promoting Bacteria

pH – potential of Hydrogen

PRRs – pattern recognition receptors

PTI – pattern-triggered immunity

qPCR – quantitative Polymerase Chain Reaction

RNA – ribonucleic acid

ROS – reactive oxygen species

rRNA – ribosomal ribonucleic acid

RT – room temperature

***S. enterica* (Se)** – *Salmonella enterica*

S. europaea – *Salicornia europaea*

SO_4^{2-} – Sulphate ion

STEC – Shiga toxin-producing *Escherichia coli*

TC – total carbon

TMAH – Tetramethylammonium hydroxide

TN – total nitrogen

Tris – Tris(hydroxymethyl)aminomethane

TSA – Tryptic Soy Agar

TSB – Tryptic Soy Broth

VOCs – Volatile Organic Compounds

XEH – xyloglucan endohydrolysis

XET – xyloglucan endotransglycosylation

Abstract

This PhD thesis investigates the complex interactions between the halophyte *Salicornia europaea* L. and three major human pathogenic microorganisms (HPMOs): *Escherichia coli*, *Salmonella enterica*, and *Listeria monocytogenes* in field and *in vitro* experiments. *S. europaea* was used as model crop based on its nutritional and antimicrobial qualities as a sustainable crop for saline agriculture with possible raw consumption. Given the rising incidence of foodborne illnesses linked to raw vegetables contaminated with HPMOs, there is a critical need for innovative and sustainable antimicrobial strategies in agriculture and food safety. Therefore, the links between the chemical composition of plant shoots (e.g., lignin and lipid content) and soil properties (e.g., salinity and pH) with the colonization of HPMOs were analysed. The persistence of HPMOs in *S. europaea* was investigated using plant transcriptomics. Additionally, plant endophytic and rhizosphere bacteria were investigated on their production of volatile organic compounds (mVOCs) with potential to inhibit the HPMOs.

It was hypothesized that: (i) chemical traits of plants and soils control HPMOs' abundance and can therefore serve as indicators of food safety risk; (ii) the persistence of HPMOs in *S. europaea* can be limited by the plant's native microbiome and internal salinity; (iii) inhibition of HPMOs can be based on mVOCs production of endophytic and rhizosphere bacteria.

To address these hypotheses, three different experimental approaches were employed:

1. field experiment: the chemical composition of *S. europaea* shoots and soils from two French field sites was analysed using GC-MS jointly with the abundance of HPMOs on them to identify potential biomarkers of the HPMOs' contamination;
2. *in vitro* experiment: interactions between *S. europaea* and HPMOs were assessed at varying salinity levels (0, 50, 100 and 200 mM NaCl), focusing on plant growth, HPMOs' abundance using selective media and qPCR of shoot and root samples, and plant transcriptomics of plant samples in responses to HPMOs colonization;
3. functional assay to identify antagonists: endophytic and rhizosphere bacteria isolated from *S. europaea* were tested for their inhibitory effects on HPMOs using mVOC-mediated interactions and identification of volatiles using a bipartite *in vitro* assay

coupled with head space - solid phase microextraction - gas chromatography - mass spectrometry (HS-SPME-GC-MS).

Negative correlations were found between the lignin content in shoots and the abundance of *S. enterica*, as well as between the lignin content in bulk soil organic matter and the abundance of *E. coli*, suggesting a potential protective role of lignin. Conversely, shoot lipid content was positively correlated with the abundance of *E. coli*. The soil pH and the soil salinity were negatively correlated with the abundance of HPMOs levels in bulk soil. This indicates the advantage of growth of *S. europaea* on saline soils for food safety. In the *in vitro* experiment a marked decline in the abundance of HPMOs in plant tissues was revealed, despite an initially high bacterial abundance in sterile sand, suggesting a natural reduction from soil to plant. *E. coli* was not found in plant tissues, whereas *S. enterica* and *L. monocytogenes* persisted and induced significant transcriptional changes, notably under specific salinity (0 and 100 mM NaCl). Transcriptomic analysis revealed no substantial changes in the gene expression in response to application of *E. coli*, but notable shifts in response to the other HPMOs (*S. enterica* and *L. monocytogenes*), involving genes linked to stress responses, biosynthesis of secondary metabolite and cellular responses to extracellular stimuli, e.g., biosynthesis of phosphoethanolamine N-methyltransferase and pentacyclic triterpenoid. Distinct inhibition patterns emerged among bacterial taxa. Bacilli, Actinomycetes, and Gammaproteobacteria predominantly suppressed the growth of *L. monocytogenes* and *E. coli*. Key strains identified for mVOC profiling included *Bacillus pumilus* CSR28, *Xanthomonadales* sp. CSE34, *Streptomyces champavatii* CSR4, and *Bacillus pseudomycoides* CSE4, with dimethyl disulfide (DMDS) highlighted as a principal and potential antimicrobial mVOC. Other detected mVOCs, such as cyclohexane and methylcyclopentane, varied across bacterial and pathogen co-cultures, including in the HPMOs' monocultures.

Concluding, this PhD thesis highlights high diversity of interactions between *S. europaea*-and HPMOs, revealing that only some of these microorganisms are capable of persisting within the plant tissues. Soil pH and salinity emerge as a key controls and indicator of the risk of HPMOs' contamination in *S. europaea*, and can be used to enhance the safety for human consumption. Moreover, HPMOs trigger notable changes in the plant's gene expression, suggesting that the plant actively responds to certain HPMOs. Furthermore, it demonstrates that specific endophytic and rhizosphere bacteria associated with *S. europaea* generate mVOCs which are capable to suppress major foodborne pathogens, positioning these bacteria as viable candidates for the biocontrol of HPMOs for an increased food safety in agriculture.

Abstrakt (PL)

Niniejsza rozprawa doktorska bada złożone interakcje pomiędzy halofitem *Salicornia europaea* L. a trzema głównymi ludzkimi drobnoustrojami chorobotwórczymi (HPMOs, ang. Human Pathogenic Microorganisms): *Escherichia coli*, *Salmonella enterica* i *Listeria monocytogenes* w doświadczeniach polowych i *in vitro*. *S. europaea* została wykorzystana jako roślina modelowa ze względu na swoje wartości odżywcze i właściwości przeciwdrobnoustrojowe, jako zrównoważona uprawa do rolnictwa na glebach zasolonych z możliwością spożycia na surowo. W związku ze wzrastającą liczbą chorób przenoszonych przez żywność, związanych z warzywami spożywanymi na surowo i skażonymi HPMOs, istnieje pilna potrzeba innowacyjnych i zrównoważonych strategii przeciwdrobnoustrojowych w rolnictwie i bezpieczeństwie żywności. Dlatego przeanalizowano związki pomiędzy składem chemicznym pędów roślin (np. zawartością ligniny i lipidów) oraz właściwościami gleby (np. zasoleniem i pH) a kolonizacją przez HPMOs. Trwałość HPMOs w *S. europaea* badano za pomocą transkryptomiki roślin. Ponadto analizowano bakterie endofityczne i ryzosferowe pod kątem ich zdolności do syntezy lotnych związków organicznych (mVOC) o potencjale hamującym HPMOs.

Postawiono następujące hipotezy: (i) parametry chemiczne roślin i gleb kontrolują liczebność HPMOs i mogą służyć jako wskaźniki ryzyka dla bezpieczeństwa żywności; (ii) trwałość HPMOs w *S. europaea* może być ograniczana przez natywny mikrobiom rośliny i jej wewnętrzne zasolenie; (iii) hamowanie HPMOs może wynikać z produkcji mVOC przez bakterie endofityczne i ryzosferowe.

Aby zweryfikować te hipotezy, zastosowano trzy różne podejścia eksperymentalne:

1. doświadczenie polowe: skład chemiczny pędów *S. europaea* oraz gleb z dwóch lokalizacji we Francji analizowano za pomocą GC-MS wraz z liczebnością HPMOs w celu identyfikacji potencjalnych biomarkerów skażenia HPMOs;

2. doświadczenie *in vitro*: oceniano interakcje między *S. europaea* a HPMOs przy różnych poziomach zasolenia (0, 50, 100 i 200 mM NaCl), koncentrując się na wzroście roślin, liczebności HPMOs przy użyciu podłoży selektywnych i qPCR próbek pędów i korzeni oraz transkryptomice roślin w odpowiedzi na kolonizację przez HPMOs;

3. test funkcjonalny w celu identyfikacji antagonistów: bakterie endofityczne i ryzosferowe izolowane z *S. europaea* testowano pod kątem ich właściwości hamujących wobec HPMOs z wykorzystaniem interakcji wywołanych przez mVOC oraz identyfikacji lotnych związków przy wykorzystaniu dwuetapowego testu *in vitro* połączonego z techniką HS-SPME-GC-MS.

Stwierdzono ujemne korelacje pomiędzy zawartością ligniny w pędach a liczebnością *S. enterica*, jak również pomiędzy zawartością ligniny w glebowej materii organicznej a liczebnością *E. coli*, co sugeruje potencjalną ochronną rolę ligniny. Natomiast zawartość lipidów w pędach była dodatnio skorelowana z liczebnością *E. coli*. Odczyn pH gleby i jej zasolenie były ujemnie skorelowane z liczebnością HPMOs w glebie. Wskazuje to na przewagę *S. europaea* rosnącej na glebach zasolonych z punktu widzenia bezpieczeństwa żywności. W doświadczeniu *in vitro* wykazano wyraźny spadek liczebności HPMOs w tkankach roślin, pomimo początkowo wysokiej liczebności bakterii w jałowym piasku, co sugeruje naturalne ograniczenie od gleby do rośliny. *E. coli* nie wykryto w tkankach roślin, natomiast *S. enterica* i *L. monocytogenes* przetrwały i wywoływały istotne zmiany w analizach transkryptomicznych, szczególnie przy określonym zasoleniu (0 i 100 mM NaCl). Analiza transkryptomiczna wykazała brak istotnych zmian w ekspresji genów w odpowiedzi na obecność *E. coli*, ale zauważalne zmiany w odpowiedzi na pozostałe HPMOs (*S. enterica* i *L. monocytogenes*), obejmujące geny związane z reakcjami stresowymi, biosyntezą wtórnych metabolitów oraz odpowiedziami komórkowymi na bodźce zewnętrzne, np. biosyntezą fosfoetanoloaminy N-metylotransferazy i pentacyklicznych triterpenoidów. Zaobserwowano różne wzorce hamowania wśród taksonów bakteryjnych. Bacilli, Actinomycetes i Gammaproteobacteria głównie hamowały wzrost *L. monocytogenes* i *E. coli*. Kluczowe szczepy zidentyfikowane do profilowania mVOC obejmowały *Bacillus pumilus* CSR28, *Xanthomonadales* sp. CSE34, *Streptomyces champavatii* CSR4 oraz *Bacillus pseudomycoides* CSE4, przy czym dimetylodisulfid (DMDS) został wyróżniony jako główny i potencjalny przeciwdrobnoustrojowy mVOC. Inne wykryte mVOC, takie jak cykloheksan i metylocyklopentan, różniły się w zależności od współkultur bakterii i patogenów, w tym także w monokulturach HPMOs.

Podsumowując, niniejsza rozprawa doktorska podkreśla dużą różnorodność interakcji pomiędzy *S. europaea* a HPMOs, ujawniając, że tylko niektóre z tych mikroorganizmów są zdolne do przetrwania w tkankach roślin. Odczyn pH gleby i zasolenie wyłaniają się jako kluczowe czynniki kontrolne i wskaźniki ryzyka skażenia *S. europaea* przez HPMOs i mogą

być wykorzystane w celu zwiększenia bezpieczeństwa konsumpcji. Ponadto HPMOs wywołują istotne zmiany w ekspresji genów rośliny, co sugeruje, że roślina aktywnie reaguje na niektóre z tych drobnoustrojów. Co więcej, wykazano, że określone bakterie endofityczne i ryzosferowe związane z *S. europaea* wytwarzają mVOC zdolne do hamowania głównych patogenów przenoszonych przez żywność, co czyni je potencjalnymi kandydatami do biokontroli HPMOs w celu zwiększenia bezpieczeństwa żywności w rolnictwie.

1. Introduction

1.1. **Soil salinization: a pressing contemporary issue**

Salinization is connected to low rainfall and global issues like population growth and climate change (Vengosh, 2014). Fluctuating water levels and the mixing of seawater with groundwater can significantly impact soils, causing rapid salinization of agricultural lands and groundwater (Vengosh, 2014). This rise in salinity will disrupt agricultural production systems, alter natural vegetation, and change land-use patterns (Vengosh, 2014). The vulnerability is heightened because approximately 70% of the world's population resides on coastal flatlands, making these areas more susceptible to these changes and intensifying issues like desertification and salinization in arid and semiarid regions (Okur and Örçen, 2020). Drylands in South America, southern Australia, Mexico, the southwestern United States, and South Africa are predicted to be at the highest risk for increased soil salinity based on long-term models, while at European scale the Mediterranean coastline stands out (Daliakopoulos et al., 2016; Hassani et al., 2021). Climate change is expected to increase soil salinity in dryland areas of Spain, Morocco, and northern Algeria (Hassani et al., 2021). By 2100, the western and southern Sahara, central Indian drylands, desert soils in southeastern Mongolia, and northern China are also projected to become more saline due to climate change (Hassani et al., 2021). Using treated wastewater or brackish water, which contains high levels of chloride, sodium, and boron, is best for crops that can tolerate salt (Vengosh, 2014). This type of water requires special soil treatment (Vengosh, 2014). Crop production losses due to salinization in arid and semiarid regions worldwide vary from 18% to 43% (Singh, 2021). In areas with high salt levels, planting crops that are highly tolerant of salt, e.g., spinach, barley, date palm, sugar beet and asparagus, is often recommended (Singh, 2021). This rising global salinization trend underscores the urgent need for crops capable of thriving in high-salinity environments. Within this context, halophytes, specifically *Salicornia europaea* L. emerges as a viable solution not only for sustainable saline agriculture but also for food safety applications, as explored in this dissertation.

Halophytes, comprising less than 2% of terrestrial plant life, have evolved unique strategies to thrive in salty environments. Notably, they can store salts within cell vacuoles and expel them through specialized leaf glands. These salt-tolerant plants hold potential for long-term restoration of areas affected by salinity (Litalien and Zeeb, 2019).

1.2. **Revealing the agronomic potential of *Salicornia europaea* as a valuable halophyte**

This background section provides essential ecological and agronomic context for understanding the growth conditions and environmental adaptability of *S. europaea*, which are critical to the experimental design and interpretation of this thesis—particularly in relation to salinity and pH as key factors influencing food safety risks associated with human pathogenic microorganisms (HPMOs). *Salicornia*, a prominent genus of halophytes, plays a crucial ecological and economic role worldwide. This plant thrives in saline coastal regions and inland salt marshes due to its remarkable ability to withstand high salt concentrations, up to 1 M NaCl with optimum salinity for biomass production in the range between 200 and 400 mM NaCl under laboratory conditions (Cárdenas-Pérez et al., 2021; Cárdenas-Pérez et al., 2022; Orzoł et al., 2025). Environmental studies have shown that *Salicornia* thrives in soils with a pH of 7–8, reflecting its adaptation to neutral to slightly alkaline saline habitats (Hrynkiewicz et al., 2019; Marangi et al., 2024). Despite its salt tolerance, high salinity levels can inhibit its germination. Consequently, many coastal halophytes, including *Salicornia*, tend to germinate during spring when soil salinity decreases due to increased freshwater availability and favourable temperatures (Singh et al., 2014). An EU-supported initiative in Portimão, southern Portugal, aimed to regenerate land previously abandoned due to excessive soil salinity. The initiative focused on establishing a 4,600 m^2 intensive production unit of greenhouses for the cultivation of certified organic *S. europaea* (https://eu-cap-network.ec.europa.eu/sites/default/files/2024-07/eu-cap-network-good-practice-report-salivitae.pdf). In Europe, the protection of salt marshes gained special significance with the adoption of Council Directive 92/43/EEC in 1992. Notably, Baltic coastal meadows and temperate inland salt marshes were classified as endangered and included in the Red List of European habitats (Janssen et al., 2016).

S. europaea L., a notable species within the genus, belongs to the Amaranthaceae family under the subfamily Salicornioideae. It is commonly known as glasswort, sea beans, sea asparagus, or samphire (Kim et al., 2021; Cárdenas-Pérez et al., 2022). The species has garnered attention for its numerous health benefits, prompting researchers to explore its potential as both a functional food and a medicinal plant. Crude extracts of *S. europaea* have demonstrated various therapeutic properties (Kim et al., 2021). *S. europaea* is highly versatile in its uses. It can be consumed raw, cooked, or marinated and serves as livestock feed. Additionally, it holds potential for biofuel production and has promising applications in the pharmaceutical and cosmetic industries (Fussy and Papenbrock, 2024).

Studies have shown that *S. europaea* exhibits reduced growth under extreme salinity conditions (e.g., 1000 mM NaCl) compared to lower salt concentrations (Cárdenas-Pérez et al., 2022). High salinity leads to a decline in photosynthetic pigment content; however, the plant demonstrates a high tolerance to salinity by mitigating excessive H_2O_2 production (Cárdenas-Pérez et al., 2022). Optimal growth has been observed at moderate salt concentrations of 15 g/L NaCl, with fresh mass declining at higher levels. Interestingly, plants grown without added salt (0 g/L NaCl) exhibited higher total phenolic compound contents across various harvests (Fussy and Papenbrock, 2024). Laboratory studies revealed that nutrient solutions with NaCl concentrations of 170 milliequivalents per Liter (meq/L) and 340 meq/L supported optimal growth for *S. europaea*, while seed germination occurred from February to June under lowest soil salinity and was highest in distilled water controls rather than saline treatments (Ungar et al., 1979). The plant's salt tolerance is attributed to its ability to accumulate and compartmentalize Na^+ and Cl^- ions in vacuoles since it lacks salt glands or bladders (Calone et al., 2022). Irrigation practices also significantly influence *S. europaea*'s total lipid content: lipid levels increased with the transition from fresh to brackish water but declined when irrigated with seawater (Araus et al., 2021). Salinity poses challenges for germination. A significant decline in germination indices was observed as NaCl concentrations increased; the most pronounced reductions occurred between 400 and 600 mM NaCl (Calone et al., 2020). This observation aligns with our findings, although we did not assess germination percentage, as the plants were collected at the seedling stage (8 weeks old). Despite this limitation, *S. europaea* demonstrates resilience under moderate saline conditions. However, the effects of salinity on *S. europaea*'s growth remain ambiguous; greenhouse experiments involving salinities ranging from 0 to 1000 mM NaCl yielded conflicting results regarding whether the plant grows better in saline or non-saline conditions (Puccinelli et al., 2024).

S. europaea contains a diverse array of metabolites, including oleanane triterpenoid saponins, caffeoylquinic acid derivatives, flavonoids, chromones, sterols, lignans, and aliphatic compounds (Kim et al., 2021). However, caution is advised when comparing yield data since high yields are often derived from dried plant material extractions (Kim et al., 2021). Plants grown with standard nutrient solutions exhibited higher concentrations of ascorbate compounds (ascorbate and dehydroascorbate), total chlorophylls, carotenoids, phenols, and flavonoids compared to those irrigated with wastewater (Puccinelli et al., 2024). This diverse metabolite profile of *S. europaea*, particularly its phenolic and

triterpenoid compounds, may partially explain the observed plant transcriptomic responses to HPMOs reported in this thesis. The transcriptome of *S. europaea* has been primarily studied under varying salinity conditions, revealing a wide array of genes involved in ion homeostasis and osmotic regulation, including cation transporters and enzymes associated with the synthesis of low-molecular-weight osmolytes (Ma et al., 2013; Furtado et al., 2019). These publications strengthen the biological foundation for why *S. europaea*'s endogenous metabolites, and their modulation under saline conditions, can influence HPMOs' colonization, plant defence transcriptomes, and metabolite-based food safety indicators.

1.3. **Human pathogen contamination in crops**

Plants constitute over 80% of human diets and are the primary nutritional source for livestock (FAO, 2020; Rizzo et al., 2021). Despite increased efforts to improve hygiene, outbreaks related to microbial contamination of lightly processed foods, like produce, continue to occur worldwide (Dandie et al., 2019). The origins of these outbreaks have been attributed to multiple contamination routes, including pre-harvest elements such as soil, seeds, irrigation water, and animal excrement, as well as post-harvest procedures like storage, handling, and packaging (Miceli and Settanni, 2019). While microbial research has traditionally cantered on the soil and rhizosphere, emerging evidence highlights the importance of seed-associated and epiphytic microorganisms in influencing plant health and performance (Truyens et al., 2015; Nelson, 2018; Bintarti et al., 2022; Zeng et al., 2023; Romão et al., 2025). Unlike root and soil microbes, seed microbiota is capable of vertical transmission, enabling the inheritance of both beneficial and pathogenic microorganisms from one generation to the next (Rodríguez et al., 2018; Khan et al., 2025; Romão et al., 2025). A range of microbiological agents that are mainly originate from the soil, including bacteria, parasites, viruses, fungi, and mycotoxins, can trigger incidents of foodborne illness (De Corato, 2020; Paseka et al., 2020; Steffan et al., 2020; Samaddar et al., 2021; Glaize et al., 2021; Gareth et al., 2024). Crops grown in soil contaminated with human pathogens are at greater risk of becoming contaminated themselves. In the United States, produce-based foods accounted for the majority (51%) of outbreak-associated diseases during a ten-year study (Painter et al., 2013). This percentage was higher than that associated with other food categories, such as meat, fish, and dairy (Painter et al., 2013). Consuming tainted products

can lead to both chronic and acute health consequences, potentially resulting in mortality (Sarma et al., 2017). Foodborne illnesses pose a substantial global health burden, with reports indicating that they affect 600 million people annually (Foodborne Disease Burden Epidemiology Reference Group, 2015). The accelerated production of vegetables to meet growing demand has increased the potential for contamination by pathogenic microbes, raising concerns about consumer safety (Balali et al., 2020). Arguably, soil harbours some of the most diverse biological communities on Earth (Nielsen et al., 2015). The physical characteristics of soil are also crucial in regulating the establishment and survival of pathogens. Soil texture as the proportion of sand, silt, and clay influences the persistence of various pathogens in soils. For example, a fine-textured clayey soil may favour pathogen survival (Obayomi et al., 2019). When irrigating food crops, particularly lightly processed items like lettuce, spinach, parsley, and other leafy greens, there is significant concern regarding opportunistic and human pathogens (Dandie et al., 2019). Indeed, many opportunistic human pathogens colonizing fresh produce exhibit an endophytic existence. They use vegetables as an alternative host for environmental survival and as a vehicle to colonize human and animal hosts after consumption (Mendes et al., 2013). An interesting case is *Bacillus cereus*, which is both a leading cause of toxin-induced foodborne illnesses and, intriguingly, one of the most notable bacteria with plant-stimulating properties (Jovanovic et al., 2021; Kulkova et al., 2023). Although the use of sewage sludge as fertilizer can foster sustainable agriculture and nutrient recycling, it also introduces potential risks related to increased chemical and microbiological hazards (Goberna et al., 2018). For these reasons its use is regulated, partly forbidden. Irrigation practices and distribution networks must be maintained to the highest standards possible to ensure that the potential for contamination is minimized (Dandie et al., 2019; Balali et al., 2020).

1.4. **Plant–HPMOs interaction and foodborne illness outbreaks**

Over the past ten years, the majority of foodborne illness outbreaks related to fresh produce have been associated with *Salmonella* spp., pathogenic *Escherichia coli*, and *Listeria monocytogenes* (Gareth et al., 2024). Although fruits and vegetables are frequently implicated in foodborne illness outbreaks, the levels of certain human pathogenic microorganisms (HPMOs) (*E. coli*, *S. enterica* and *L. monocytogenes*) found on these crops are typically low. This low prevalence can make it challenging to effectively control

contamination (De Oliveira Elias et al., 2019). Pathogens have the ability to colonize and penetrate the aerial parts of plants, including through stomata, scar tissue, and wounds (Işık et al., 2020).

The surface of plants poses several challenges for the colonization of human pathogens. Physical barriers, such as tough cell walls and waxy cuticles, act as the initial line of defence against these invaders (George and Brandl, 2021). Additionally, bacteria must be resilient enough to withstand dry environments and harmful ultraviolet radiation (George and Brandl, 2021). Seasonal changes and extreme weather conditions can also affect surface characteristics, either facilitating or hindering the ability of human pathogens to invade plant tissues (George and Brandl, 2021). Once pathogens establish themselves, they must compete for nutrients and contend with inhibitory substances like reactive oxygen species (ROS) (George and Brandl, 2021). Moreover, the native microbiome of the phyllosphere can further impede the colonization of foreign cells through competition or by producing antimicrobial compounds (George and Brandl, 2021). In summary, while several steps involved in the colonization of plants by enteric pathogens have been identified, information regarding the mechanisms activated during this process remains limited. What is certain is that the nonspecific adhesion of bacterial cells to plant surfaces is followed by their irreversible attachment, followed by active production of exopolysaccharides, multiplication, colonization of the plant surface, and persistence (Kyere et al., 2019; Truong et al., 2021). Plants initiate their primary immune defence—known as pattern-triggered immunity (PTI)—by detecting conserved molecular signatures from microbes or pathogens, such as bacterial flagellin, via transmembrane pattern recognition receptors (PRRs) (Bigeard et al., 2015). Nonetheless, pathogens may evade this defence by releasing virulence effectors that either inhibit PTI signalling or avoid recognition by PRRs (Guo et al., 2009). Although this rationale has traditionally been applied to the interactions between plants and phytopathogens, the possibility of a comparable mechanism occurring in HPMO–plant interactions should not be dismissed. Although human pathogens cannot directly enter root cells, earlier studies indicate that enteric pathogens may colonize the interior of roots passively, often through wounds caused by transplantation or at the sites where lateral roots emerge (Zheng et al., 2013). It has been proposed that vegetable seeds may become contaminated with soil-borne bacterial pathogens either directly through contact with pathogen cells or indirectly via soil particles carrying the pathogens (Agarwal and Sinclair, 1997). It is worth noting that, although HPMOs differ from plant pathogens in

their interactions with host plants, both early studies and findings from the present thesis suggest that HPMOs' inoculation may elicit similar transcriptomic changes in plants (Jacob et al., 2021). Indeed, lettuce and *Arabidopsis* plants inoculated with HPMOs exhibited alterations in their transcriptomic profiles, particularly in the phenylpropanoid biosynthetic process and the ethylene-activated signalling pathway—both of which involve transcripts associated with plant immune defence, similar to those observed in this thesis (Jacob et al., 2021).

HPMOs have been reported worldwide as causing diseases in humans. Approximately 265,000 infections caused by Shiga toxin-producing *E. coli* (STEC) occurs each year in the United States, with symptoms ranging from mild diarrhea to severe conditions such as ischemic colitis and hemolytic uremic syndrome. In some cases, these infections can be fatal (Scallan et al., 2011; Tack et al., 2021). Healthy ruminant animals, such as cattle and goats, often carry STEC in their intestinal tracts. Transmission to humans can occur through various routes, including consumption of contaminated food or water, contact with infected animals or their surroundings, or direct person-to-person spread (Griffin and Tauxe, 1991; Tack et al., 2021). Between 2010 and 2017, it was reported that 71% of the STEC outbreaks, which affected thousands of individuals, were caused by the O157 strain. This strain, the most commonly identified *E. coli* in the U.S., is responsible for severe cases of STEC infections. Notably, *E. coli* O157:H7 is also a primary pathogen behind foodborne illness outbreaks in Canada (Coulombe et al., 2020; Tack et al., 2021). In 2020, seven out of the ten multistate foodborne illness outbreaks in the USA were linked to produce (Centers for Disease Control and Prevention, 2021). *Salmonella* from contaminated seeds has the potential to survive for extended periods in both lettuce and hydroponic farming environments, presenting significant risks of cross-contamination (Li et al., 2022). However, a study found that planting tomatoes with *Salmonella*-contaminated seeds or using contaminated irrigation water did not lead to the presence of the pathogen on the stems, leaves, or fruit (Miles et al., 2009). Many studies performed under laboratory conditions confirmed that *L. monocytogenes* can colonize and persist on plants. Indeed, inoculation of this pathogen at the surface of roots or leaves resulted in population increase and colonization of parsley, lettuce, corn salad, spinach, mustard spinach, cultivated rocket, wild rocket, carrot, radish and many other plants (Truong et al., 2021). The rise of antibiotic-resistant pathogens has sparked greater interest in the effectiveness of plant extracts as antimicrobials. Many plant extracts have been shown to effectively combat enteric

pathogens (Friedman, 2015). Applying bioactive plant compounds to fruit and vegetables, either directly on the plant tissue or through the wash water, has been shown to reduce contamination on post-harvest produce with varying levels of effectiveness (George and Brandl, 2021).

1.5. The potential role of endophytic and rhizosphere bacteria in HPMOs' suppression: mVOCs

Both plants and microorganisms release volatile organic compounds (VOCs) that enable communication within and across species. Microbial VOCs (mVOCs) provide significant advantages to plants, especially in agriculture, by suppressing plant pathogen growth, activating plant defence mechanisms, and promoting plant growth and development (Poveda, 2021). However, the full ecological roles of microbial volatiles remain unclear, and more research is required in this area (Poveda, 2021). Furthermore, only a limited number of studies have investigated the effects of mVOCs on the suppression of HPMOs. The majority of the existing research on mVOCs focuses on their action against plant pathogens. It is essential to recognize that some mVOCs produced by specific bacteria may exhibit similar effects on HPMOs as those observed with plant pathogens. The profiles of mVOCs are assessed using gas chromatography-mass spectrometry (GC-MS), a method that allows for effective separation, identification, and quantification of components within complex mixtures (Veselova et al., 2019). mVOCs typically possess low boiling points and small molecular sizes, averaging around 300 Da (Veselova et al., 2019). These compounds are mainly byproducts of primary and secondary metabolism, often formed by the oxidation of glucose and other intermediates (Schmidt et al., 2015). mVOCs have the capacity to influence the metabolome, genome, and proteome, making them promising biostimulants and bioprotectants, even under open-field conditions (Chung et al., 2016). mVOCs are small molecules that belong to various chemical families, including alkenes, alcohols, ketones, organic acids, terpenes, benzenoids, and pyrazines. Notably, the composition of volatilomes is species-specific and can change depending on the microorganisms' growth conditions (Almeida et al., 2023). As previously mentioned, some endophytic and rhizosphere bacteria, along with their associated mVOCs, which have demonstrated antibacterial and antifungal activity, may also possess anti-HPMOs activity. Indeed, three rhizobacterial isolates, such as *Bacillus amyloliquefaciens* and *Bacillus thuringiensis*, were shown to inhibit the growth

of two HPMOs (*Bacillus cereus* and *Enterococcus faecalis*) (Ajilogba and Babalola, 2019). These rhizobacteria produced several compounds, including dimethylfuvene, formic acid 2-methylpropyl ester, tridecane, acetic acid butyl ester, paraldehyde, s-(+)-1,2 propanediol, tropone, phthalan, and p-xylene (Ajilogba and Babalola, 2019). Several endophytic strains from *Origanum vulgare* ssp. displayed bactericidal and/or bacteriostatic properties against most strains of the *Burkholderia cepacia* complex (Polito et al., 2022). These endophytes also synthesized mVOCs with well-established antimicrobial effects, including dimethyl disulfide, dimethyl trisulfide, and monoterpenes (Polito et al., 2022). mVOCs offer significant potential for addressing infectious diseases and antibiotic resistance, paving the way for a new generation of antimicrobial agents that could treat previously hard-to-manage infections (Ueda and Beppu, 2017; Yu et al., 2022; Koilybayeva et al., 2023). Moreover, sulphur-containing compounds, such as dimethyl disulfide (DMDS) and dimethyl trisulfide (DMTS), are recognized for their strong inhibitory effects against a broad range of phytopathogens (Weisskopf et al., 2021). These sulphides are commonly produced by soil-associated bacteria including *Bacillus*, *Pseudomonas*, and *Serratia*, and are thought to disrupt microbial cell membranes or induce oxidative stress (Kai et al., 2009). Other important classes of antimicrobial mVOCs include alkanes, which can interfere with membrane stability, and alcohols, which inhibit microbial growth by altering metabolic processes and signalling mechanisms (Effmert et al., 2012; Weisskopf et al., 2021). Together, these mVOCs contribute to the ecological role of the endophytic and rhizosphere bacteria in plant protection and microbial competition, including phytopathogens and HPMOs, forming a chemical defence network within the plant environment.

1.6. **Influence of the chemical composition of plants and soils on endophytes**

A comprehensive introduction to this topic is thoroughly presented in P1, Annex I (Marangi et al., 2024).

Pathogenic bacteria penetrate plant tissues and multiply within the extracellular spaces. In response, plants have developed an immune system capable of detecting and restricting pathogen growth (Lee et al., 2019). Furthermore, the properties of the soil play a significant role in shaping the microbial community present.

Research on the influence of soil pH on HPMOs' survival remains limited. Most investigations have been conducted under controlled laboratory conditions to mimic the

effects of pH on HPMOs' persistence, with some studies performed in the field (Arcari et al., 2020; Cheng et al., 2021). Acidic environments, characterized by high proton concentrations, pose significant challenges for unicellular organisms. The protonation of biological molecules can alter their charge, structure, and function, potentially leading to detrimental effects on cellular integrity (Arcari et al., 2020). Following bio-activation of the soil, there was an observable increase in the abundance of beneficial microorganisms, which correlates positively with plant pathogens suppression and elevated pH levels (Cheng et al., 2021). A recent study indicated that the complete inhibition of four foodborne pathogens – *S. enterica*, *E. coli*, *L. monocytogenes* and *Staphylococcus aureus*– occurred within a pH range of 3.80 to 3.87 (Caballero-Guerrero et al., 2022). Additionally, the populations of *E. coli*, *S. enterica*, and *L. monocytogenes* in bulk soil decreased as soil pH increased, a trend also associated with saline soil types (Marangi et al., 2024). Notably, higher concentrations of NaCl (5%) typically suppress the growth of *E. coli* and impair virulence traits like biofilm formation, resistance to oxidative stress, and motility (Li et al., 2021).

Some soil microorganisms are capable of adapting their physiological metabolism to cope with salinity, for this reason they are considered halotolerant (Zhang et al., 2024). Certain halotolerant bacteria can establish themselves as endophytes in plant roots, where they produce antimicrobial metabolites to defend against pathogens (Nabti et al., 2015). Notably, the open reading frames (ORFs) in Cluster_111 are present exclusively in three halotolerant strains, implying a role for taurine accumulation as an osmoprotective mechanism (Zhou et al., 2023). Additionally, these halotolerant bacteria contain genes associated with multiple glutamate biosynthesis pathways (Zhou et al., 2023). For example, ORFs in Cluster_113 are annotated as members of the hydantoinase B/oxoprolinase family, including 5-oxoprolinase, which catalyses the conversion of 5-oxo-L-proline into L-glutamate, thereby contributing to salt tolerance (Niehaus et al., 2017). *B. halotolerans*, a halotolerant bacterial species, mitigates pathogen threats in crops like wheat, rice, date palm, and tomato through a multifaceted strategy involving siderophore and phytohormone synthesis, exopolysaccharide secretion, and the emission of antifungal and nematocidal agents (Rafanomezantsoa et al., 2025). Genomic and metabolomic profiling further underscored its capacity to generate diverse secondary metabolites that enhance its anti-pathogenic efficacy and plant-growth promotion (Rafanomezantsoa et al., 2025).

Plants have a natural defence mechanism against infections that involves the production of various protective metabolites, including lignin (Ninkuu et al., 2023). Lignin is a complex

biopolymer predominantly found in the secondary cell walls of plants (Gallego-Giraldo et al., 2018). It plays a crucial role not only in plant growth and development but also in how plants respond to a range of biotic and abiotic stresses (Cesarino, 2019). Lignin is widely recognized for its contribution to disease resistance against pathogens (Zhao and Dixon, 2014). The resistance mechanisms attributed to lignin involve the formation of physical barriers that impede pathogen entry and restrict the movement of toxins and nutrients from pathogens to the host plant (Weng and Chapple, 2010). Both the overall lignin content and stress-induced lignin are vital for enhancing disease resistance; their combined effects significantly bolster this resistance (Ma et al., 2018). Furthermore, the presence of lignin in plants negatively impacts the motility of pathogenic bacteria (Lee et al., 2019). These insights regarding plant pathogens may also extend to human pathogens like *S. enterica* (Marangi et al., 2024).

2. Hypotheses

S. europaea, a salt-tolerant halophyte, thrives in high-salinity soils. Its unique ecological niche and microbial associations present a compelling system to explore natural mechanisms of resistance against HPMOs. We suggest that environmental factors such as soil and plant chemistry may play critical roles in suppressing the growth of HPMOs. Additionally, the colonization of *S. europaea* by HPMOs may vary between strains, altering the plant transcriptome in different ways. Moreover, plant-associated bacteria capable of emitting mVOCs *in vitro* may inhibit the growth of certain HPMOs. Investigating these interconnected factors in *S. europaea* may not only enhance our understanding of plant-microbe-HPMOs interactions but also identify biomarkers and biocontrol strategies relevant to food security in marginal soils. In light of these observations, we hypothesize that:

1. specific physicochemical characteristics of the soil surrounding *S. europaea*, particularly pH and lignin content, may be significantly correlated with the plant's susceptibility to contamination by HPMOs. These variables may influence HPMOs' colonization, thereby serving as reliable environmental biomarkers for predicting infection risk and informing early detection strategies for food security and sustainable agriculture;
2. while HPMOs may successfully initiate colonization when introduced into a sterile sand, their long-term persistence will be significantly reduced in *S. europaea* at varying levels of salinity. This may be due to the plant-associated bacteria, and the high salinity. Furthermore, we expect that the plant gene expression profile in response to HPMOs' inoculation will be detectable at the transcriptomic level, reflecting molecular adjustments associated with HPMOs' recognition and stress adaptation;
3. endophytic and rhizosphere bacteria associated with *S. europaea* may actively inhibit the growth of HPMOs through the production of mVOCs. These volatiles, known for their antimicrobial properties, may represent a valid eco-friendly alternative to the use of standard chemical products in agriculture.

3. Research objectives

Understanding how halophyte like *S. europaea* interact with HPMOs offers valuable insight into natural defence strategies in extreme environments. Within this context, the present study seeks to uncover how *S. europaea* responds to HPMOs, what roles its native endophytic and rhizosphere bacteria play in limiting HPMOs' growth, and how environmental conditions shape the outcomes of these interactions. In accordance with these observations, we aimed to:

1. identify and quantify critical environmental and biochemical factors—such as soil pH, lignin content, and salinity levels—in both the soil and tissues of *S. europaea* that influence the establishment and abundance of HPMOs. This objective seeks to uncover how abiotic conditions and host-derived compounds contribute to HPMOs' regulation, with potential applications in developing biomarker-based monitoring systems for plant health;
2. investigate the temporal and spatial dynamics of colonization by HPMOs in *S. europaea*, and to assess how this interaction alters the plant's gene expression profile. This objective includes evaluating the extent of HPMOs establishment, persistence, and any physiological responses at the molecular level using transcriptomic analysis to uncover key pathways activated or suppressed in response to inoculation;
3. identify and select endophytic and rhizosphere bacterial strains from *S. europaea* that exhibit inhibitory activity against HPMOs, with a specific focus on the role of mVOCs. This objective aims to determine the spectrum and mechanisms of inhibition provided by native microbiota, thereby elucidating potential biocontrol agents inherent to the plant's microbiome.

4. Materials and methods

4.1. **HPMOs in *S. europaea*: analyses of shoots and soil chemistry**

A comprehensive section of the materials and methods to this topic is thoroughly presented in P1, Annex I (Marangi et al., 2024).

Samples of *S. europaea*, its rhizosphere and bulk soil were collected in October 2022 from two salt marshes in France differing in site age and salinity: an old sandy marsh (F1, municipality of Plurien, 48.634379, −2.415823) and a young muddy marsh (F2, municipality of Beaussais-sur-Mer, 48.582263, −2.159779). At each site, three 1×1 m plots were established, from which five plants and adjacent soil were collected (15 plants per site). Bulk soil samples were also taken. All samples were stored at 4°C and transported to Nicolaus Copernicus University in Poland. Sampling complied with environmental protection regulations with the permission of the General Director for Environmental Protection (DZP-WG.6400.13.2022.EP.1).

For thermochemolysis, plant (10 mg) and soil (100 mg) samples were placed in modified Pasteur pipettes and treated with tetramethylammonium hydroxide (TMAH). The system, connected to a charcoal-filled pipette and flushed with nitrogen, was heated to 220 °C for 6 minutes after a 5-minute reaction time. Following cooling, the samples were transferred to vials, rinsed with a dichloromethane/methanol mixture, and sonicated at 35 °C for 5 minutes. The suspension was then left to settle for 55 minutes. For GC/MS analysis, 1 µL of the sample was injected into a Thermo Scientific Trace 1310-GC with a 60 m BP5 column at an injector temperature of 300 °C. Helium was used as the carrier gas at a constant flow of 1 mL/min. A splitless injection was followed by split ratios of 1:100 (45–90 s) and 1:5 (after 90 s). The temperature program began at 100 °C for 5 min, increased at 5 K/min to 280 °C, with a total run time of 120 min. The GC was coupled to a Thermo Scientific DFS magnetic sector mass spectrometer. Compound classes—carbohydrates, lignin, and lipids—were identified based on peak areas and assigned using the NIST 2017 database.

At each site, three plots (A, B, C) with five replicates were used. Rhizosphere and/or bulk soil (1 g) and surface-sterilized plant organs (roots and shoots) were collected. Shoots and roots were homogenized in 2% NaCl, and serial dilutions were prepared for both plant (10^{-1}–10^{-2}) and soil (10^{-1}–10^{-3}) samples. Dilutions (100 µL) were plated in triplicate on selective media to quantify HPMOs, targeting *L. monocytogenes*, *E. coli*, *S. enterica*, and *B. cereus* using ISO-

standard chromogenic agars. Plates were incubated at 37 °C for 2–7 days, and colony-forming units (CFU) were counted, normalized to 1 g of dry weight, and expressed as $\log_{10}$ CFU g^{-1}. Soil samples were air-dried, sieved (2 mm), and analysed for total carbon (Ct) and nitrogen (Nt) using an Elementar Vario CNS analyser. Calcium carbonate ($CaCO_3$) was measured volumetrically, with total inorganic carbon (TIC) and total organic carbon (TOC) calculated accordingly. Bioavailable phosphorus (Pca) was determined colorimetrically. Soil pH ($CaCl_2$), electrical conductivity (EC), and concentrations of Mg, Ca (via atomic absorption spectrometry), K, Na (via optical emission spectrometry), HCO_3^- (via titration), and SO_4^{2-}, Cl^-, Br^- (via ion chromatography) were measured. Soil texture was assessed using 10 g of bulk soil through a multi-step process involving carbonate removal, organic matter digestion, dispersion with pyrophosphate, ultrasonic treatment, and sedimentation. Silt, clay, and sand fractions were separated, dried, weighed, and used to calculate the total soil texture composition.

Data were analysed using R (versions 4.4.0 and 5.2-0). Normality and variance homogeneity were tested using Shapiro–Wilk and Levene's tests, respectively. Differences were assessed using one-way ANOVA and Tukey's test ($p < 0.05$), and Pearson correlation coefficients were used for association analyses.

4.2. ***In vitro*** **pot-experiment**

Biological material

The *S. europaea* seeds used in the *in vitro* experiment were purchased from AlsaGarden (France). Three strains of HPMOs bacteria were used in the experiments: *E. coli* (non-pathogenic, PCM 2057), *S. enterica* subsp. *enterica* (PCM 2565) and *L. monocytogenes* (PCM 2191), all from the microbial collection of Department of Microbiology at Nicolaus Copernicus University in Toruń (Poland). Bacterial strains were maintained as starting stock in glycerol and stored at -80°C in Eppendorf tubes.

Experimental design

The experimental design included: (i) four inoculation variants - a control group (not inoculated with bacteria) and three groups inoculated with bacteria: *E. coli*, *S. enterica*, and *L. monocytogenes*, (ii) four salinity treatments: 0 mM, 50 mM, 100 mM, and 200 mM NaCl. A total of 2000 plants were analysed, with 125 plants for each of the 16 variants of the experiment

(Figure 1). The *in vitro* experiment was conducted under sterile conditions in sealed magenta boxes (107 x 94 x 96 mm, Duchefa, Netherlands), which were maintained in plant growth chambers under controlled cycles of light and darkness (16 hours of light/8 hours of darkness) at a constant temperature of 21°C. The growing medium for the plants was sand (0.5-1.4 mm, KREISEL, Poland) in a volume of 150 mL/magenta box and Hoagland's medium (30 mL per box) (Hoagland and Arnon, 1950) with four different salinity levels (0 g/L, 2.92 g/L, 5.84 g/L and 11.68 g/L NaCl), which were sterilized before use in an autoclave (0,8 atm., 121˚C, 20 min). Seeds of *S. europaea* were placed in the magenta boxes at a density of approximately 30 seeds per box. Seeds of *S. europaea* were not surface-sterilized prior to sowing, for several biological and technical reasons. Firstly, sterilization procedures carry the risk of removing native epiphytic bacteria, which may play a role in modulating plant–HPMOs interaction. At the same time, seeds may also carry some HPMOs. For this reason, the qPCR analyses in this thesis were compared to a control (non-inoculated). Secondly, due to the extremely small size of *S. europaea* seeds, standard sterilization treatments resulted in a marked reduction in germination rates, compromising experimental consistency and plant viability.

Before preparing the bacterial suspension for plant inoculation, a portion of the bacterial cells was taken with a sterile loop from the starting stock (stored at -80°C) and transferred to 35 ml of Tryptic Soy Broth (TSB; Biomaxima, Poland) and incubated for 24h at 37°C. After this time, the grown bacterial cells were centrifuged using a vortex and the bacterial suspension was prepared in saline solution (0.85% NaCl) at a concentration of 1.5×10^8 CFU/mL. Inoculation of germinated *S. europaea* plants was carried out four weeks after sowing. In each bacterial variant of the experiment, 5 ml of the prepared bacterial suspension was spread evenly on the surface of the sand, while in the control variant, 5 ml of a sterile solution of 0.85% NaCl was spread. After 8 weeks of plant cultivation and 4 weeks after inoculation, we proceeded to measure plant growth parameters, determine HPMOs' abundance in their organs, and prepare samples for transcriptomic analysis.

A total of 25 plants were selected from each magenta box and measured and weighed: total biomass (measured as total plant weight in g), shoot length and root length (in mm). After measurements: 5 plants were used for evaluation of total bacterial abundance and abundance of HPMO bacteria in selective media, 10 plants were used for DNA isolation and quantitative PCR (qPCR) (stored at -20°C), 10 plants were reserved for transcriptomic analyses (stored at -80°C). All procedures were carried out under a laminar flow hood to ensure sterile conditions.

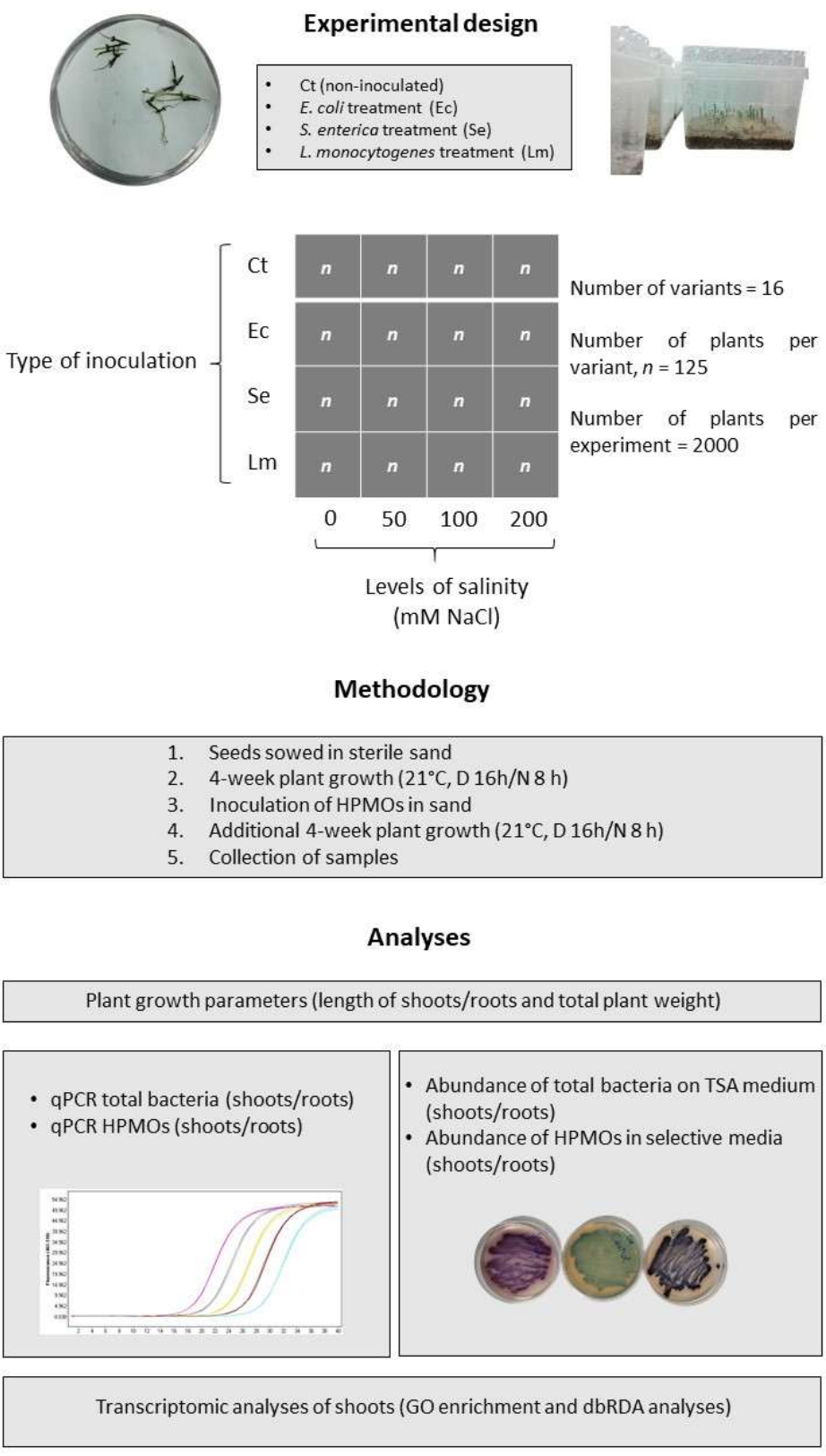

Figure 1. Presentation of the experimental design: the pot experiment and the analyses performed.

Particularly, plants of *S. europaea* were cultivated in sterile sand at varying levels of salinity (0, 50, 100, 200 mM NaCl) including four different treatments (non-inoculated, *E. coli*, *S. enterica* and *L. monocytogenes*). Eight weeks after sowing, plants were collected and surface sterilised for different analyses: plant growth parameters, abundance and detection of HPMOs and total bacteria in shoots and roots, and transcriptomic analyses of shoots.

Abundance of total bacteria and HPMOs in selective media

Before analysis all plants were surface sterilized using 0.85% NaCl (three washes of 30 s each) followed by a single wash with 5% hydrogen peroxide (H_2O_2) for 5 min. After sterilization, the roots and shoots were separated using a sterile scalpel. For the assessment of total bacteria and HPMOs, the shoots (200 mg) and roots (100 mg) were milled in 0.85% NaCl at a ratio of 1:9, and two dilutions (10^{-1} and 10^{-2}) were prepared from the resulting mixture. From each dilution 100 µL was pipetted onto Tryptic Soy Agar (TSA; Biomaxima, Poland) and selective media (in triplicate) including Chromogenic *Salmonella* LAB-AGAR™ with *Salmonella* Chromogenic Supplement, Chromogenic *Listeria* according to Ottaviani and Agosti LAB-AGAR™ Base with Chromogenic *Listeria* Kit Supplement, and *E. coli* Chromogenic Medium (Biomaxima, Poland). Colony counts were performed seven days after streaking on the Petri plates, incubated at 37°C. The results were expressed as CFU/g, which were then transformed into $\log_{10}$ values for analysis.

Genomic DNA isolation from shoots and roots of *S. europaea*

Five and two biological replicates were prepared for shoots and roots, respectively, resulting in a total of seven samples per variant. Genomic DNA was isolated using the Plant and Fungi DNA Purification Kit (EURx, Poland) according to the manufacturer's instructions. The DNA concentrations were determined using a Qubit™ dsDNA HS Assay Kit (Invitrogen™). The isolated DNA was then stored at −20°C. The genomic DNA was isolated in order to be used for the detection of HPMOs and total bacteria in shoots and roots through real-time qPCR.

Real-Time quantitative PCR assay: detection of HPMOs in shoots and roots of *S. europaea*

The absolute quantification of each analysed HPMO and the total 16S rRNA gene copy numbers in the shoots and roots of *S. europaea* was carried out using the LightCycler 480 system along with the LightCycler 480 SYBR Green I Master Kit (Roche). The qPCR reactions were set up in a total volume of 10 µL, comprising 5 µL of 2x SYBR Green I Master Mix

(Roche), 2 µL of PCR-grade water, 0.5 µL of each specific primer (10 pmol/µL), and 2 µL of DNA template (5 ng/µL for shoots and 2.5 ng/µL for roots). The cycling conditions included an initial denaturation step at 95°C for 5 minutes, followed by 40 cycles of 10 seconds of denaturation at 95°C, 20 seconds of annealing at the optimal temperature for the primer pair (Table 1), and 20 seconds of elongation at 72°C. A melting curve analysis was conducted with a continuous temperature increase from 65°C to 95°C. Positive (DNA of specific bacterial strains) and negative controls (molecular-grade water) were included and analyzed alongside the experimental samples. The qPCR analyses were performed with five biological replicates for shoots and two biological replicates for roots, each with three technical replicates. Standard curves for the quantification of specific gene copy numbers for each strain were generated using PCR-amplicons. The amplicons were purified using AMPure XP (Beckman Coulter) and their concentrations were determined with a Qubit™ dsDNA HS Assay Kit (Invitrogen™, USA) and a Qubit fluorometer (ThermoFisher Scientific, USA). Standard curves were established by performing 5-fold serial dilutions of amplicons, resulting in a copy number range from 100,000,000 to 1,280 copies per reaction. These standard curves were utilized to evaluate the reaction efficiency for each primer set. Absolute quantification results were expressed as the number of specific bacterial gene copies detected in 1 ng of total plant DNA.

Table 1. Oligonucleotide sequences and annealing temperature (AT) used in qPCR. The design of the primers was carried out by Dr. Edyta Deja-Sikora (Department of Microbiology, Faculty of Biological and Veterinary Sciences, Nicolaus Copernicus University, Lwowska 1, Torun, 87-100, Poland), with the primers for *E. coli*, *L. monocytogenes* and total bacteria adopted from Szymańska et al. (2024), Amagliani et al. (2010), and Johnson et al. (2011) respectively.

Oligo name	**Sequence (5 → 3)**	**Detected bacteria**	**AT**
EcRTF1	GAAGGGAGTAAAGTTAATAC	*E. coli*	50°C
EcRTR1	AGTATCAGATGCAGTTCC		
SeqPCRr	ATTTCACATCCGACTTGACAG	*S. enterica*	61°C
SeqPCRf	GGGGAGGAAGGTGTTGTG		
634F	ACTTCGGCGCAATCAGTGA	*L. monocytogenes*	54°C
770R	TTGCAACTGCTCTTTAGTAACAGCTT		
357F	CCTACGGGAGGCAGCAG	Total bacteria	50°C
515R	TTACCGCGGCKGCTGGCAC		

RNA isolation

RNA isolation was carried out by Dr. Marcin Sikora (Centre for Modern Interdisciplinary Technologies, Nicolaus Copernicus University in Toruń, Wileńska 4, PL-87-100 Toruń, Poland). A total of 100 mg of tissue was homogenized in 1.2 ml of RNA Extracol reagent (Eurx, Gdansk, Poland) using a bead-beating method. The homogenization was performed with a PowerLyzer 24 (MO BIO Laboratories, CA, USA) at 4000 cpm for 45 s and repeated twice. The tissue was disrupted using a mixture of iron beads with diameters of 42.5 mm and 61.5 mm. 300 µL of chloroform was added to the lysate, and the mixture was vortexed for 20 s. The sample was centrifuged at 14,000 × g for 10 minutes at 4 °C. Then, 450–500 µL of the aqueous phase was carefully transferred to a new 2 ml microcentrifuge tube and further extracted with 500 µL of a chloroform–isoamyl alcohol mixture (24:1, v/v). RNA was precipitated with 0.7 volume of 2-propanol, washed twice with 75% ethanol and air-dried no longer than 10 min. RNA pellet was resuspended in nuclease-free water. Remaining DNA was digested by DNAse I (Eurx, Gdansk, Poland) according to manufacturer protocol. RNA was further purified using Canvax CleanEasy mini spin columns (Canvax Biotech, Kordoba, Spain) as described by Deja-Sikora et al. (2024). RNA concentration was measured with NanoDrop 2000 (Thermo Fisher Scientific, Waltham, MA, USA). RNA integrity was checked with Agilent RNA 6000 Nano Kit and 2100 Bioanalyzer using Plant RNA Assay (Agilent Technologies, CA, USA). RNA samples with RIN values above 8 were used for transcriptomic libraries preparation.

Library was prepared using NEBNext Ultra II Directional RNA Library Prep Kit Illumina (New England Biolabs, Ipswich, MA, USA; protocol section 4) according manufacturer protocol. PCR products were purified using AMPure XP beads (Beckman Coulter Life Sciences, Indianapolis, IN, USA). The purified products were quantified by NanoDrop™ 2000 spectrophotometer (Thermo Fisher Scientific) and quality check was done using Agilent RNA 6000 Nano Kit and 2100 Bioanalyzer (Agilent Technologies, CA, USA).

Development of depletion protocols

The development of depletion protocols was carried out by Dr. Marcin Sikora (Centre for Modern Interdisciplinary Technologies, Nicolaus Copernicus University in Toruń, Wileńska 4, PL-87-100 Toruń, Poland) and Dr. Edyta Deja-Sikora (Department of Microbiology, Faculty of Biological and Veterinary Sciences, Nicolaus Copernicus University, Lwowska 1, Torun, 87-100, Poland). Small RNAs were removed from total RNA using carboxylate-modified magnetic beads. Briefly, 20 µL of total RNA (containing at least 3 µg) was mixed with 16 µL of 5 M guanidinium thiocyanate and 4 µL of nuclease-free water, and the mixture was incubated

at RT for 10 min. Next, 40 µL of SpeedBeads™ magnetic carboxylate-modified particles (Cytiva, Marlborough, MA, USA), suspended in 50% ethanol, was added and the sample was incubated for 15 min. The tube was then placed on a magnetic rack for 10 min, and the supernatant was removed. The beads were washed twice with 200 µL of 80% ethanol, then air-dried for 3 min. RNA was eluted by adding 20 µL of nuclease-free water. The tube was removed from the magnetic rack and gently mixed for 10 min at RT. After incubation, it was returned to the magnetic rack for 5 min, and the supernatant containing the RNA fraction depleted of small RNAs was transferred to a fresh tube.

Plant rRNA was depleted using Sera-Mag™ Magnetic Streptavidin-Coated Particles (Cytiva, Marlborough, MA, USA) and a custom biotinylated probe mixture (Annex II, Table 1). For each sample, 200 µL of beads was washed three times with 1 volume of 1× binding and wash (B&W) buffer (0.5 M Tris–HCl, pH 7.0; 0.5 M Tris–HCl, pH 8.0; 0.25 M EDTA; 2.5 M NaCl). Next, beads were resuspended in 60 µL of 2× B&W buffer (1 M Tris–HCl, pH 7.0; 1 M Tris–HCl, pH 8.0; 0.5 M EDTA; 5 M NaCl) supplemented with 1 µL of RNase inhibitor (Eurx, Gdansk, Poland).

Separately, 2 µg of size-selected total RNA was combined with 1.5 µL of SSC buffer (0.15 M NaCl, 0.015 M sodium citrate), 0.8 µL of the biotinylated rRNA probe mix, and nuclease-free water to a final volume of 30 µL. The mixture was incubated in a C1000 Touch™ Thermal Cycler (Bio-Rad, Hercules, CA, USA) at 70 °C for 5 minutes, followed by a gradual cooling to 25 °C (1 °C per 30 seconds) to allow probe hybridization.

Next, 30 µL of the prepared bead suspension in 2× B&W buffer was added to the annealed RNA–probe mixture. The sample was mixed gently by pipetting and incubated at RT for 5 min, then transferred to 50 °C for another 5 min. After incubation, the tube was placed on a magnetic rack for 5 min, and 55–60 µL of the supernatant (containing rRNA-depleted RNA) was carefully transferred to a fresh 200 µL tube, avoiding bead carryover.

To further deplete residual ribosomal RNA, 30 µL of nuclease-free water and 30 µL of fresh bead suspension were added to the collected supernatant. The binding and incubation steps were repeated. During two-round depletion, 100–110 µL of the final supernatant was collected. RNA was precipitated by adding 0.1 volume of 3 M sodium acetate and 3 volumes of chilled 96% ethanol. After incubation at –20 °C for 1 h samples were centrifuged at 14,000 × g at 4 °C for 30 min. The resulting RNA pellet was washed twice with 1 ml of 80% cold ethanol, air-dried, and resuspended in 10 µL of nuclease-free water.

Transcriptomic analyses of *S. europaea* shoots

Bioinformatics analyses of transcriptomic data were carried out by Prof. Marcin Gołębiewski (Interdisciplinary Centre for Modern Technologies, Nicolaus Copernicus University, Torun, Poland). Raw reads were denoised with rcorrector v.1.0.4 (Song and Florea, 2015). Reads containing unfixable errors were removed using the 'FilterUncorrectabledPEfastq.py' script (https://github.com/harvardinformatics/TranscriptomeAssemblyTools/tree/master/utilities) and quality trimming as well as adapter removal was performed using TrimGalore v.0.6.7 (https://github.com/FelixKrueger/TrimGalore). Reads mapping to ribosomal RNAs were removed (mapping with Bowtie2 v.2.4.2 to SILVA v.138.1). Clean reads were assembled with Trinity v.2.15.1 (Grabherr et al., 2011), and the resulting transcripts were annotated using TransDecoder and Trinotate (Bryant et al., 2017). Clean reads were mapped to assembled transcriptome with HiSat2 v.2.2.1 (Kim et al., 2019). Transcripts were quantified using stringtie v. 2.2.0 (Pertea et al., 2015) and differentially expressed genes and transcripts were identified using ballgown v. 2.36.0 (Frazee et al., 2015) in R 4.4.1. GO enrichment was performed using topGO v. 2.56.0 (Alexa and Rahnenfuhrer, 2023).

4.3. *In vitro* bipartite assay coupled with HS-SPME-GC-MS

Bacterial strain collection

A total of 58 endophytic and rhizosphere bacterial isolates belonging to Bacilli, Gammaproteobacteria, Actinomycetes and Alphaproteobacteria, were included in this study. These isolates were previously characterized and taxonomically identified by Dr. Szymańska et al. (2016). Of these, 46 strains had been fully identified (Table 2), while the remaining 12 were unclassified. In the present study, we performed taxonomic identification for the 12 previously unidentified isolates. All 58 endophytic and rhizosphere bacteria were analysed and tested against 3 HPMOs: *E. coli* (non-pathogenic, PCM 2057), *S. enterica* subsp. *enterica* (PCM 2565) and *L. monocytogenes* (PCM 2191). The endophytic and rhizosphere bacteria and the HPMOs used in this experiment came from the collection at the Department of Microbiology (Nicolaus Copernicus University, Torun, Poland) stored in glycerol stock at -80°C.

Table 2. List of the 58 endophytic and rhizosphere bacteria used for the realisation of the bipartite *in vitro* assay. Detailed description in the work of Szymańska et al. (2016).

ID code	Bacteria	Class
CSR28	*Bacillus pumilus*	Bacilli
CSR1	*Bacillus toyonensis*	Bacilli
CSR14	*Bacillus pumilus*	Bacilli
CSR12	*Bacillus pumilus*	Bacilli
CSE31	*Bacillus sp.*	Bacilli
CSE32	*Bacillus pumilus*	Bacilli
ISE27	*Bacillus cereus*	Bacilli
ISE8	*Bacillus sp.*	Bacilli
ISE28	*Bacillus weihenstephanensis*	Bacilli
ISE11	*Bacillus cereus*	Bacilli
CSR23	*Bacillus pumilus*	Bacilli
CSR25	*Bacillus toyonensis*	Bacilli
CSE22	*Bacillus baekryungensis*	Bacilli
ISR12	*Bacillus sp.*	Bacilli
ISR22	*Bacillus cereus*	Bacilli
ISR13	*Bacillus sp.*	Bacilli
ISR8	*Bacillus mycoides*	Bacilli
ISR25	*Bacillus sp.*	Bacilli
CSR2	*Bacillus pumilus*	Bacilli
ISR5	*Bacillus sp.*	Bacilli
CSE34	*Xanthomonadales sp.*	Gammaproteobacteria
CSE6	*Serratia marcescens*	Gammaproteobacteria
ISE14	*Serratia plymuthica*	Gammaproteobacteria
ISE12	*Pseudomonas sp.*	Gammaproteobacteria
CSE5	*Serratia marcescens*	Gammaproteobacteria
CSE16	*Hafnia psychrotolerans*	Gammaproteobacteria
CSE25	*Salinicola socius*	Gammaproteobacteria
ISR14	*Serratia plymuthica*	Gammaproteobacteria
ISR2	*Serratia plymuthica*	Gammaproteobacteria
CSR13	*Microbacterium oxydans*	Actinomycetes
CSR21	*Microbacterium foliorum*	Actinomycetes
CSR36	*Dietzia sp.*	Actinomycetes

CSR4	*Streptomyces champavatii*	Actinomycetes
CSR15	*Microbacterium oxydans*	Actinomycetes
ISE7	*Microbacterium thalassium*	Actinomycetes
ISE29	*Streptomyces sp.*	Actinomycetes
ISE16	*Rhodococcus erythropolis*	Actinomycetes
ISR1	*Streptomyces sp.*	Actinomycetes
ISE22	*Williamsia sp.*	Actinomycetes
ISE5	*Microbacterium oxydans*	Actinomycetes
ISR6	*Mycobacterium sacrum*	Actinomycetes
ISR7	*Microbacterium oxydans*	Actinomycetes
ISR30	*Oerskovia paurometabola*	Actinomycetes
ISR15	*Rhodococcus erythropolis*	Actinomycetes
CSR16	*Mycobacterium vaccae*	Actinomycetes
CSE28	*Thalassospira permensis*	Alphaproteobacteria

DNA isolation and identification of bacteria

Identification of the 12 selected bacterial isolates was conducted through 16S rRNA gene sequencing. Genomic DNA was extracted utilizing the Bacterial & Yeast Genomic DNA Purification Kit (EURx), following the manufacturer's protocol with a modified elution volume of 50 µL. DNA concentration and purity were measured using a NanoDrop 2000 UV-Vis spectrophotometer. The extracted DNA served as the template for polymerase chain reaction (PCR) targeting the 16S rRNA gene, using the primer pair 27F (5′-AGA GTT TGA TCC TGG CTC AG-3′) and 1492R (3′-CTA CGG CTA CCT TGT TAC GA-5′) (Mapelli et al., 2013). DNA samples were stored at −20°C until further use. PCR reactions were carried out using Taq PCR Master Mix (Qiagen, Hilden, Germany). The cycling conditions were as follows: one cycle of 2 min at 95 °C, followed by 30 cycles of 1 min at 94 °C, 1 min at 55 °C, and 2 min at 72 °C, and one final cycle of 5 min at 72 °C. Amplification products were visualized on 1.0% (w/v) agarose gels stained with Simply Safe (EURx) to verify their size and presence, compared to a known bacterial strain (Control). Sequencing was carried out using the same primer pair, and forward and reverse reads were assembled using Sequencher 5.1 software (Gene Codes 20). The resulting sequences were compared against entries in the GenBank database, with a minimum of 97% identity required for confident taxonomic identification.

Bipartite *in vitro* assay - selection of endophytic and rhizosphere bacteria inhibiting the growth of HPMOs

Tryptic Soy Agar (TSA) (Biomaxima S.A., ul. Vetterów 5, 20-277 Lublin, Poland) culture medium was prepared, autoclaved (121°C for 21 minutes) and distributed in a total volume of 25 mL for each bipartite Petri plate. When the Petri plates dried, a portion of endophytic and rhizosphere bacteria was transferred in one side of each bipartite Petri plate (Figure 2) with a sterile inoculum loop from a specific Petri plate containing a determined endophytic or rhizosphere bacterium. After 3-5 days (at 26°C), based on the growth of the endophytic/rhizosphere bacteria, an inoculum of the HPMOs was distributed in a 3-cm-long line in the middle of the second side of the bipartite Petri plate following a draft picture at the bottom of the Petri plate. All the Petri plates were sealed with parafilm and secured with transparent cook foil. Each endophytic and rhizosphere bacterium had 3 variants (*S. enterica*, *L. monocytogenes*, *E. coli*) with 2 replicates each. In total, there were 6 replicates (3 per one plate).

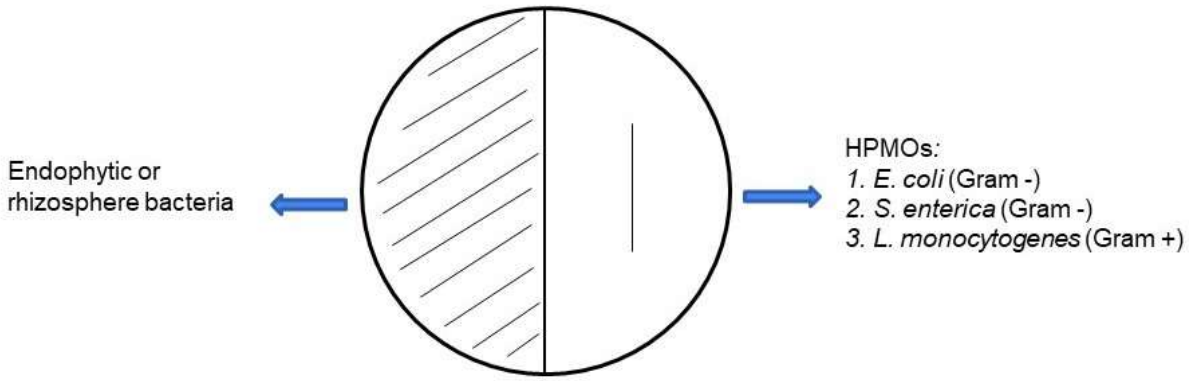

Figure 2. Representation of the performed bipartite assay to evaluate the width of the HPMOs in relationship to the presence of the endophytic or rhizosphere bacteria.

The inoculum of the HPMOs was prepared as follows. A volume of 30 mL of Tryptic Soy Broth (TSB) (BD BBL™, Becton, Dickinson and Company, Sparks, MD 21152 USA) was added in 100 mL flasks; a portion of HPMO from glycerol stock at -80°C was transferred onto a Petri plate and allowed to incubated for 24 hours at 37°C. After overnight growth, a portion of HPMO from Petri plate was inoculated into the TSB flasks with a sterile inoculum loop. After 24 hours at 37°C, a fresh Petri plate with TSA medium received a volume of 100 µL of HPMO-TSB medium and then distributed all over the surface of the new Petri plate. 24 hours after (at 37°C), the inoculum of HPMO was distributed in a 3-cm-long line in the middle of the second side of the bipartite Petri plate. 3 and 7 days (at 37°C) after the realisation of the bipartite assay, a

measurement of the HPMO's width was detected and calculated by comparing to control; in total 6 measurements were considered for each sample. Particularly, the percentage of growth of the HPMOs in bipartite Petri plate compared to control was calculated:

$$Wf = \frac{Wi * 100}{Wc}$$

Wf = % of growth of HPMOs

Wi = width of HPMOs

Wc = width of HPMOs (control)

mVOCs analysis through HS-SPME-GC-MS

The four bacterial strains—*Bacillus pumilus* CSR28, *Xanthomonadales* sp. CSE34, *Streptomyces champavatii* CSR4, and *Bacillus pseudomycoides* CSE4—that exhibited significant inhibition of HPMOs in the bipartite *in vitro* assay were further analysed for their production of mVOCs using HS-SPME-GC-MS. The HS-SPME-GC-MS was carried out by Dr. Robert Gąsior (Central Laboratory of the National Research Institute, Jurajska 44, Aleksandrowice, 32-084 Morawica). In addition, *E. coli*, *S. enterica*, and *L. monocytogenes* were included in the analysis. To assess whether the selected strains produced mVOCs active against these HPMOs, co-cultures were established and analysed as follows: *B. pumilus* CSR28 with *E. coli* and *L. monocytogenes*; *Xanthomonadales* sp. CSE34 with *E. coli*, *S. enterica*, and *L. monocytogenes*; *S. champavatii* CSR4 with *E. coli* and *S. enterica*; and *B. pseudomycoides* CSE4 with *E. coli* and *S. enterica*. Fresh bacterial cultures were prepared on TSA by incubating the selected bacterial strains for 3 days at 26 °C, and the HPMOs (*E. coli*, *S. enterica*, and *L. monocytogenes*) for 24 hours at 37 °C. For co-culture experiments, the selected bacterial strains were inoculated onto one half of a TSA-filled bottle and incubated for 3 days at 26 °C. After this incubation period, a single HPMO was streaked onto the opposite half of the same TSA-filled bottle, and the bottles were incubated at 37 °C for an additional 7 days. All bottles were sealed with a septum to retain headspace volatiles. Following the incubation period, mVOC profiles were analysed using HS-SPME-GC-MS. Each bacterial treatment was performed in triplicate.

A gas chromatography-mass spectrometry method (GC-MS-QP 2020 NX, Shimadzu, Duisburg, Germany) was developed for VOCs analysis. Volatiles were isolated by headspace

solid-phase microextraction using 120µm DVB/CAR-WR/PDMS SPME Smart Arrow (Shim-Pol, Warszawa, Poland). A semi-polar column –Zebron ZB-5MSi 30m x 0.25mm, 0.25µm column (Phenomenex; Shim-Pol, Warszawa, Poland) – was used for volatiles separation. The injection was performed using the AOC-6000 Plus Shimadzu (Shimadzu, Duisburg, Germany). The autosampler rack was cooled to about +3 °C and the sample was equilibrated at 50 °C for 30 min before injection. The SPME Smart Arrow exposition time was 15 min at 50 °C and then VOCs were desorbed in the splitless port for 2 min. The quadrupole electron ionization (70 eV) mass spectrometer was operated in full scan mode in a range of 35–450 m/z. The total time of the analysis was 60 min. The remaining GC-MS operating conditions were as follows: column temperature range of 37 °C to 240 °C, injector temperature of 220 °C, helium as the carrier gas (3 mL/min, 99.99% purity; Linde Gaz Polska, Kraków, Poland), ion source temperature of 230 °C, and interface temperature of 240 °C.

4.4. **Statistical analysis**

The statistical analysis of plant growth parameters, bacterial abundance on selective media, and bacterial abundance quantified through qPCR was performed using R software. This statistical analysis was performed by Prof. Marcin Gołębiewski (Interdisciplinary Centre for Modern Technologies, Nicolaus Copernicus University, Torun, Poland). For comparison of plant growth parameters and bacterial abundance across multiple groups, the Kruskal-Wallis's test was used to assess differences in distributions among groups. This non-parametric test was applied to determine if there were significant differences in the data across three or more independent groups. In cases where the Kruskal-Wallis's test indicated significant differences, pairwise comparisons were carried out using the Wilcoxon rank-sum test (Mann-Whitney U test) to identify which specific groups differed from each other. All tests were conducted at a significance level of $p < 0.05$.

Statistical analyses were performed in R (RStudio, agricolae package) to identify the most significant bacteria for mVOCs analysis. The raw data were assessed for normality using the Shapiro-Wilk test, which indicated that the data were not normally distributed ($p < 0.05$). Therefore, non-parametric methods were applied to evaluate significance. The Kruskal-Wallis's test was used to compare the groups, with a significance level set at $p < 0.05$. Post-hoc pairwise comparisons were conducted using the Dunn test, with p-values adjusted for multiple

comparisons ($p < 0.05$). Statistical analysis of mVOCs was performed by Dr. Jakub Wojtasik (Centre for Statistical Analysis, Nicolaus Copernicus University in Toruń, Poland) using a t-test to compare the mVOCs emitted by bacterial cultures against the control samples, which consisted of TSA medium only. This approach allowed for the identification of significant differences in mVOC production attributable to bacterial activity relative to the baseline medium.

5. Results

5.1. **HPMOs in *S. europaea*: impact of shoots and soil chemistry**

A comprehensive section of the results to this topic is thoroughly presented in P1, Annex I (Marangi et al., 2024).

To better understand the physicochemical and HPMOs dynamics within the study sites, we compared soil properties, chemical composition of plant shoots, and HPMOs' associations across old and young marsh soils. This section presents the observed differences in pH, salinity, soil texture, as well as key HPMOs' correlations that highlight potential interactions between soil chemistry and HPMOs' abundance.

At the old marsh site, soil pH levels were generally slightly alkaline, ranging from 7.4 to 7.8 in both bulk and rhizosphere soils, with the exception of the rhizosphere soil in plot A, which was closer to neutral (pH 6.6–7.3). In contrast, at the young marsh site, the bulk soil maintained a slightly alkaline pH (7.4–7.8), while the rhizosphere soil was moderately alkaline, with pH values ranging from 7.9 to 8.4. Electrical conductivity measurements indicated that soils at the old marsh site had varying salinity levels: the bulk soil was moderately saline ($8 < EC < 16$ mS cm^{-1}), and the rhizosphere soil was strongly saline ($EC \geq 16$), except in plot C, where it remained moderately saline. At the young marsh site, the pattern was reversed—the bulk soil was strongly saline, while the rhizosphere soil was moderately saline. Soil texture also differed between the two sites, with the old marsh characterized by loamy sand or clayey sand, and the young marsh exhibiting a finer texture of loamy silt or clayey silt.

Chemical analyses revealed no statistically significant differences in carbohydrate content across any of the sample types or locations. However, lignin content showed significant differences ($p < 0.05$) between shoots and rhizosphere soils at both sites, with the rhizosphere consistently having the highest lignin levels and shoots the lowest. Lipid content also varied significantly ($p < 0.05$) between bulk soil samples, with the young marsh site showing a higher lipid concentration than the old marsh.

Microbial correlations revealed several notable associations, primarily involving *E. coli*, *S. enterica*, and *L. monocytogenes*, but not *B. cereus*. In plant shoots, the abundance of *S. enterica* was negatively correlated with lignin content ($p = 0.0130$; $r = –0.82$), while *E. coli* abundance was positively correlated with lipid content ($p = 0.0304$; $r = 0.75$). In the bulk soil, *E. coli*

abundance was negatively associated with lignin content ($p = 0.0494$; $r = –0.81$) and also negatively correlated with soil pH ($p = 0.0306$; $r = –0.85$). Similarly, *L. monocytogenes* and *S. enterica* abundances were negatively correlated with pH ($p = 0.0013$; $r = –0.97$ and $p = 0.0283$; $r = –0.86$, respectively). In the rhizosphere soil, however, *L. monocytogenes* showed a positive correlation with pH ($p = 0.036$; $r = 0.84$). These interactions were visually summarized in a correlation network graph, illustrating both strong and weak relationships among the physicochemical and microbial variables across soil types and locations. The comparative analysis of old and young marsh soils revealed distinct physicochemical profiles and notable patterns in HPMOs' associations. While pH and salinity varied between bulk and rhizosphere soils at both sites, soil texture differences aligned with marsh age. Organic compound distributions showed consistent trends, particularly elevated lignin in rhizosphere soils. HPMOs' correlations highlighted specific associations between key HPMOs and soil chemistry—especially pH and lignin content—suggesting that HPMOs' dynamics are strongly influenced by localized soil conditions. These findings underscore the complex interplay between soil physicochemical properties and HPMOs' ecology in marsh environments.

5.2. *In vitro* pot experiment: abundance of HPMOs, plant growth parameters and HPMOs-modulated plant gene expression profiles

Plant growth parameters

In this section, we present the findings related to the growth parameters of *S. europaea* assessed during our study. These parameters include length of shoots and roots (mm), and total plant weight (g), which collectively provide insights into the overall health and productivity of the plants under investigation.

In the analysis of plant biomass (Figure 3), measured as total plant weight (g), most of the significant differences were observed in non-inoculated (Ct) plants and in *L. monocytogenes* treatments. A consistent pattern across all inoculated and non-inoculated treatments was the significantly reduced total plant weight observed at 200 mM NaCl. In the non-inoculated plants (Ct) (Figure 3a), the control group (0 mM NaCl) displayed markedly higher biomass compared to plants exposed to 50, 100, and 200 mM NaCl, with reductions of 20%, 26.5%, and 37%, respectively. Additionally, plants treated with 50 mM NaCl were 20.5% heavier than those subjected to 200 mM NaCl. For the *E. coli* treatment group (Figure 3b), significant differences were identified between plants at 200 mM NaCl and those at lower salinity levels. Specifically,

plants exposed to 200 mM NaCl exhibited reduced biomass compared to those at 0, 50, and 100 mM, with decreases of 29%, 24%, and 25.5%, respectively. In the *S. enterica* treatment group (Figure 3c), plants grown at 50 mM NaCl showed significantly greater biomass compared to those at 0, 100, and 200 mM NaCl, with increases of 26%, 28%, and 26%, respectively. Similarly, in the *L. monocytogenes* treatment group (Figure 3d), plants subjected to 50 mM NaCl exhibited significantly higher weights than those grown at both 0 and 200 mM NaCl, with increases of 18% and 46%. Additionally, plants grown at both 0 and 100 mM NaCl were significantly heavier than those exposed to the highest salinity level (200 mM), with differences of 34% and 46%, respectively. Across all treatments, 200 mM NaCl consistently led to the lowest plant biomass, confirming high salinity as a major growth inhibitor. Notably, 50 mM NaCl enhanced biomass in *S. enterica* and *L. monocytogenes* treatments, indicating that HPMOs can shape plant responses to moderate salinity. Non-inoculated controls also showed progressive biomass reduction with increasing salinity, supporting a dose-dependent stress effect.

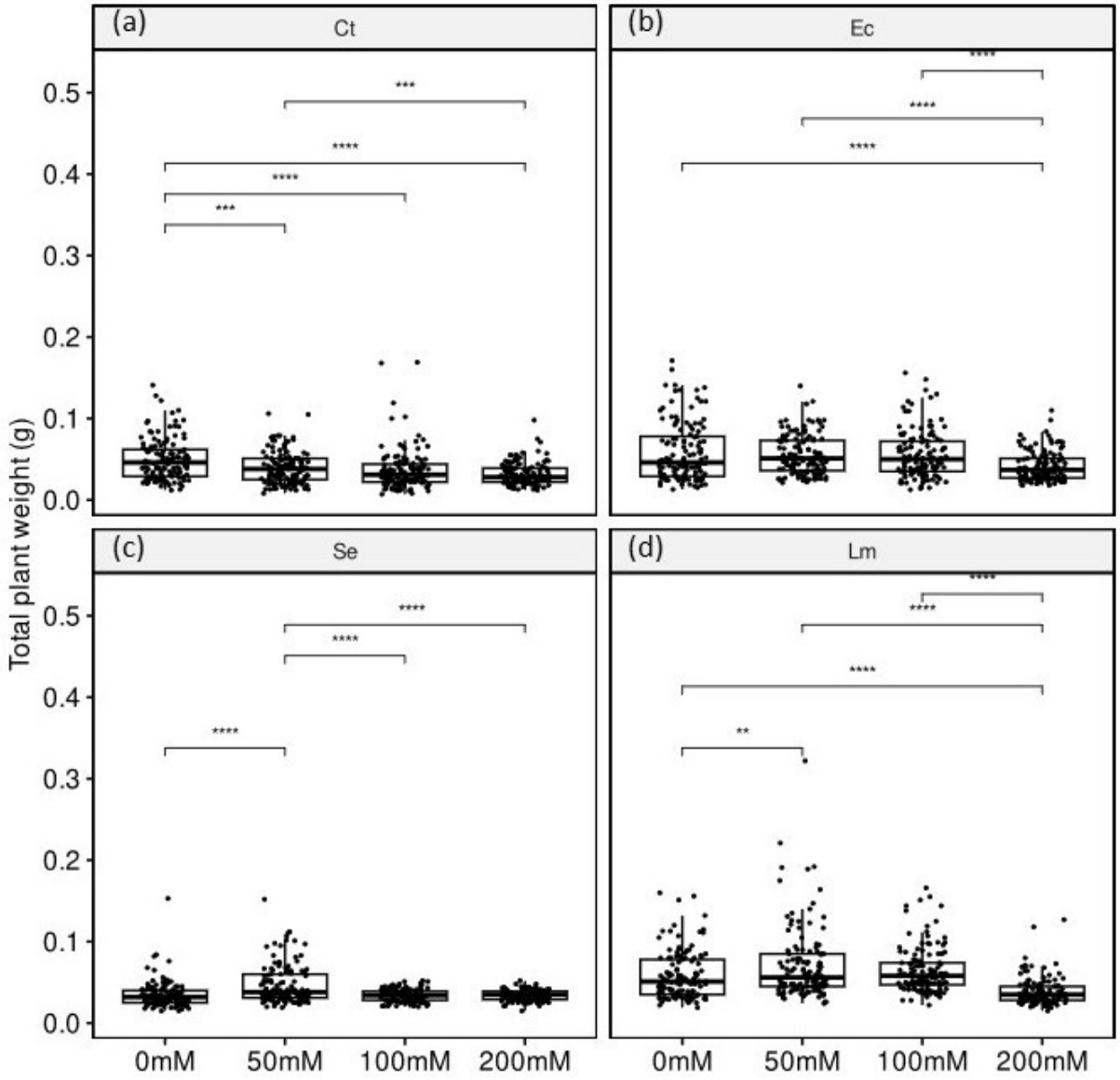

Figure 3. Total plant weight (g) measured at varying salinity levels (0, 50, 100, and 200 mM NaCl) across four different treatments: non-inoculated (Control - Ct) (a), *E. coli* (b), *S. enterica* (c), and *L. monocytogenes* (d) after 8 weeks of growth. Statistical significance was determined at $p < 0.05$ ($n = 125$).

A comparison of the total plant weight percentage for different inoculation treatments relative to non-inoculated controls (Figure 4) showed that *E. coli* and *L. monocytogenes* treatments increased total plant biomass, particularly at 50 and 100 mM NaCl concentrations. In contrast, *S. enterica* treatment led to a decrease in total plant weight at both 0 and 100 mM NaCl concentrations. This comparative analysis revealed that *E. coli* and *L. monocytogenes* treatments enhanced plant biomass at moderate salinity levels (50 and 100 mM NaCl), indicating a potential growth-promoting effect. In contrast, *S. enterica* treatment reduced

biomass at both 0 and 100 mM NaCl, suggesting a possible negative impact on plant growth under these conditions.

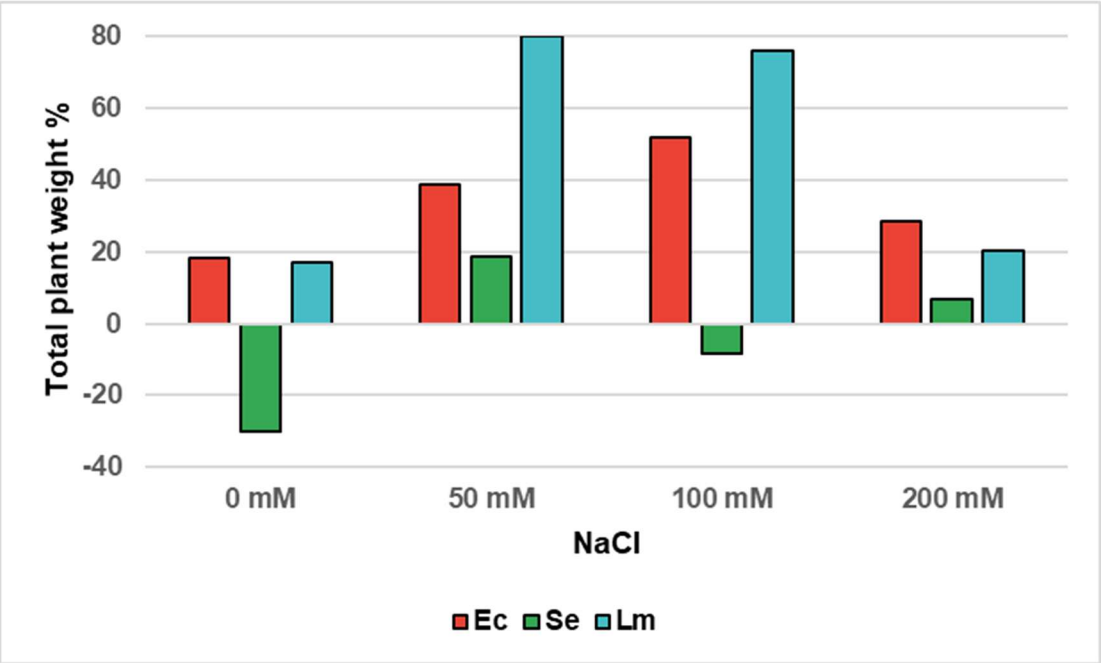

Figure 4. Comparison of the percentage total biomass of *S. europaea* for the different variants of HPMOs' inoculation relative to the control without inoculation after 8 weeks of growth. Abbreviations: Ec - *E. coli*; Se - *S. enterica*; Lm - *L. monocytogenes*.

Shoot length analysis (Figure 5) revealed a consistent trend of reduced growth in plants exposed to 200 mM NaCl, with the most pronounced statistical differences observed under *L. monocytogenes* treatment across salinity levels. In contrast, plants treated with 50 mM NaCl generally exhibited longer shoots compared to other salinity levels in both non-inoculated and inoculated groups. In the control group (non-inoculated) (Figure 5a), plants treated with 50 mM NaCl had significantly longer shoots than those treated with 0, 100, and 200 mM NaCl, with increases of 15%, 14.5%, and 9%, respectively. Similarly, under *E. coli* treatment (Figure 5b), plants in the 50 mM NaCl group exhibited greater shoot length compared to the 0 and 200mM groups by 17% and 15%. Additionally, plants treated with 100 mM NaCl showed longer shoots than those in the 0 and 200 mM groups, with increases of 20% and 15%. For *S. enterica* treatment (Figure 5c), plants exposed to 50 mM NaCl had longer shoots than those in the 0, 100, and 200 mM variants, with differences of 12%, 15%, and 18%, respectively. Under *L. monocytogenes* treatment (Figure 5d), plants at 0 mM NaCl exhibited shorter shoots than those at 50 and 100 mM by margins of 12% and 9%, but they were still longer than those at 200 mM

by 8.5%. Furthermore, plants treated with both 50 mM and 100 mM NaCl consistently displayed greater shoot length compared to those at 200 mM NaCl, with increases of 20% and 17%. Shoot length was significantly influenced by both salinity levels and microbial treatments. Plants exposed to moderate salinity (50 mM NaCl) consistently showed the greatest shoot growth across all inoculation variants, including non-inoculated controls and treatments with *E. coli*, *S. enterica*, and *L. monocytogenes*. In contrast, high salinity (200 mM NaCl) markedly reduced shoot length, with the most pronounced growth inhibition observed under *L. monocytogenes* treatment. These results highlight that moderate salinity conditions favour plant growth regardless of microbial exposure, while high salinity combined with certain HPMOs can exacerbate growth reduction.

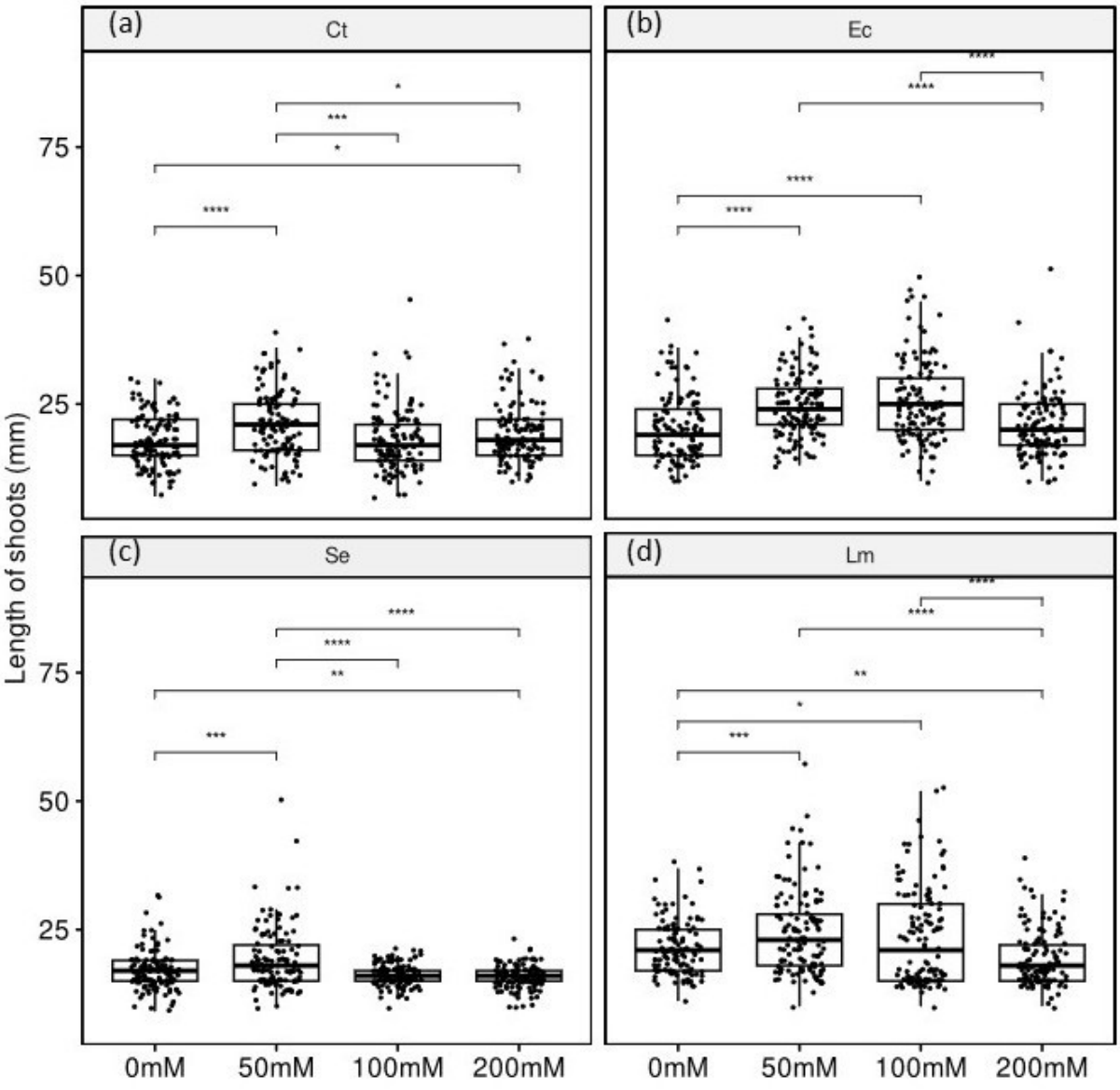

Figure 5. Length of shoots (mm) measured at varying salinity levels (0, 50, 100, and 200 mM NaCl) across four different treatments: non-inoculated (Control) (a), *E. coli* (b), *S. enterica* (c), and *L. monocytogenes* (d) after 8 weeks of growth. Statistical significance was determined at $p < 0.05$ ($n = 125$).

The length of roots (Figure 6), similar to total plant weight (Figure 3) and shoot length (Figure 5), was significantly reduced in the majority of treatments at 200 mM NaCl. The non-inoculated control plants exhibited the highest number of statistical differences across the various salinity levels, mirroring the patterns observed for total plant weight. In the control group (non-inoculated) (Figure 6a), plants treated with 0 mM NaCl had root lengths that were 14% and 27% longer than those treated with 50 and 200 mM NaCl, respectively. Additionally, roots in the 50 mM variant were longer than those in the 200 mM group by 15%. Notably, plants in the 100 mM variant showed root lengths that exceeded those in both the 50 and 200 mM groups by 19% and 32%, respectively. For the *E. coli* treatment (Figure 6b), significant differences were noted between the 0 and 50 mM groups, with roots in the 0 mM group being 7% longer. Moreover, plants in the 100 and 200 mM groups had longer roots than those in the 50 mM group by 13% and 12%, respectively. In contrast, root length under *S. enterica* treatment (Figure 6c) did not show significant variation across different salinity levels; however, plants in the 0 mM group had roots that were longer than those in the 200 mM group by 6%. Regarding *L. monocytogenes* treatment (Figure 6d), plants subjected to the 200 mM condition displayed shorter roots compared to those in the 0, 50, and 100 mM groups, with reductions of 17%, 20%, and 19%, respectively. Root length was generally reduced at the highest salinity level (200 mM NaCl) across most treatments, paralleling trends seen in shoot length and total plant weight. Non-inoculated plants showed the greatest sensitivity to salinity changes, with significant root length differences between all salinity variants. In contrast, *E. coli*-treated plants displayed inconsistent patterns, with shorter roots at 50 mM but relatively longer roots at 100 and 200 mM compared to 50 mM. *S. enterica* treatment had minimal influence on root length across salinity levels, showing only a slight decrease at 200 mM. Meanwhile, *L. monocytogenes* treatment led to noticeably shorter roots at 200 mM, with reductions of up to 20% compared to lower salinity levels. These findings suggest that while high salinity broadly suppresses root development, HPMOs' effects on root length vary depending on the species and salt concentration. Root length responses to salinity varied by treatment: non-inoculated and *L. monocytogenes*-treated plants showed clear reductions at high salinity, *E. coli* showed mixed effects, and *S. enterica* had minimal influence across salinity levels.

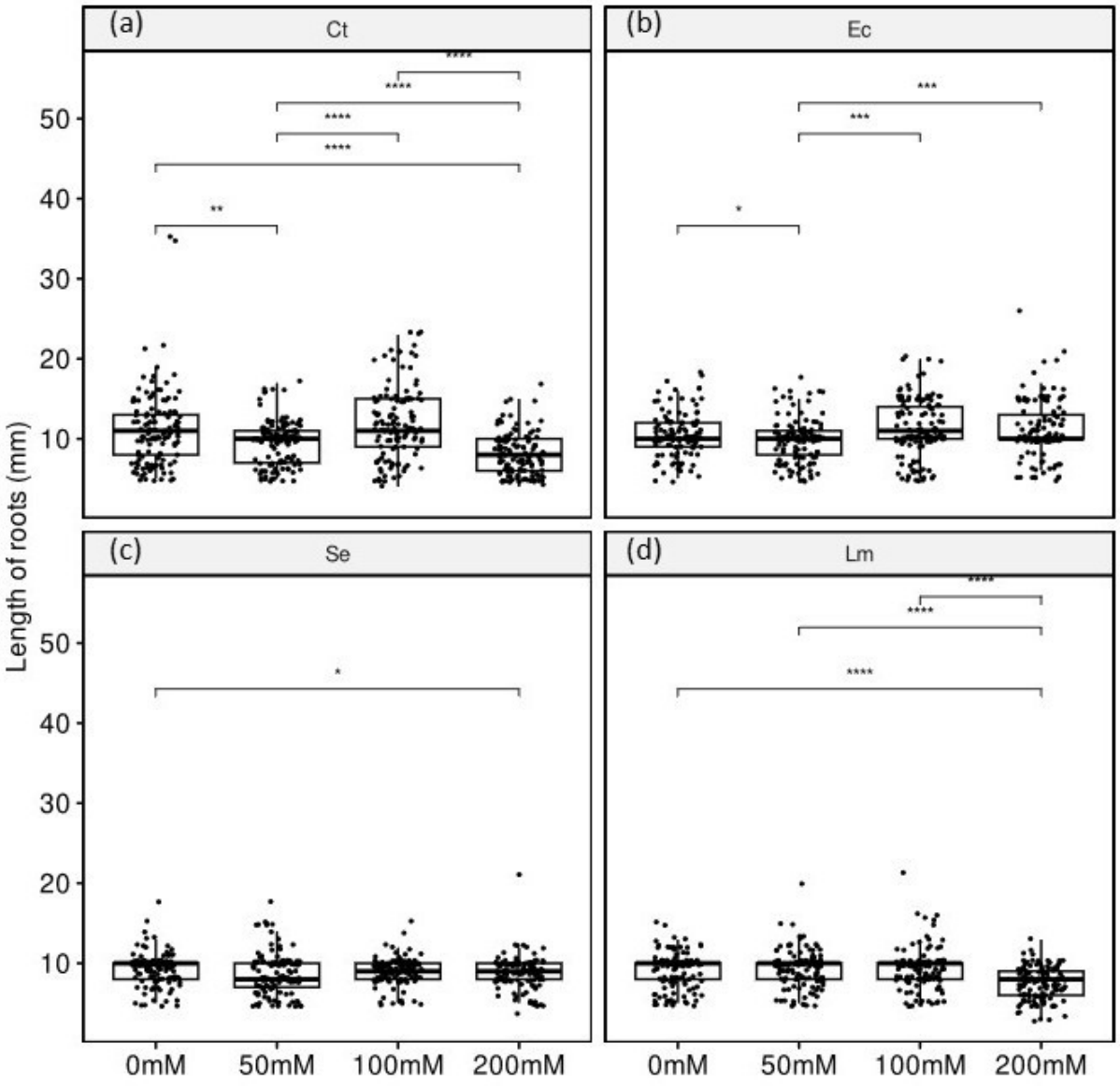

Figure 6. Length of roots (mm) of *S. europaea* measured at varying salinity levels (0, 50, 100, and 200 mM NaCl) across four different treatments: non-inoculated (Control) (a), *E. coli* (b), *S. enterica* (c), and *L. monocytogenes* (d) after 8 weeks of growth. Statistical significance was determined at $p < 0.05$ (n = 125).

Abundance and detection of total bacteria in shoots and roots of *S. europaea*

In this section, we present a comprehensive analysis of total bacterial counts in both *S. europaea* shoots and roots, obtained from two distinct methodologies: traditional culture on TSA medium (log CFU g^{-1}) and qPCR (log bacterial 16SrRNA gene copy ng^{-1}). By employing both techniques, we aim to provide a robust comparison of bacterial populations, highlighting the strengths and limitations of each method. The findings will clarify how effective TSA is in

growing viable bacteria and how sensitive qPCR is in detecting bacterial DNA. This will provide valuable insights into microbial quantification for our study.

Overall, we observed more significant statistical differences in total bacterial counts measured *via* qPCR compared to those on TSA medium. While bacterial abundance on TSA was consistent across shoots and roots, qPCR results showed a notably higher bacterial presence in shoots than in roots.

In the bacterial count analysis on TSA medium from shoot samples (Figure 7), statistical differences were primarily observed under the *E. coli* treatment. The control treatment (non-inoculated) (Figure 7a) showed consistent bacterial counts across salinity levels, except for plants subjected to 100 mM NaCl, which had a 25% higher bacterial count compared to those at 50 mM NaCl. For the *E. coli* treatment (Figure 7b), plants at 0 mM NaCl exhibited significantly higher bacterial counts than those at 50, 100, and 200 mM NaCl, with increases of 5% for each salinity level. In contrast, in the *S. enterica* treatment (Figure 7c), plants exposed to 200 mM NaCl had a 10% higher bacterial count than those at 50 mM NaCl. No statistically significant differences were observed in the *L. monocytogenes* treatment (Figure 7d) across the different salinity groups. Thus, in shoots, bacterial count analysis on TSA medium revealed significant differences primarily under *E. coli* treatment, where bacterial counts were highest at 0 mM NaCl, while *S. enterica* treatment showed increased counts at 200 mM NaCl and a reduction at 50 mM NaCl, and *L. monocytogenes* exhibited no significant variations across salinity levels. Bacterial counts in shoot samples varied primarily under the *E. coli* treatment, with the highest counts at 0 mM NaCl and reductions at higher salinities. *S. enterica* showed a modest increase in bacterial counts at 200 mM, while *L. monocytogenes* exhibited no significant changes across salinity levels. The control group remained largely stable, except for a slight increase at 100 mM NaCl.

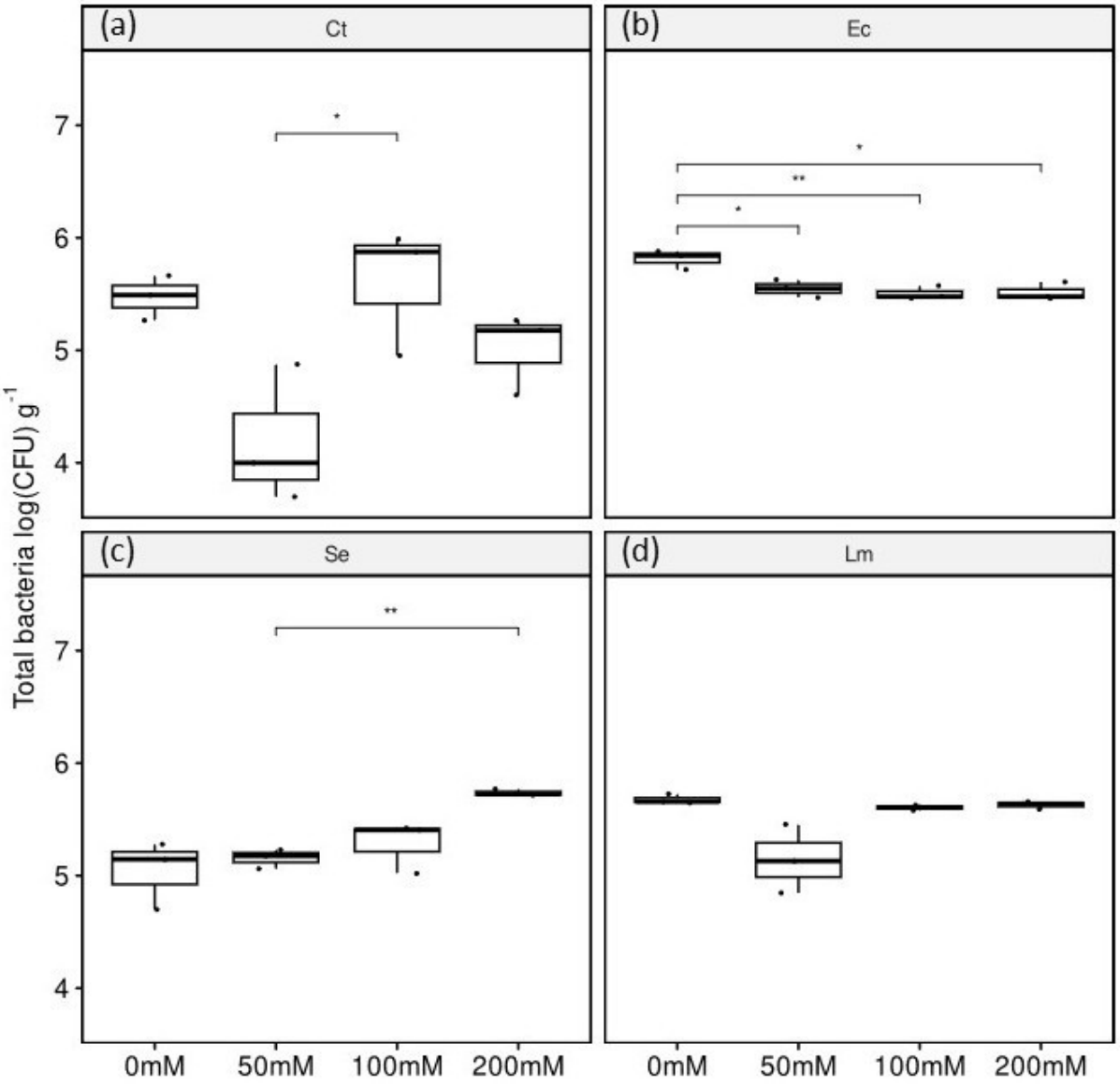

Figure 7. Total bacteria count on TSA medium measured in shoots of *S. europaea* at varying salinity levels (0, 50, 100, and 200 mM NaCl) across four different treatments: non-inoculated (Control - Ct) (a), *E. coli* (b), *S. enterica* (c), and *L. monocytogenes* (d) after 8 weeks of growth. Statistical significance was determined at $p < 0.05$ ($n = 3$).

In the analysis of total bacterial counts on TSA medium from root samples (Figure 8), a consistent trend was observed at 200 mM NaCl, where roots exhibited higher bacterial counts. In the control treatment (non-inoculated) (Figure 8a), plants at 50 mM NaCl had lower bacterial counts than those at 0, 100, and 200 mM NaCl, with reductions of 7%, 7%, and 8%, respectively. For the *E. coli* treatment (Figure 8b), plants exposed to 200 mM NaCl had significantly higher bacterial counts than those at 0, 50, and 100 mM NaCl, with increases of 7%, 9%, and 7%, respectively. In the *S. enterica* treatment (Figure 8c), plants at 50 mM NaCl

had lower bacterial counts than those at 0, 100, and 200 mM NaCl, with reductions of 13%, 14%, and 17%, respectively. No significant differences in bacterial counts were found in the *L. monocytogenes* treatment (Figure 8d) across the salinity groups. Total bacterial count analysis from root samples revealed consistently higher counts at 200 mM NaCl and lower at 50 mM NaCl, with the most significant differences observed in non-inoculated, *E. coli*-, and *S. enterica* – treated plants, while *L. monocytogenes* treatment showed no significant variations across salinity levels.

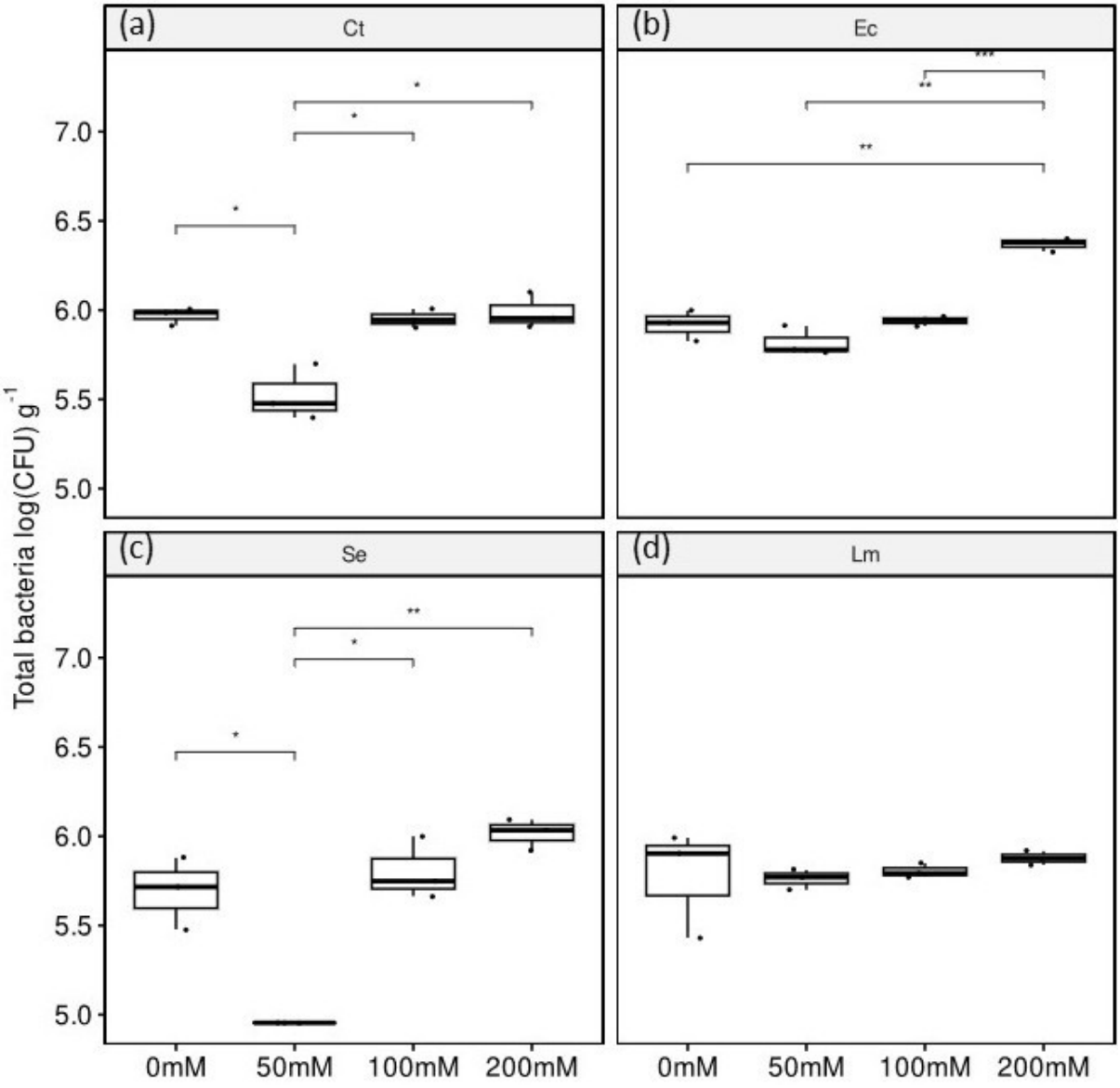

Figure 8. Total bacteria count on TSA medium measured in roots of *S. europaea* at varying salinity levels (0, 50, 100, and 200 mM NaCl) across four different treatments: non-inoculated (Control) (a), *E. coli* (b), *S. enterica* (c), and *L. monocytogenes* (d) after 8 weeks of growth. Statistical significance was determined at $p < 0.05$ ($n = 3$).

qPCR analysis of total bacterial counts in shoots (Figure 9) revealed more significant differences in the control (non-inoculated) treatment across salinity levels than in inoculated treatments. In the control treatment (non-inoculated) (Figure 9a), plants at 0 mM NaCl had lower bacterial counts than those at 50, 100, and 200 mM NaCl, with reductions of 38%, 21%, and 21%, respectively. Additionally, plants at 50 mM NaCl had higher bacterial counts than those at 100 and 200 mM NaCl, with increases of 22% and 21%. For the *E. coli* treatment (Figure 9b), plants at 50 mM NaCl had greater bacterial counts than those at 0, 100, and 200 mM NaCl, with increases of 28%, 21%, and 21%, respectively. In the *S. enterica* treatment (Figure 9c), plants at 0 mM NaCl had fewer bacteria than those at 50 and 100 mM NaCl, with reductions of 18%. Conversely, plants at 200 mM NaCl had fewer bacteria than those at both 50 and 100 mM NaCl, with reductions of 22%. For the *L. monocytogenes* treatment (Figure 9d), plants at 50 mM NaCl exhibited significantly lower bacterial counts compared to those at 0 and 100 mM NaCl, with reductions of 32% and 35%, respectively. The qPCR analysis of total bacterial counts in shoots showed that the control (non-inoculated) plants experienced the most pronounced changes across salinity levels, with bacterial counts increasing at 50, 100, and 200 mM NaCl compared to 0 mM. In contrast, *E. coli*-inoculated plants had the highest bacterial counts at 50 mM NaCl, while *S. enterica* counts peaked at 50 and 100 mM NaCl but declined at 0 and 200 mM. *L. monocytogenes*-inoculated plants showed the lowest bacterial counts at 50 mM NaCl, with higher counts at 0 and 100 mM NaCl. Overall, salinity influenced the total bacteria abundance differently depending on the inoculation, with the control showing the greatest variability.

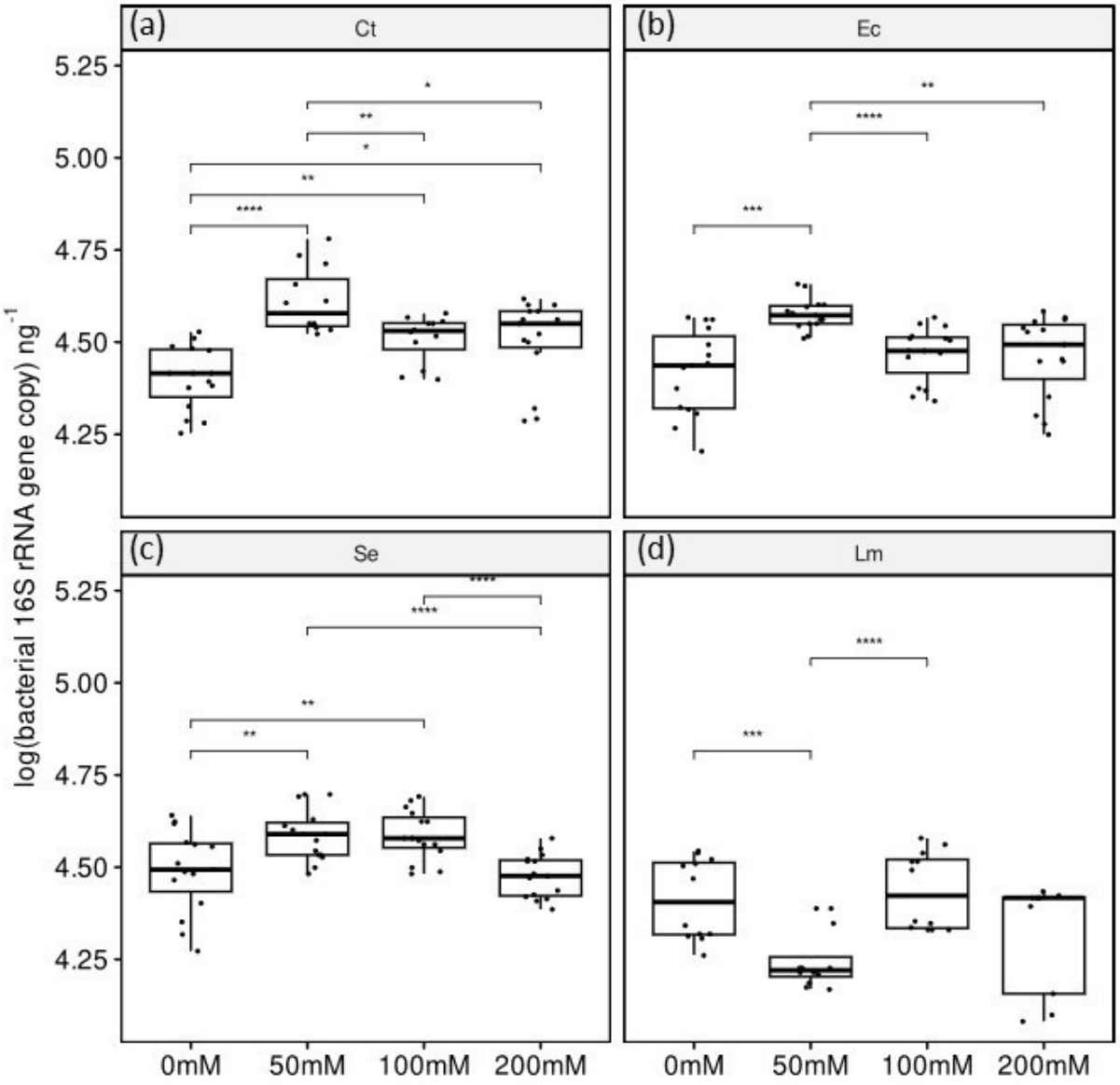

Figure 9. Total bacteria count (16S rRNA) on qPCR measured in shoots of *S. europaea* at varying salinity levels (0, 50, 100, and 200 mM NaCl) across four different treatments: non-inoculated (Control - Ct) (a), *E. coli* (b), *S. enterica* (c), and *L. monocytogenes* (d) after 8 weeks of growth. Statistical significance was determined at $p < 0.05$ ($n = 15$).

Regarding the qPCR analysis of total bacteria in roots (Figure 10), in the control treatment (non-inoculated) (Figure 10a), no statistically significant differences in bacterial counts were observed across the various salinity levels. In the *E. coli* treatment (Figure 10b), plants at 50 mM NaCl had higher bacterial counts than those at 0, 100, and 200 mM NaCl, with increases of 40%, 28%, and 41%, respectively. Similarly, in the *S. enterica* treatment (Figure 10c), plants at 50 mM NaCl had greater bacterial counts than those at 0 and 200 mM NaCl, with increases of 34% and 33%, respectively. In the *L. monocytogenes* treatment (Figure 10d), plants at 0 mM

NaCl exhibited lower bacterial counts than those at 50 and 200 mM NaCl, with reductions of 45% and 50%, respectively. Plants at 100 mM NaCl also had lower bacterial counts than those at 50 and 200 mM NaCl, with reductions of 23% and 30%. Root bacterial counts (qPCR) were influenced by both inoculation type and salinity. *E. coli* and *S. enterica* treatments showed peak colonization at 50 mM NaCl, while *L. monocytogenes* treatment had higher counts at 50 and 200 mM NaCl. Non-inoculated plants showed no significant salinity effects. This highlights species-specific responses to salinity in root colonization.

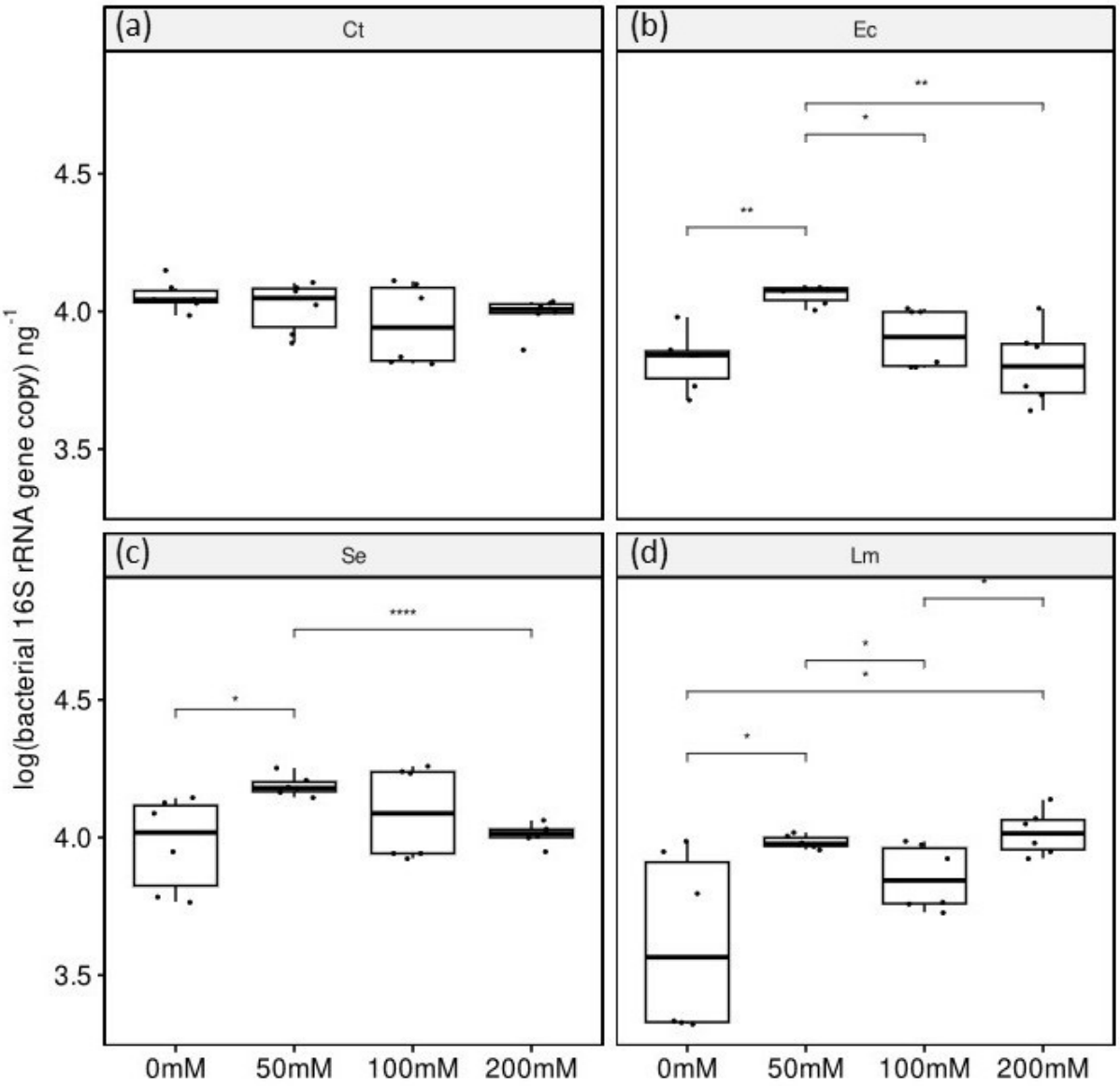

Figure 10. Total bacteria count (16S rRNA) on qPCR measured in roots of *S. europaea* at varying salinity levels (0, 50, 100, and 200 mM NaCl) across four different treatments: non-inoculated (control - Ct) (a), *E. coli* (b), *S. enterica* (c), and *L. monocytogenes* (d) after 8 weeks of growth. Statistical significance was determined at $p < 0.05$ ($n = 6$).

Abundance and detection of HPMOs in shoots and roots of *S. europaea*

In this study, we assessed the abundance of HPMOs in selective media (Figure 11) and their quantification in the shoots and roots of *S. europaea* using qPCR (Appendix III, Figures 1-6, pages 117-122). Our results highlight variations in HPMOs populations between plant tissues, providing insight into HPMOs dynamics in different levels of salinity. In contrast to *L. monocytogenes*, the abundance of *E. coli* and *S. enterica* showed a similar trend to the qPCR detection results. All qPCR detections of HPMOs were below the limit of detection (1.28 x 10^3); however, these values are still reported for comparison with non-inoculated plants (Ct) (Appendix III, Figures 1-6, pages 117-122). Our findings from both selective media and qPCR detection consistently showed a greater abundance of HPMOs in the roots rather than in the shoots. In selective media, the abundance of HPMOs in the shoots (Figure 11a) showed more notable differences in plants treated with *L. monocytogenes*. However, no consistent patterns were observed when comparing all three HPMOs across different salinity levels. In *E. coli*-treated plants, there were no significant differences, with the pathogen only detected at 50 mM NaCl. For *L. monocytogenes*-treated plants, the highest colonization occurred at 100 mM NaCl, where bacterial levels were 16%, 25%, and 29% higher compared to 0, 50, and 200 mM NaCl, respectively. In *S. enterica*-treated plants, no colonization was observed at 50 mM NaCl, making these plants significantly different from those grown at 0, 100, and 200 mM NaCl. In examining the abundance of HPMOs in the roots (Figure 11b), we noted a consistent trend among plants treated with *E. coli*, similar to our findings in the shoots. However, unlike the shoots, weobserved more significant differences in plants treated with *S. enterica*. Specifically, *S. enterica* was not detected in the roots of plants at 200 mM NaCl, resulting in significant differences compared to the other salinity levels (0, 50, and 100 mM NaCl). For *L. monocytogenes*-treated plants, the lowest abundance was recorded at 50 mM NaCl, which was 15% lower than the levels observed at both 0 and 100 mM NaCl.

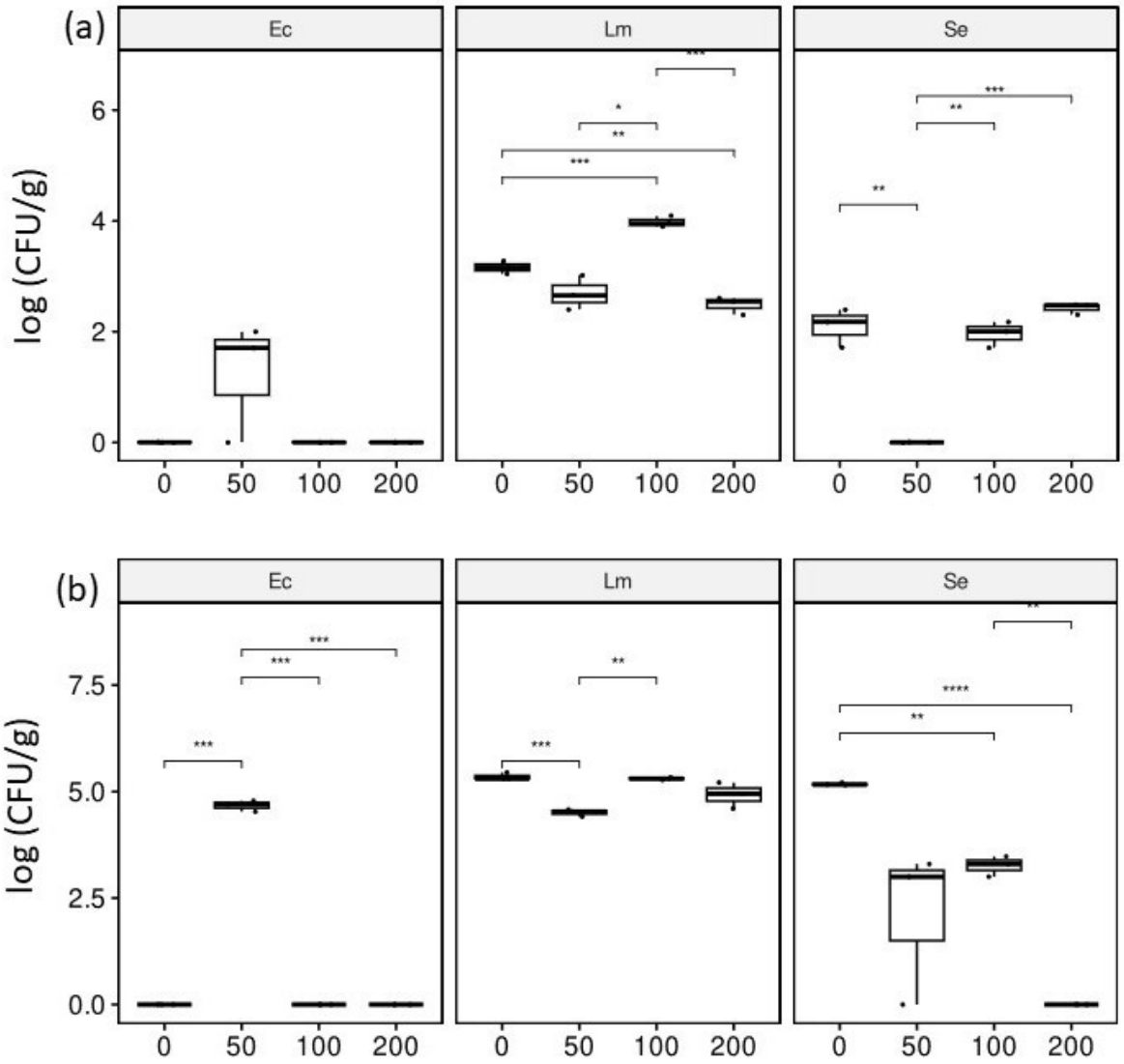

Figure 11. The abundance of *E. coli* (Ec), *L. monocytogenes* (Lm), and *S. enterica* (Se) in selective media (log CFU g^{-1}) measured in the shoots (a) and roots (b) of *S. europaea* at varying salinity levels: 0, 50, 100, and 200 mM NaCl after 8 weeks of growth. Statistical significance was assessed at $p < 0.05$ ($n = 3$).

In our analysis of HPMOs using qPCR, we found no evidence of detection in the *E. coli* and *L. monocytogenes* treated plants (Appendix III, Figures 1-4, pages 117-120). When detections did occur, they were not significantly different from those in the non-inoculated control plants. It is noteworthy that while amplification was observed in all samples, the melting profiles differed from the bacterial control, leading us to classify these as non-specific and treat them as negative. The qPCR results indicated that *S. enterica* was detected in the shoots and roots (Appendix III, Figures 5,6, pages 121,122), with higher concentrations found in the roots compared to the shoots. Specifically, in the shoots, *S. enterica*-treated plants (Appendix III, Figure 5, page 121)

exhibited increased pathogen detection at 50, 100, and 200 mM NaCl, with detection rates of 100%, 99%, and 100%, respectively, compared to the non-inoculated control. In terms of root samples (Annex III, Figure 6, page 122), *S. enterica*-treated plants consistently showed a higher presence of pathogens than the non-inoculated controls across all saline treatments (0, 50, 100, and 200 mM NaCl), with detection rates of 100%, 88%, 100%, and 97%, respectively.

Transcriptomic analyses

Distance-based redundancy analysis (dbRDA) was performed to assess the influence of inoculation treatment and salinity levels on *S. europaea* transcriptomic responses in shoots (Figure 12). Separate ordination plots were generated for each inoculation treatment: non-inoculated (Control), *E. coli*-inoculated, *S. enterica*-inoculated, and *L. monocytogenes*-inoculated across four salinity levels (0, 50, 100, and 200 mM NaCl). The significance of the observed patterns was statistically evaluated using permutational multivariate analysis of variance (PERMANOVA), with corresponding F-statistics and p-values indicating the effects of salinity within each inoculation condition. Additionally, homogeneity of multivariate dispersions (beta dispersion) was tested to determine whether observed differences were driven by shifts in dispersion rather than location within the ordination space.

dbRDA analysis revealed that the impact of salinity on the global transcriptomic profiles of *S. europaea* shoots varied depending on the inoculation treatment. In the non-inoculated (Ct) plants (Figure 12a), salinity had a significant effect on gene expression patterns (PERMANOVA: $F = 2.04$, $p = 0.003$), while multivariate dispersion remained unchanged (Betadisper: $F = 0.18$, $p = 0.908$), indicating that observed transcriptomic shifts were driven by differential gene expression rather than changes in dispersion. A similar trend was observed in *E. coli*-treated plants (Figure 12b), where salinity significantly influenced transcriptomic profiles (PERMANOVA: $F = 1.68$, $p = 0.017$), yet no significant differences in dispersion were detected (Betadisper: $F = 0.96$, $p = 0.443$). In contrast, no significant effect of salinity on transcriptomic profiles was detected in *S. enterica*-treated plants (PERMANOVA: $F = 1.18$, $p = 0.258$) (Figure 12c) or *L. monocytogenes*-treated plants (Figure 12d) (PERMANOVA: $F = 1.27$, $p = 0.163$). Likewise, multivariate dispersion did not differ across salinity levels in either *S. enterica* (Betadisper: $F = 2.05$, $p = 0.165$) or *L. monocytogenes* (Betadisper: $F = 0.34$, $p = 0.799$) treatments, suggesting that salinity did not induce major shifts in gene expression or dispersion in these cases.

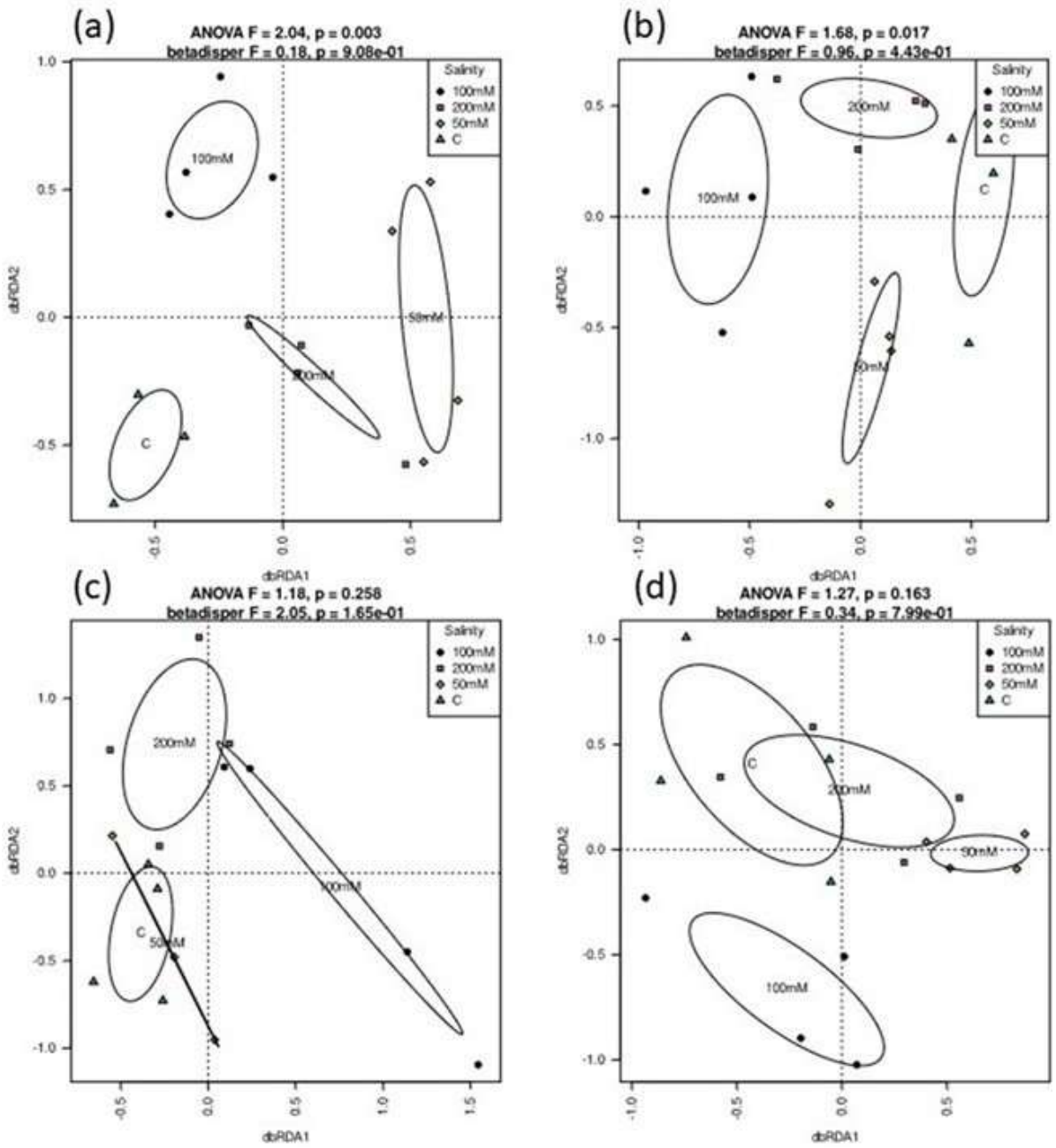

Figure 12. Distance-based redundancy analysis (dbRDA) visualizing the impact of salinity (0 = C, 50, 100, and 200 mM NaCl) on *S. europaea* shoots subjected to different inoculation treatments: (a) non-inoculated control, (b) *E. coli* inoculated, (c) *S. enterica* inoculated, and (d) *L. monocytogenes* inoculated plants.

Circos plots were utilized to illustrate the number of genes that fit into each category for each variant and treatment. These plots were based on the results of gene ontology enrichment analyses. Differential gene expression related to biological processes showed distinct associations with saline variants across bacterial treatments. In *S. enterica* treatment, all saline variants were associated with differential gene expression. For *L. monocytogenes*, associations

were observed with 0, 100, and 200 mM NaCl concentrations. In contrast, *E. coli* treatment showed a limited association with 0, 50, and 100 mM NaCl concentrations. These findings align with the quantification of HPMOs using both selective media and qPCR. Notably, the majority of genes were associated with plants treated with *S. enterica* and *L. monocytogenes* at a concentration of 100 mM NaCl. In these treatments, genes were linked to distinct biological processes (Figure 13), notably responses to stress, nitrogen and organonitrogen compound metabolism, and responses to external biotic stimuli. These biological processes were predominantly localized (Figure 14) in the cytoplasm, plastid, and membrane, with fewer occurrences in the mitochondrion and nucleus.

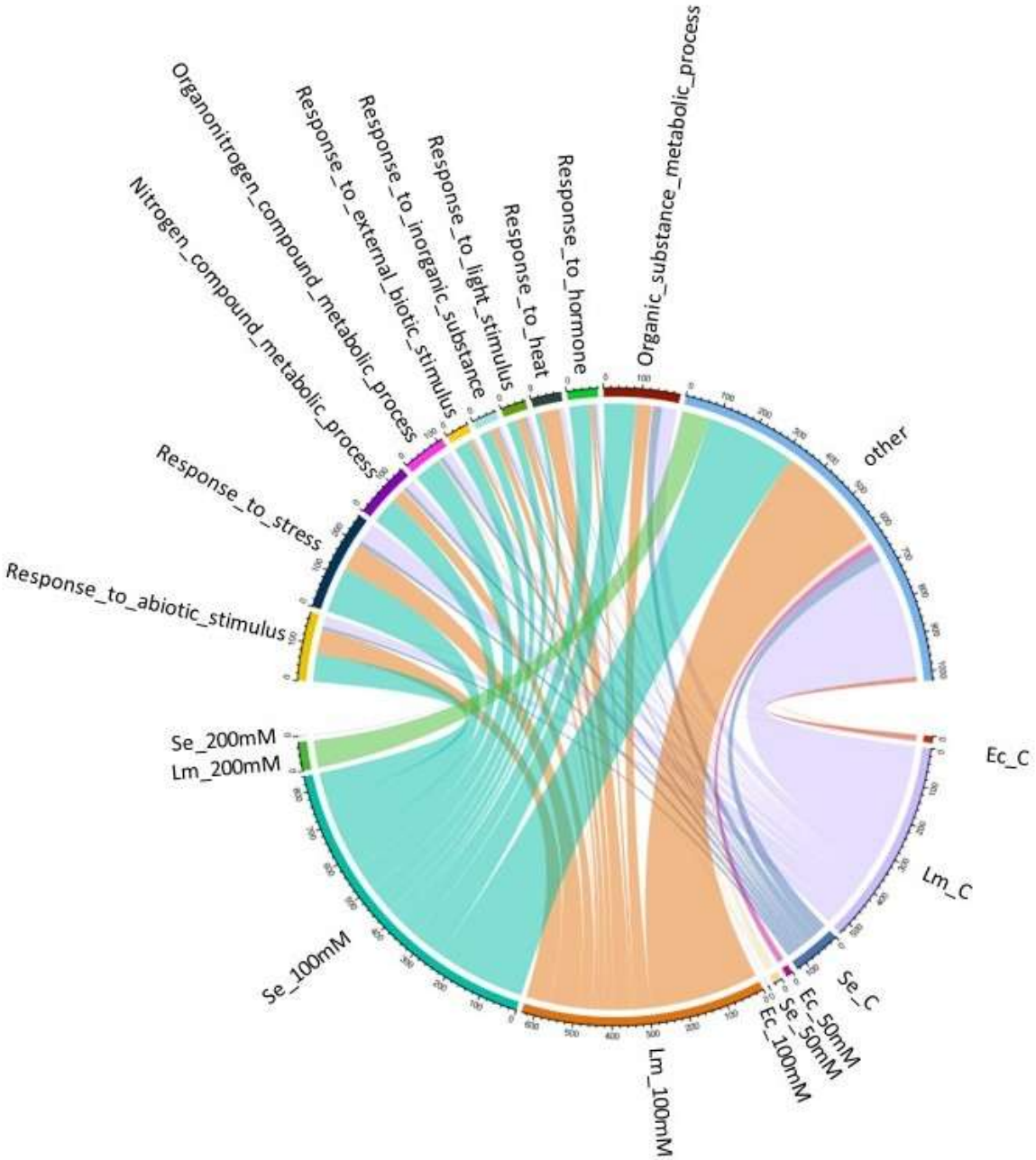

Figure 13. Circos plots illustrating biological process categories across inoculation treatments of *S. europaea* with *E. coli* (Ec), *S. enterica* (Se), and *L. monocytogenes* (Lm) under four salinity levels (0, 50, 100, and 200 mM NaCl).

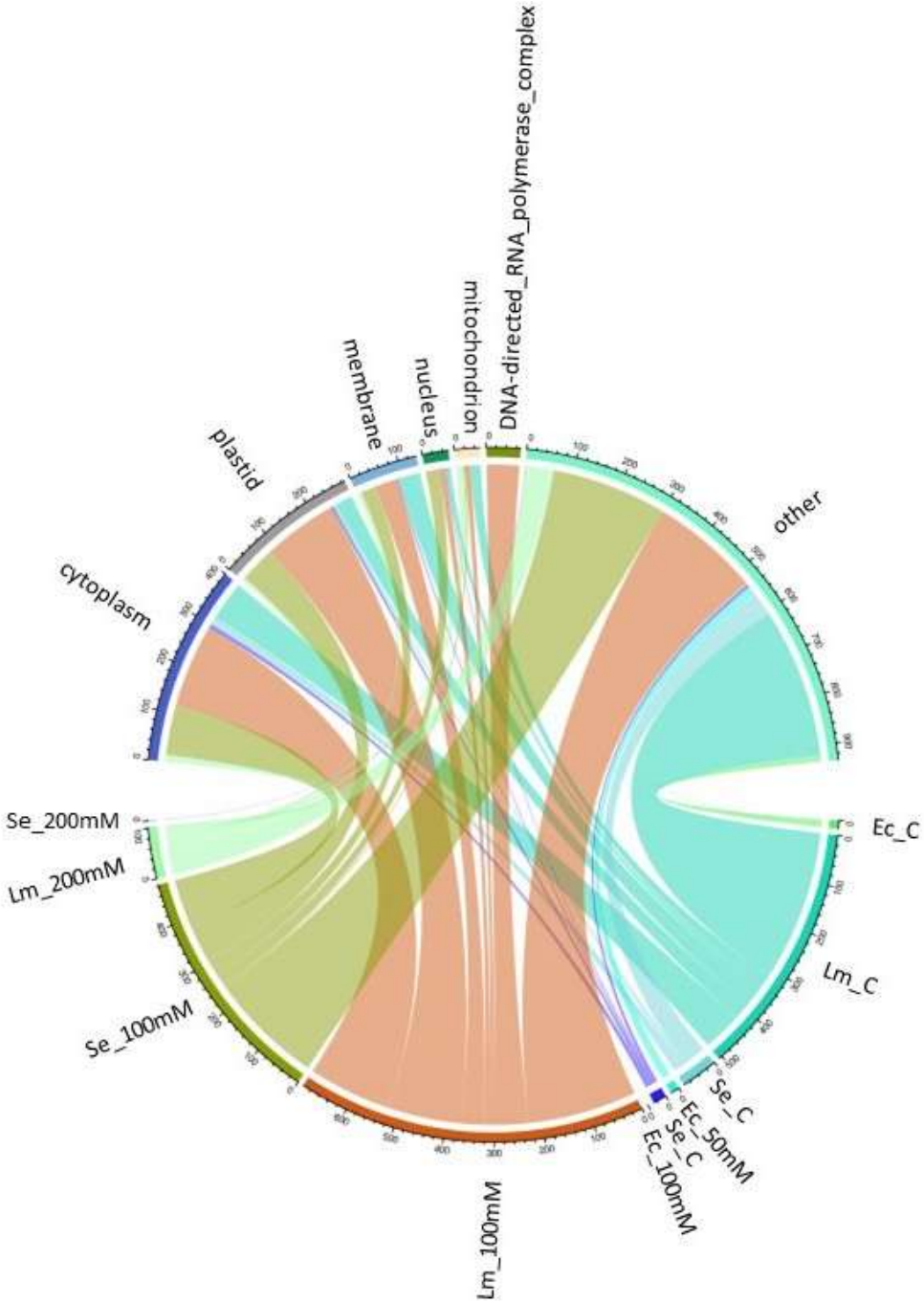

Figure 14. Circos plots illustrating cellular compartment categories across inoculation treatments of *S. europaea* with *E. coli* (Ec), *S. enterica* (Se), and *L. monocytogenes* (Lm) under four salinity levels (0, 50, 100, and 200 mM NaCl).

Consistent with the absence of *E. coli* detection in shoots and roots using both selective media and qPCR, transcriptomic analyses showed no significant gene expression changes associated with *E. coli* treatment across all saline variants.

In *S. europaea* shoots treated with *S. enterica*, we observed significant changes in gene expression across different NaCl concentrations. At 0, 50, and 100 mM NaCl, the gene encoding phosphoethanolamine N-methyltransferase was upregulated in non-inoculated control plants but downregulated in those inoculated with *S. enterica*, as indicated by fold change values. The biosynthesis of choline and phosphatidylcholine was associated with transcripts related to this enzyme. At 0 mM NaCl, the biosynthesis of pentacyclic triterpenoids was downregulated in *S. enterica*-treated plants compared to non-inoculated controls. In the same treatment and salinity variant, non-inoculated plants showed upregulation of xyloglucan endohydrolysis (XEH) and/or endotransglycosylation (XET) compared to *S. enterica*-treated plants. In non-inoculated plants at 0 mM NaCl, there was an upregulation of hydroquinone: oxygen oxidoreductase activity, which is involved in the lignin catabolic process, compared to *S. enterica*-treated plants. Finally, at 100 mM NaCl, plants treated with *S. enterica* exhibited upregulation of cellular responses to extracellular stimuli, which helps protect cells from the toxic effects of hydrogen peroxide.

At 0 mM NaCl, the biosynthesis of pentacyclic triterpenoids was downregulated in *L. monocytogenes*-treated plants compared to non-inoculated controls, a pattern similar to that observed with *S. enterica* treatment. In this condition, the gene encoding phosphoethanolamine N-methyltransferase, which is involved in the biosynthesis of choline and phosphatidylcholine, was upregulated in non-inoculated control plants but downregulated in those inoculated with *L. monocytogenes*. Additionally, under both 0 mM and 100 mM NaCl conditions, non-inoculated plants showed upregulation of XEH and/or XET compared to inoculated-treated plants. At 0 mM NaCl, *L. monocytogenes* treatment resulted in downregulation of the class III peroxidase subfamily, which is linked to plant-type cell wall organization. Conversely, in the same salinity condition, inoculated plants exhibited upregulation of cellular responses to extracellular stimuli, potentially helping protect cells from the toxic effects of hydrogen peroxide.

5.3. **Selection of *S. europaea* endophytes and their mVOCs identification**

Taxonomic identification of unknown bacterial isolates

A total of twelve bacterial strains were identified based on 16S rRNA gene sequence analysis (Table 3). The isolates were assigned to three major bacterial classes: Bacilli, Actinomycetes, and Gammaproteobacteria. Among the Bacilli, four strains were identified: *B. pseudomycoides* CSE4, *Paenibacillus* sp. ISR16, *B. mycoides* CSE27, and *B. zhangzhouensis* CSE23. The Actinomycetes class included *Streptomyces* sp. CSR7, CSR6, and CSE3, as well as *S. mediolani* CSR34 and CSR30, *S. zaomyceticus* ISR17, and *S. peucetius* CSR27. A single strain, *Stutzerimonas stutzeri* ISE9, was classified within the Gammaproteobacteria.

Table 3. Identified bacterial strains isolated as determined by 16S rDNA nucleotide sequencing.

No of strain	**Strain**	**GenBank Accession number**	**Blast NCBI**	**Coverage**	**Percentage of identity**	**bp**
1	CSE4 *Bacillus pseudomycoides*	PV642498	*Bacillus pseudomycoides* NR_113991	99%	1413/1420 (99.51%)	1423
2	CSR7 *Streptomyces* sp.	PV642499	*Streptomyces cyaneofuscatus* NR_041226	99%	1379/1396 (98.78%)	1398
3	ISE9 *Stutzerimonas stutzeri*	PV642500	*Stutzerimonas stutzeri* NR_118798	99%	1414/1414 (100%)	1417
4	CSR6 *Streptomyces sp.*	PV642501	*Streptomyces cyaneofuscatus* NR_041226	100%	1386/1402 (98.86%)	1402
5	ISR16 *Paenibacillus* sp.	PV642502	*Paenibacillus alkaliterrae* NR_043293	97%	1353/1376 (98.33%)	1409

6	CSE27 *Bacillus mycoides*	PV642503	*Bacillus mycoides* NR_036880	100%	1423/1423 (100%)	1423
7	CSE3 *Streptomyces sp.*	PV642504	*Streptomyces cyaneofuscatus* NR_041226	99%	1379/1396 (98.78%)	1398
8	CSE23 *Bacillus zhangzhouensis*	PV642505	*Bacillus zhangzhouensis* NR_148786	100%	1420/1422 (99.93%)	1421
9	CSR34 *Streptomyces mediolani*	PV642506	*Streptomyces mediolani* NR_112465.1	100%	1390/1391 (99.93%)	1391
10	ISR17 *Streptomyces zaomyceticus*	PV642507	*Streptomyces zaomyceticus* NR_112376	99%	1399/1401 (99.86%)	1402
11	CSR27 *Streptomyces peucetius*	PV642508	*Streptomyces peucetius* NR_112574	100%	1385/1393 (99.43%)	1393
12	CSR30 *Streptomyces mediolani*	PV642509	*Streptomyces mediolani* NR_112465	100%	1399/1402 (99.79%)	1400

Screening of endophytic and rhizosphere bacteria highlights selective inhibition of HPMOs

The bipartite *in vitro* assay revealed distinct antagonistic profiles among bacterial classes (Figure 15). Isolates belonging to the Bacilli and Actinomycetes classes exhibited predominant inhibitory activity against *L. monocytogenes*, with several strains also inhibiting *E. coli*. Similarly, members of the Gammaproteobacteria class demonstrated inhibition of *L.*

monocytogenes and *E. coli*, with a few also active against *S. enterica*. Notably, the sole isolate representing Alphaproteobacteria displayed broad-spectrum inhibitory effects against all three HPMOs: *E. coli*, *S. enterica*, and *L. monocytogenes*. A general trend emerged in which nearly all tested endophytic and rhizosphere bacteria were effective in suppressing *L. monocytogenes*, but showed limited ability to inhibit *S. enterica*. Interestingly, despite these antagonistic interactions, some isolates from Bacilli, Gammaproteobacteria, and Actinomycetes classes also promoted the growth of *E. coli* and *S. enterica*. Based on statistical significance ($p < 0.05$), the the top significant bacterial strains were selected, representing the highest significant levels of growth inhibition against *E. coli*, *S. enterica*, and *L. monocytogenes*. Indeed, the bipartite *in vitro* assay allowed to identify several endophytic and rhizosphere bacterial isolates with inhibitory activity against the three HPMOs. Against *E. coli*, the following isolates demonstrated notable inhibition, along with their respective percentages: CSR28 (45%), CSR12 (44%), CSR13 (44%), CSE4 (46%), CSE28 (47%), CSR4 (46%), CSE5 (56%), CSE34 (47%), CSE27 (49%), CSE31 (50%), and CSE6 (55%). For *S. enterica*, the isolates showing measurable inhibition included: CSE4 (41%), CSR4 (35%), CSE34 (42%), and CSE5 (60%). In the case of *L. monocytogenes*, a uniform inhibition percentage (57%) was observed across a broader set of isolates: CSE28, CSE31, CSE32, CSE34, CSR1, CSR12, CSR13, CSR14, CSR21, CSR28, and CSR34. Based on overlapping inhibitory activity against two or more of the tested HPMOs, four bacterial strains were selected for subsequent mVOCs analysis: *B. pumilus* CSR28, *Xanthomonadales* sp. CSE34, *S. champavatii* CSR4, and *B. pseudomycoides* CSE4. It is important to highlight that in the vast majority of the bipartite *in vitro* assays conducted with all tested bacterial strains, a consistent trend was observed: prolonged exposure (from 3 days to 7 days) of the bacteria to HPMOs generally resulted in the HPMOs' inhibition.

Class	Bacteria	Lm 3d	Lm 7d	Ec 3d	Ec 7d	Se 3d	Se 7d
Bacilli	*Bacillus pumilus* CSR28	-46.1	-56.7	-43.0	-44.9	-35.3	-27.7
	Bacillus toyonensis CSR1	-28.1	-56.7	-37.8	-40.9	-26.6	-27.7
	Bacillus pumilus CSR14	-28.1	-56.7	-33.9	-32.1	-31.8	-34.9
	Bacillus pumilus CSR12	-28.1	-56.7	-45.6	-43.9	-37.1	-27.7
	Bacillus sp. CSE31	-28.1	-56.7	-57.3	-49.8	-26.6	-27.7
	Bacillus pumilus CSE32	-28.1	-56.7	-41.7	-40.9	-26.6	-27.7
	Bacillus cereus ISE27	-28.1	-45.8	-14.5	-13.4	-16.1	-12.0
	Bacillus sp. ISE8	-28.1	-45.8	-8.0	-11.4	-16.1	-13.3
	Bacillus weihenstephanensis ISE28	-28.1	-45.8	142.2	-12.4	-16.1	-22.9
	Bacillus cereus ISE11	-28.1	-45.8	6.2	2.4	-16.1	-19.3
	Bacillus pumilus CSR23	-19.2	-35.0	14.0	15.2	-3.8	-1.2
	Bacillus toyonensis CSR25	-10.2	-35.0	-0.3	-0.6	-19.6	-10.8
	Bacillus baekryungensis CSE22	-10.2	-35.0	-31.3	-27.2	-26.6	-30.1
	Bacillus sp. ISR12	-10.2	-24.2	16.6	10.2	-19.6	-12.0
	Bacillus cereus ISR22	-10.2	-24.2	-10.6	-13.4	-0.3	-25.3
	Bacillus sp. ISR13	-10.2	-24.2	16.6	14.2	-9.1	-3.6
	Bacillus mycoides ISR8	-10.2	-24.2	-6.7	-8.5	-9.1	-12.0
	Bacillus sp. ISR25	-4.2	-24.2	19.2	24.0	1.4	9.6
	Bacillus pumilus CSR2	-10.2	-18.8	14.0	15.2	-23.1	-22.9
	Bacillus sp. ISR5	4.8	-18.8	29.5	16.1	-16.1	6.0
	Bacillus mycoides CSE27	-10.2	-45.8	-36.5	-48.8	-19.6	-28.9
	Bacillus pseudomycoides CSE4	-10.2	-38.6	-43.0	-45.9	-26.6	-41.0
	Bacillus zhangzhouensis CSE23	-28.1	-35.0	-37.8	-32.1	-26.6	-27.7
	Paenibacillus sp. ISR16	-10.2	8.3	14.0	12.2	-0.3	1.2
Gammaproteobacteria	*Xanthomonadales sp* . CSE34	-28.1	-56.7	-45.6	-46.8	-37.1	-42.2
	Serratia marcescens CSE6	-31.1	-47.7	-50.8	-54.7	-33.6	-31.3
	Serratia plymuthica ISE14	-28.1	-45.8	-6.7	-9.4	-2.1	-6.0
	Pseudomonas sp. ISE12	-19.2	-45.8	-13.2	-11.4	-16.1	-15.7
	Serratia marcescens CSE5	-10.2	-45.8	-49.5	-55.7	-58.0	-60.2
	Hafnia psychrotolerans CSE16	-25.1	-45.8	-27.5	-23.2	-23.1	-19.3
	Salinicola socius CSE25	-10.2	-42.2	-48.2	-54.7	-9.1	-9.6
	Serratia plymuthica ISR14	-10.2	-24.2	16.6	-26.2	10.1	6.0
	Stutzerimonas stutzeri ISE9	-28.1	-45.8	14.0	10.2	-16.1	-2.4
	Serratia plymuthica ISR2	-10.2	-24.2	7.5	0.4	-3.8	-2.4
Actinomycetes	*Microbacterium oxydans* CSR13	-28.1	-56.7	-37.8	-43.9	-31.8	-27.7
	Microbacterium foliorum CSR21	-28.1	-56.7	-33.9	-40.9	-26.6	-20.5
	Dietzia sp. CSR36	-28.1	-45.8	-31.3	-27.2	-31.8	-27.7
	Streptomyces champavatii CSR4	-28.1	-45.8	-41.7	-45.9	-31.8	-34.9
	Microbacterium oxydans CSR15	-28.1	-45.8	-37.8	-40.9	-26.6	-27.7
	Microbacterium thalassium ISE7	-28.1	-45.8	-9.3	-4.5	-14.3	-21.7
	Streptomyces sp. ISE29	-28.1	-45.8	-2.8	-10.4	-12.6	-6.0
	Rhodococcus erythropolis ISE16	-28.1	-45.8	19.2	8.3	-5.6	2.4
	Streptomyces sp. ISR1	-22.2	-45.8	8.8	1.4	-5.6	-9.6
	Williamsia sp. ISE22	-19.2	-45.8	11.4	14.2	-10.8	7.2
	Microbacterium oxydans ISE5	-10.2	-45.8	-1.5	6.3	4.9	9.6
	Mycobacterium sacrum ISR6	-10.2	-24.2	23.1	18.1	27.6	19.3
	Microbacterium oxydans ISR7	-10.2	-24.2	16.6	18.1	-2.1	1.2
	Oerskovia paurometabola ISR30	-1.2	-24.2	16.6	18.1	6.6	13.3
	Rhodococcus erythropolis ISR15	-4.2	-18.8	20.5	17.1	6.6	1.2
	Mycobacterium vaccae CSR16	-1.2	-9.7	-22.3	-23.2	-26.6	-24.1
	Streptomyces mediolani CSR34	-28.1	-56.7	-26.2	-35.0	-21.3	-13.3
	Streptomyces sp. CSR6	-28.1	-45.8	-26.2	-23.2	-31.8	-27.7
	Streptomyces sp. CSE3	-28.1	-45.8	-30.0	-23.2	-26.6	-24.1
	Streptomyces sp. CSR7	-28.1	-44.0	-24.9	-20.3	-2.1	10.8
	Streptomyces mediolani CSR30	7.8	-24.2	-37.8	-40.9	-0.3	9.6
	Streptomyces zaomyceticus ISR17	-10.2	-17.0	19.2	15.2	15.4	14.5
	Streptomyces peucetius CSR27	-10.2	-11.5	14.0	16.1	-5.6	19.3
Alphaproteobacteria	*Thalassospira permensis* CSE28	-28.1	-56.7	-45.6	-46.8	-37.1	-27.7

Figure 15. Heat map showing the mean percentage growth of HPMOs in bipartite Petri plates relative to the control (n = 6). Bacterial strains: Lm (*L. monocytogenes*), Ec (*E. coli*), Se (*S. enterica*). Time points: 3d (3 days) and 7d (7 days). The data are shown using a color scale, ranging from green (-60%) to red (140%).

Significant shifts in mVOCs profiles among HPMOs-inhibiting bacterial strains

The four bacterial strains (*B. pumilus* CSR28, *Xanthomonadales* sp. CSE34, *S. champavatii* CSR4, and *B. pseudomycoides* CSE4) that demonstrated significant level of inhibition of HPMOs in the bipartite *in vitro* assay were further analysed for their mVOCs using HS-SPME-GC-MS. Not all selected strains demonstrated significant inhibition against all three HPMOs. Therefore, the HS-SPME-GC-MS analysis was conducted based on the specific strains that showed the highest significant inhibition against each individual HPMO. For each mVOC produced by the selected bacterial strains, the absolute difference and significance ($p < 0.05$) were calculated, according to % peak area, by comparison to the control samples containing only TSA medium. Overall, the significant absolute differences (Figure 16) revealed that some mVOCs were produced in higher amounts by the control samples, while others were more abundant in the bacterial treatments.

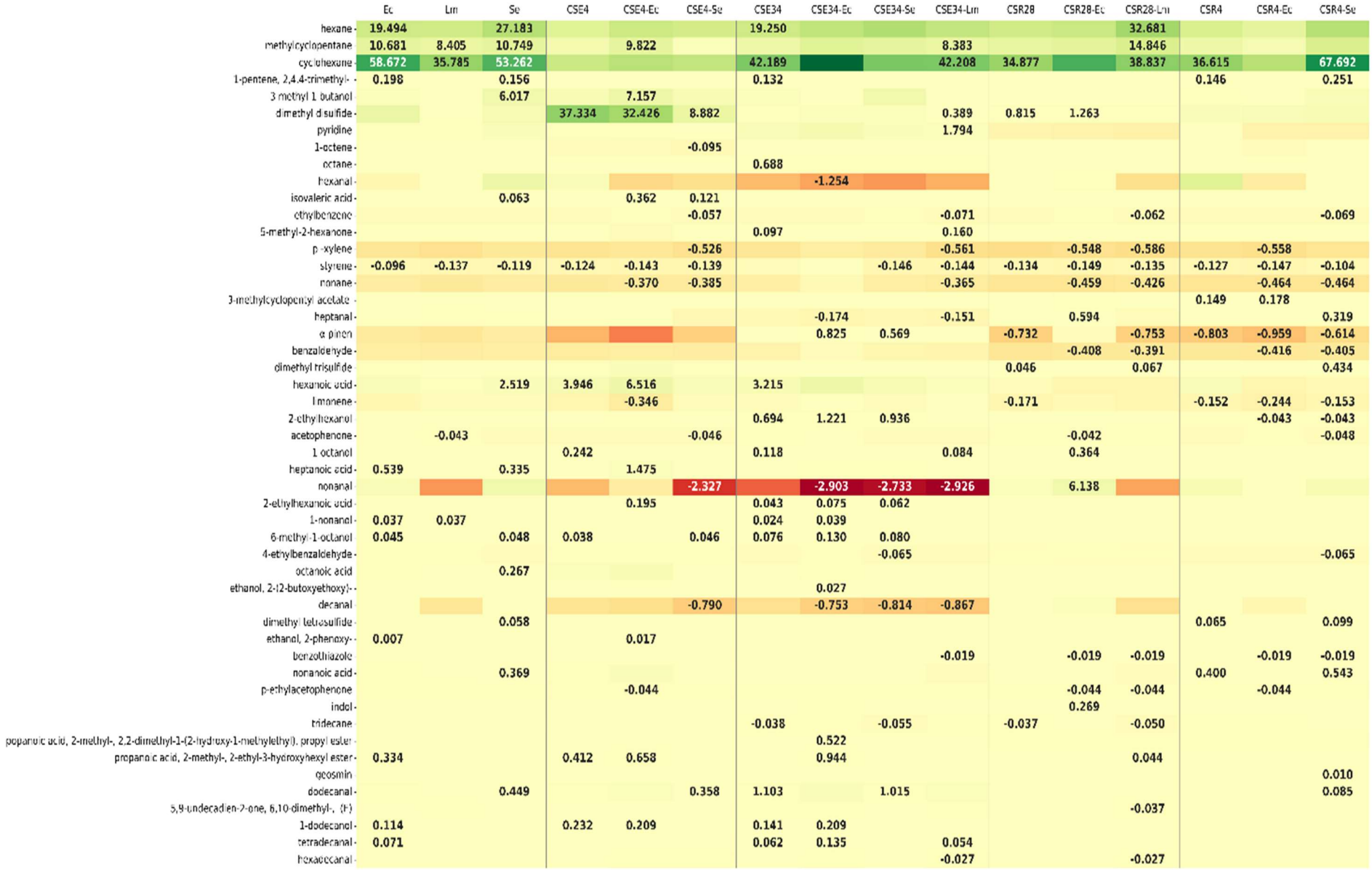
Ec Lm Se CSE4 CSE4-Ec CSE4-Se CSE34 CSE34-Ec CSE34-Se CSE34-Lm CSR28 CSR28-Ec CSR28-Lm CSR4 CSR4-Ec CSR4-Se
hexane 19.494 27.183 19.250 32.681
methylcyclopentane 10.681 8.405 10.749 9.822 8.383 14.846
cyclohexane 58.672 35.785 53.262 42.189 42.208 34.877 38.837 36.615 67.692
1-pentene, 2,4,4-trimethyl- 0.198 0.156 0.132 0.146 0.251
3 methyl 1 butanol 6.017 7.157
dimethyl disulfide 37.334 32.426 8.882 0.389 0.815 1.263
pyridine 1.794
1-octene -0.095
octane 0.688
hexanal -1.254
isovaleric acid 0.063 0.362 0.121
ethylbenzene -0.057 -0.071 -0.062 -0.069
5-methyl-2-hexanone 0.097 0.160
p -xylene -0.526 -0.561 -0.548 -0.586 -0.558
styrene -0.096 -0.137 -0.119 -0.124 -0.143 -0.139 -0.146 -0.144 -0.134 -0.149 -0.135 -0.127 -0.147 -0.104
nonane -0.370 -0.385 -0.365 -0.459 -0.426 -0.464 -0.464
3-methylcyclopentyl acetate 0.149 0.178
heptanal -0.174 -0.151 0.594 0.319
α pinen 0.825 0.569 -0.732 -0.753 -0.803 -0.959 -0.614
benzaldehyde -0.408 -0.391 -0.416 -0.405
dimethyl trisulfide 0.046 0.067 0.434
hexanoic acid 2.519 3.946 6.516 3.215
limonene -0.346 -0.171 -0.152 -0.244 -0.153
2-ethylhexanol 0.694 1.221 0.936 -0.043 -0.043
acetophenone -0.043 -0.046 -0.042 -0.048
1 octanol 0.242 0.118 0.084 0.364
heptanoic acid 0.539 0.335 1.475
nonanal -2.327 -2.903 -2.733 -2.926 6.138
2-ethylhexanoic acid 0.195 0.043 0.075 0.062
1-nonanol 0.037 0.037 0.024 0.039
6-methyl-1-octanol 0.045 0.048 0.038 0.046 0.076 0.130 0.080
4-ethylbenzaldehyde -0.065 -0.065
octanoic acid 0.267
ethanol, 2-(2-butoxyethoxy)- 0.027
decanal -0.790 -0.753 -0.814 -0.867
dimethyl tetrasulfide 0.058 0.065 0.099
ethanol, 2-phenoxy- 0.007 0.017
benzothiazole -0.019 -0.019 -0.019 -0.019 -0.019
nonanoic acid 0.369 0.400 0.543
p-ethylacetophenone -0.044 -0.044 -0.044 -0.044
indol 0.269
tridecane -0.038 -0.055 -0.037 -0.050
propanoic acid, 2-methyl-, 2,2-dimethyl-1-(2-hydroxy-1-methylethyl), propyl ester 0.522
propanoic acid, 2-methyl-, 2-ethyl-3-hydroxyhexyl ester 0.334 0.412 0.658 0.944 0.044
geosmin 0.010
dodecanal 0.449 0.358 1.103 1.015 0.085
5,9-undecadien-2-one, 6,10-dimethyl-, (E) -0.037
1-dodecanol 0.114 0.232 0.209 0.141 0.209
tetradecanal 0.071 0.062 0.135 0.054
hexadecanal -0.027 -0.027

Figure 16. Heat map showing the significant absolute differences of mVOC between bacterial treatments and the control (TSA medium only). Green or green-shaded values indicate higher mVOC production compared to the control (TSA medium only), while red or red-shaded values indicate lower mVOC production relative to the control.

Among the mVOCs analysed, dimethyl disulfide (DMDS) (CAS No. 624-92-0) emerged as a particularly notable mVOC (Figure 17). This compound was significantly produced by CSE4 in monoculture (37.33%) and remained prominent in co-cultures with *E. coli* (32.426%) and *S. enterica* (8.88%). Notably, DMDS was not significantly detected in the monocultures of the tested HPMOs (*E. coli*, *S. enterica*, and *L. monocytogenes*). It was also detected, though at much lower peak areas, in CSR28 monoculture (0.82%) and its co-culture with *E. coli* (1.26%).

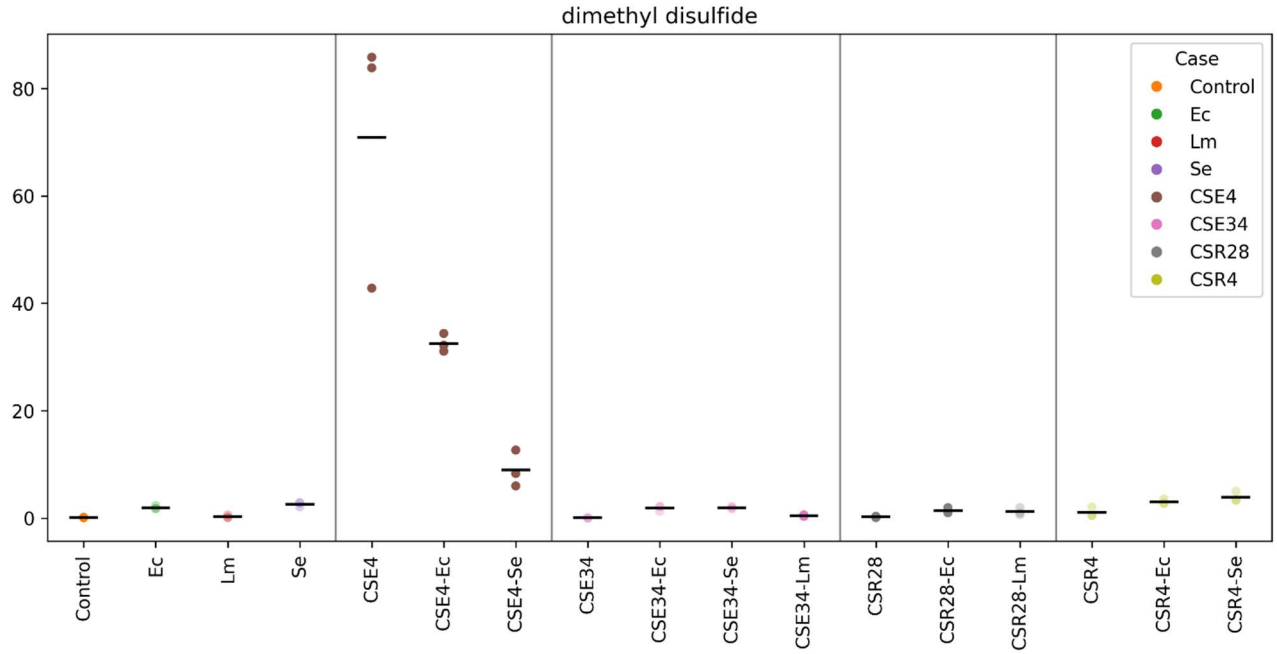

Figure 17. Relative dimethyl disulfide peak area (%) across all treatments (n = 3). Ec – *E. coli*, Lm – *L. monocytogenes*, Se – *S. enterica*, CSE4 - *B. pseudomycoides*, CSE34 – *Xanthomonadales* sp., CSR28 - *B. pumilus*, CSR4 - *S. champavatii*.

The compound hexane (CAS No. 110-54-3) (Figure 18) was prominently identified in the HPMO monocultures of *E. coli* (19.494%) and *S. enterica* (27.18%), in the endophytic bacterium CSE34 (19.25%), and in co-culture conditions involving CSR28 and *L. monocytogenes* (32.68%).

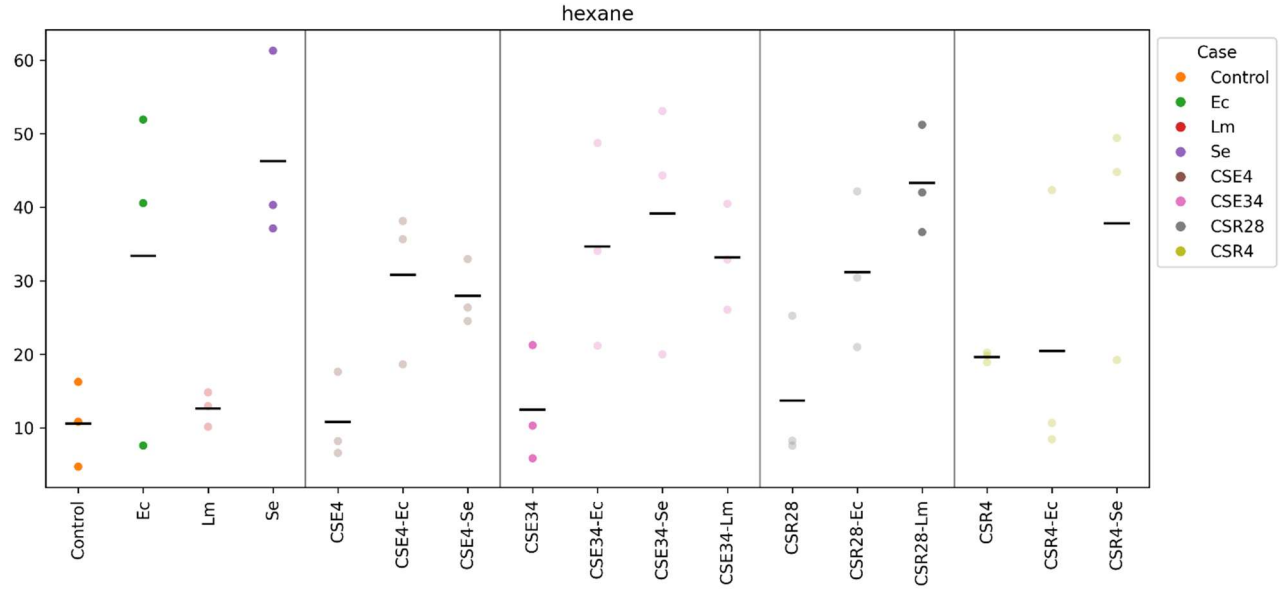

Figure 18. Relative hexane peak area (%) across all treatments (n = 3). Ec – *E. coli*, Lm – *L. monocytogenes*, Se – *S. enterica*, CSE4 - *B. pseudomycoides*, CSE34 – *Xanthomonadales* sp., CSR28 - *B. pumilus*, CSR4 - *S. champavatii*.

Methylcyclopentane (CAS No. 96-37-7) (Figure 19) was primarily detected in the monocultures of the HPMOs: *E. coli* (10.681%), *L. monocytogenes* (8.40%), and *S. enterica* (10.75%). This mVOC also appeared in co-cultures: CSE4 with *E. coli* (9.82%), CSE34 with *L. monocytogenes* (8.38%), and CSR28 with *L. monocytogenes* (14.85%).

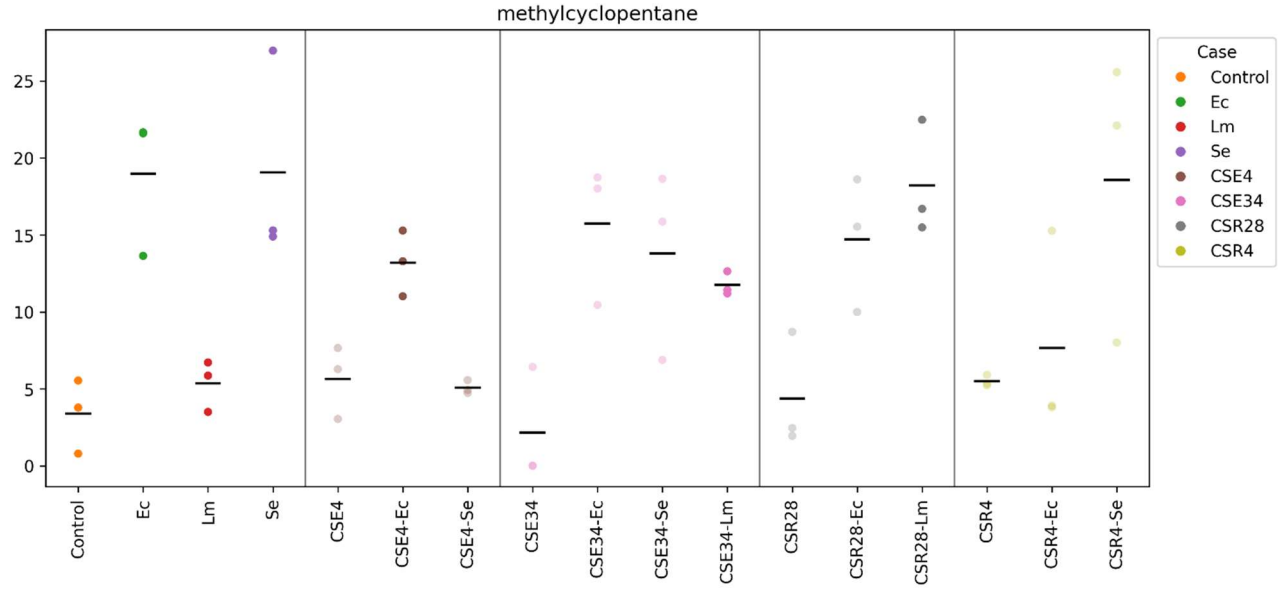

Figure 19. Relative methylcyclopentane peak area (%) across all treatments (n = 3). Ec – *E. coli*, Lm – *L. monocytogenes*, Se – *S. enterica*, CSE4 - *B. pseudomycoides*, CSE34 – *Xanthomonadales* sp., CSR28 - *B. pumilus*, CSR4 - *S. champavatii*.

Among all detected compounds, cyclohexane (CAS No. 110-82-7) (Figure 20) exhibited the highest peak area percentages. It was abundantly present in the HPMOs (*E. coli*: 58.67%; *S. enterica*: 53.26%; *L. monocytogenes*: 35.78%) and in monocultures of the endophytic and rhizosphere bacteria (CSE34: 42.19%; CSR28: 34.87%; CSR4: 36.62%), with the exception of CSE4, where it was not significantly detected. Cyclohexane was also prevalent in co-cultures of *L. monocytogenes* with CSE34 (42.21%), CSR28 (38.84%), and CSR4 (67.69%), but was notably absent in its co-culture with CSE4.

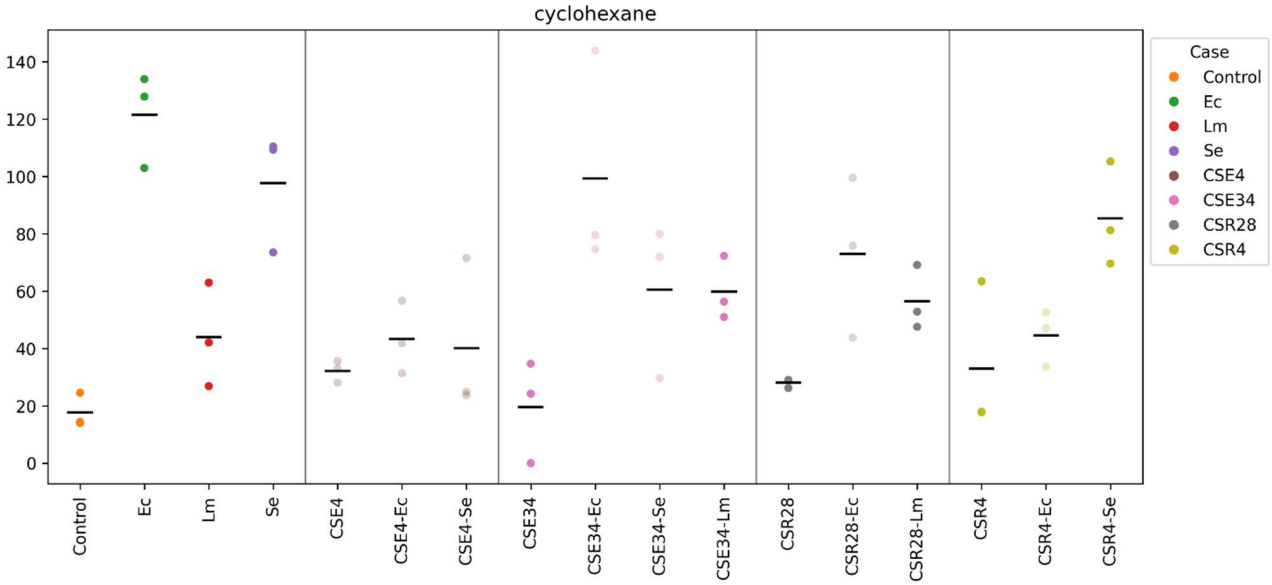

Figure 20. Relative cyclohexane peak area (%) across all treatments (n = 3). Ec – *E. coli*, Lm – *L. monocytogenes*, Se – *S. enterica*, CSE4 - *B. pseudomycoides*, CSE34 – *Xanthomonadales* sp., CSR28 - *B. pumilus*, CSR4 - *S. champavatii*.

3-Methyl-1-butanol (CAS No. 123-51-3) (Figure 21) was observed in the monoculture of *S. enterica* (6.02%) and unexpectedly in the co-culture of CSE4 with *E. coli* (7.16%), though it was absent in the CSE4 and *S. enterica* co-culture.

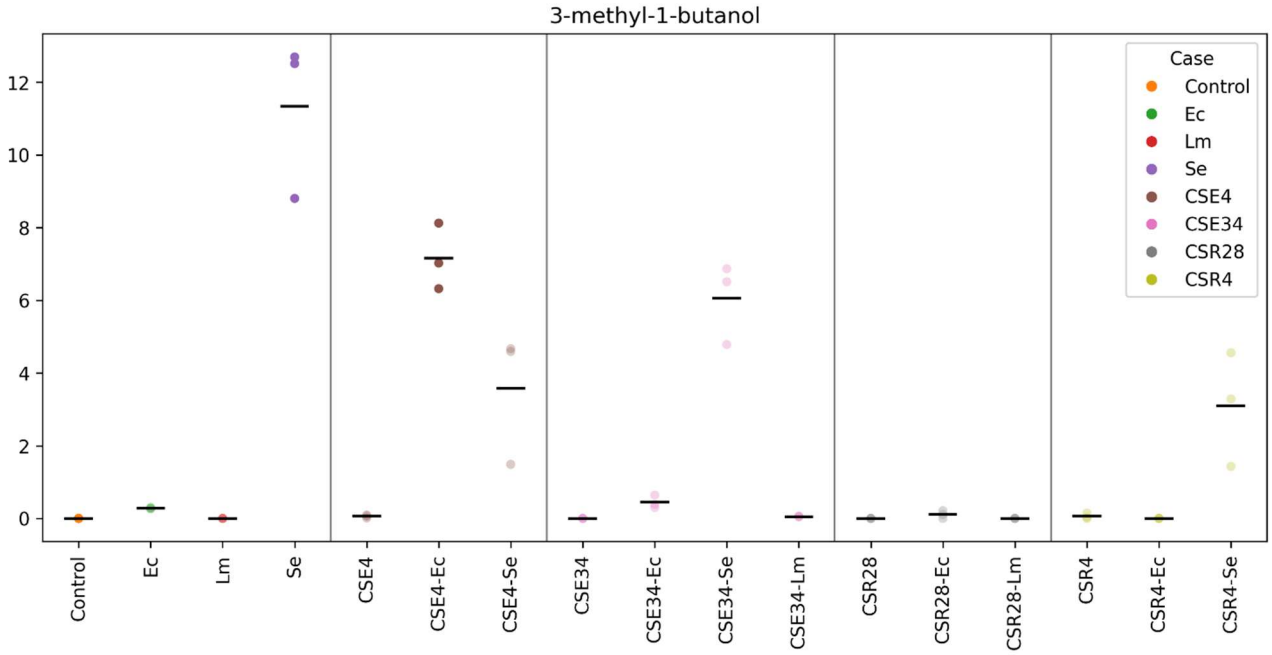

Figure 21. Relative 3-methyl-1-butanol peak area (%) across all treatments (n = 3). Ec – *E. coli*, Lm – *L. monocytogenes*, Se – *S. enterica*, CSE4 - *B. pseudomycoides*, CSE34 – *Xanthomonadales* sp., CSR28 - *B. pumilus*, CSR4 - *S. champavatii*.

Finally, nonanal (CAS No. 124-19-6) showed high abundance in the control samples (TSA-only bottles). This is further supported by the heat map data (Figure 16), where negative peak area values were primarily recorded in CSE34 monocultures and in its co-cultures with all tested HPMOs, suggesting suppression or absence of nonanal production in these conditions.

6. Discussion

6.1. **Influence of chemical traits on HPMOs dynamics in saline marsh ecosystems**

A comprehensive discussion to this topic is thoroughly presented in P1, Annex I (Marangi et al., 2024).

This study analysed the impact of environmental conditions on the abundance of human pathogenic microorganisms (HPMOs) on *S. europaea*, focusing on its chemical composition and its rhizosphere and in bulk soils at old and young marsh sites in France. The lignin content was consistently lower in plant shoots than in rhizosphere soil at both sites, confirming the naturally low lignin levels in *S. europaea* and persistence cause accumulation in the soil. A negative correlation was observed between lignin content and the abundance of *S. enterica* in shoots, as well as between lignin content and *E. coli* in bulk soil, suggesting a possible antimicrobial role of lignin or related compounds. Lipid content in plant material was positively correlated with *E. coli* abundance, with most lipids assumed to originate from the plant, though microbial contributions could not be excluded.

Additionally, several significant correlations were found between soil pH and HPMO abundance. In bulk soil, *E. coli*, *L. monocytogenes*, and *S. enterica* all showed negative correlations with pH, indicating reduced bacterial abundance at higher pH levels. In contrast, a positive correlation was found between pH and *L. monocytogenes* colonization in the rhizosphere soil. These findings suggest that pH plays a critical role in shaping microbial populations in both soil types.

Saline soils, typical of *S. europaea* habitats, are generally unfavourable for HPMOs' survival, as salt has been shown to inhibit the growth and virulence of these pathogens. According to the literature included in Marangi et al. (2024), higher NaCl concentrations generally inhibited the growth of *E. coli* and its virulence-related traits. A 5% NaCl concentration significantly reduced the growth of *S. enterica*, while a 7% NaCl concentration was the lowest to affect the growth of *L. monocytogenes*. However, the study also considers the potential for increased HPMO colonization in the future, as global climate change may raise soil temperatures to levels closer to the optimal range for these bacteria. Overall, the results highlight the importance of plant and soil chemical traits—particularly lignin, lipids, and pH—in influencing microbial colonization

and underscore the need for further research to determine causal relationships through inoculation experiments.

6.2. Gene expression and growth response of *S. europaea* to HPMOs under different salinity conditions

The inoculation of HPMOs affected differently the plant colonization and its growth parameters

Given that *S. europaea* shoots are eaten raw, the potential contamination of this plant by HPMOs has to be analysed (Ozturk et al., 2018). This highlights the novelty of our experimental design, research and results, particularly in the context of enhancing food security through the utilization of halophytes. Previous studies on the potential colonization of different plants, including *S. europaea*, by HPMOs have shown that various HPMOs can effectively penetrate plant tissues and organs (Marangi et al., 2024). Notably, studies related to different plants, such as radish, *Arabidopsis*, lettuce and tomato, assessed colonization by analysing plant materials at intervals ranging from hours to days or up to two/three weeks post-inoculation (Gu et al., 2011; Jacob et al., 2021; Szymańska et al., 2024). Through the use of both culture-dependent and culture-independent methods, we demonstrated a notable decline in HPMOs' growth by the fourth week post-inoculation, despite starting with an inoculum of millions of cells (OD = 0.5) in sterile sand, with similar pattern observed in Szymańska et al. (2024). Furthermore, although direct seed contamination with HPMOs is widely regarded as the most effective approach to ensuring high colonization in various plant tissues and organs (Szymańska et al., 2024), our study might have simulated an alternative scenario in which HPMOs were unintentionally introduced into saline and non-saline soils, potentially *via* a contaminated irrigation system in an agricultural field.

The variation in HPMOs infection across plants replicates may be attributed to biological factors, such as natural plant genome variations that can influence how individual plants respond to pathogens, leading to diverse infection outcomes (Saxena et al., 2014). To comprehensively assess HPMOs abundance, we considered both biochemical properties (selective media) and genetic material (bacterial DNA and plant RNA). We recognized that not all detected *L. monocytogenes* colonies in selective media might represent human pathogens. Missleading results can be caused e.g. by other *Listeria* species with same and/or similar shapes and colours. Conversely, qPCR results, which utilized melting profiles for high specificity,

might have been compromised by the presence of phenolic compounds in *S. europaea* during the first eight weeks of growth, potentially leading to inhibition or inaccurate detection (Sidstedt et al., 2020; Turcios et al., 2023). In general, column-based DNA extraction kits, such as the one employed in our experiments, outperformed magnetic bead-based alternatives (Vojkovska et al., 2015). The inherent complexity of food matrices, like that one of *S. europaea*—marked by low concentrations of pathogens, diverse native endophytes, and varied sample composition—makes isolating target organisms a significant challenge (Brehm-Stecher et al., 2009; Kawasaki et al., 2011). A comparative study of DNA extraction kits found that, although the PrepSeq Nucleic Acid Extraction Kit yielded higher amounts of DNA than other kits, it resulted in complete PCR inhibition (Vojkovska et al., 2015). This indicates an insufficient removal of PCR inhibitors—such as plant-derived polysaccharides, terpenoids, phenolic compounds, and tannins—a limitation that might have been similar to our study using Plant and Fungi DNA Purification Kit (Vojkovska et al., 2015). Therefore, for future experiments involving bacterial DNA isolation from *S. europaea*, we recommend optimizing the lysis of plant tissues and employing specialized kits capable of removing PCR inhibitors, such as cetyltrimethylammonium bromide-spin-based protocols, in order to obtain more accurate estimations of bacterial DNA content (Kiselev et al., 2023). In the analysis of plant growth parameters, under both inoculated and uninoculated conditions, total plant weight exhibited a consistent decline at the highest salinity level (200 mM NaCl), corroborating earlier findings that elevated salt concentrations hinder *S. europaea* germination and early development (Ungar et al., 1979; Calone et al., 2020; Cárdenas-Pérez et al., 2022). Importantly, these results suggest that the different types of inoculations tested did not provide a mitigation effect on the adaptation of *S. europaea* to salinity. Our results shown that bacterial inoculation, particularly with *E. coli* and *L. monocytogenes*, enhanced plant biomass at 50 and 100 mM NaCl, suggesting potential growth-promoting—contrasting with findings in radish (Szymańska et al., 2024). The plant growth observed in our inoculation treatments may be attributed to nutrient released from dead HPMOs cells, a mechanism similar to that reported for different bacteria, where sonicated and autoclaved bacterial cells promoted plant growth (Hayashi et al., 2022; Agake et al., 2022). Notably, different non-pathogenic *Staphylococcus* strains have been shown to modulate stress-responsive pathways and regulate ion homeostasis under saline conditions, thereby enhancing maize growth (Shahid et al., 2019). Studies on *Brassica napus* shown that PGPB inoculation, under salt stress, enhanced plant growth, water content, proline, and antioxidant activity, while reducing electrolyte leakage and H_2O_2 (Neshat et al., 2022). The plant growth promotion observed in *E. coli* and *L. monocytogenes* treatments may be linked to the HPMOs' ability to

evade plant defence mechanisms by secreting virulence effectors that suppress PTI signalling or escape recognition by pattern recognition receptors (PRRs) (Guo et al., 2009). While suggestive, our evidences are insufficient to confirm that certain HPMOs possess PGPB-like activity. Conversely, *S. enterica* reduced plant biomass at both 0 and 100 mM NaCl, indicating a negative or pathogenic interaction that impairs growth regardless of salinity, in line with previous studies (Klerks et al., 2007; Jayaraman et al., 2014; Deering et al., 2015; Szymańska et al., 2024). These findings suggest that certain HPMOs can have beneficial effects on plant biomass, while others may be harmful (Tyler and Triplett, 2008). This dichotomy highlights the complex interactions between plants and HPMOs and underscores the importance of understanding these relationships for potentially optimizing plant growth in challenging environments. With regard to total bacterial counts, our results aligned with those of Szymańska et al. (2024) using the culture-dependent method, showing higher total bacterial abundance in roots than in shoots. However, qPCR results, in our analysis, revealed a higher 16S rRNA gene copy number in shoots than roots. The physical characteristics of soil, particularly soil texture, significantly impact the establishment and survival of pathogens (Obayomi et al., 2019). The proportions of sand, silt, and clay in the soil affects the persistence of various pathogens. For example, fine-textured clayey soils may facilitate pathogen survival due to their properties (Obayomi et al., 2019), in contrast to the sterile sand in our study, which likely presents a less favourable environment for pathogen persistence. However, it is worth to consider that in the last decade, *S. europaea* extracts have been investigated for their antimicrobial properties (Rahmani et al., 2022). Notably, the phenolic and other metabolite content in this halophyte has been associated with antimicrobial activity against certain HPMOs (Castagna et al., 2022).

Plant transcriptomics analysis revealed connections with HPMOs' colonization in shoots

The lack of *E. coli* PCM 2057 detection in both shoots and roots of treated plants, as determined by selective media and qPCR, raises intriguing questions regarding its ability to associate with plant tissues. Consistent with this, no significant differential gene expression was observed in the shoots, further suggesting a limited or absent interaction. In contrast, *E. coli* PCM 2561 and the pathogenic O157:H7 strain have demonstrated the capacity to colonize a range of plant species, such as radish, leafy greens, fruits, and nuts (Deering et al., 2012; Szymańska et al., 2024). Whether this colonization ability is a key determinant of pathogenicity remains unclear and warrants deeper investigation. Although *E. coli* PCM 2057 has been studied extensively for its antimicrobial activity and detection methodologies (Kosikowska et al., 2015; Zieniuk

and Bętkowska, 2021), its potential to colonize plants remains unexplored, with the exception of the analysis presented in this thesis.

S. enterica was detected in both shoots and roots by selective media and qPCR, indicating systemic colonization, in line with previous studies (Szymańska et al., 2024). The downregulation of phosphoethanolamine N-methyltransferase in treated plants may suggest disruption of key metabolic processes, which may underlie the negative effects on plant growth. This finding aligns with previous observations in *Triticum monococcum*, where inoculation with *Blumeria graminis* f. sp. *tritici* also led to its downregulation (Bhuiyan et al., 2007). Despite these biotic stress responses, the enzyme is primarily associated with abiotic stress conditions, such as drought (Chen et al. 2019; Wang et al., 2021). Interestingly, the biosynthetic processes of choline and phosphatidylcholine have been found to be associated with transcripts related to phosphoethanolamine N-methyltransferase. The methylation of phosphoethanolamine to form phosphocholine, catalyzed by phosphoethanolamine N-methyltransferases, has emerged as a crucial biochemical step in the synthesis of the major phospholipid, phosphatidylcholine (Bobenchik et al., 2011). In plants treated with *S. enterica* at 0 mM NaCl, the biosynthesis of pentacyclic triterpenoids is suppressed compared to non-inoculated controls. The presence of these compounds in cuticular waxes across the Brassicaceae family and other plants has been associated with resistance to the pest *Plutella xylostella*, as noted by Augustin et al. (2011). Additionally, pentacyclic triterpenoids have shown antimicrobial properties (Huang et al., 2012). It is noteworthy that the downregulation observed in *S. enterica*-treated plants may be attributed to pathogen-induced alterations disrupting normal biosynthetic pathways, as evidenced by comparison with non-inoculated controls. In *S. enterica*-treated plants at 0 mM NaCl, the expression of XEH and/or XET was suppressed compared to controls. This finding aligns with previous research demonstrating a significant reduction in XET activity in fruits infected with *Penicillium*, relative to their respective controls, as infection progressed (Muñoz-Bertomeu and Lorences, 2014). In non-inoculated plants, compared to those treated with *S. enterica* in 0 mM NaCl, there is an upregulation of hydroquinone: oxygen oxidoreductase activity linked to the lignin catabolic process. Notably, similar upregulation of hydroquinone: oxygen oxidoreductase activity has been observed in plants following infection by *Globodera pallida* and *Bacillus velezensis* (Tao et al., 2023; Varandas et al., 2024). In our study, the downregulation of the lignin catabolic process in response to *S. enterica* treatment may be attributed to the enhanced biogenesis of lignin, which serves to reinforce the plant cell wall in response to the pathogen, rather than its degradation into monomers (Marangi et al., 2024). In the 100 mM NaCl variant, plants treated

with *S. enterica* exhibited upregulation of cellular responses to extracellular stimuli, which helps protect cells from the toxic effects of hydrogen peroxide (H_2O_2). This observation suggests that plants infected with *S. enterica* activated the production of H_2O_2, potentially triggering programmed plant cell death during the hypersensitive response: this response might have restricted the spread of infection (Kuźniak and Urbanek, 2000).

The discrepancy between the detection of *L. monocytogenes* in selective media and qPCR has been previously discussed. However, our analysis of differential gene expression revealed significant alterations in plants treated with *L. monocytogenes* compared to non-inoculated controls. Similar to plants treated with *S. enterica*, *L. monocytogenes* treatment resulted in the suppression of pentacyclic triterpenoid biosynthesis, a process linked to plant defense mechanisms (Augustin et al., 2011). Furthermore, the gene encoding phosphoethanolamine N-methyltransferase, which is involved in the biosynthesis of choline and phosphatidylcholine, was downregulated in *L. monocytogenes*-inoculated plants. This effect is similar to that observed in plants inoculated with *Blumeria graminis* f. sp. *tritici* (Bhuiyan et al., 2007). Additionally, the expression of XEH and XET was suppressed in *L. monocytogenes*-treated plants, aligning with previous research showing reduced XET activity in fruits infected with *Penicillium* (Muñoz-Bertomeu and Lorences, 2014). At 0 mM NaCl, *L. monocytogenes* treatment led to the downregulation of the class III peroxidase subfamily, which plays a crucial role in plant cell wall organization in response to both biotic and abiotic stresses (Duroux and Welinder, 2003; Passardi et al., 2005; Yan et al., 2019). Conversely, inoculated plants exhibited upregulation of cellular responses to extracellular stimuli, potentially protecting cells from hydrogen peroxide toxicity. This suggests that plants infected with *L. monocytogenes* may activate hydrogen peroxide production, triggering programmed cell death during the hypersensitive response, which could restrict the spread of infection (Kuźniak and Urbanek, 2000). These findings highlight the complex interactions between *L. monocytogenes* and plant hosts, involving both suppression of certain plant biosynthetic pathways and activation of defence mechanisms. Understanding these interactions can provide valuable insights into how plants respond to this pathogen and how these responses might be manipulated to enhance plant resistance and food security.

6.3. **Bacterial mVOCs as emerging bioactive agents: insights from *S. europaea* microbiome and its inhibitory effects on foodborne pathogens**

The role of mVOCs in inhibiting human pathogens of major concern remains underexplored, despite substantial progress in understanding their effects against phytopathogens (Wang et al., 2021; Naz et al., 2022; Diyapoglu et al., 2022; Wang et al., 2023; Ling et al., 2023; Zhao et al., 2023). In particular, the inhibition of HPMOs—such as *E. coli*, *S. enterica*, and *L. monocytogenes*—via mVOCs has received limited attention in the current literature. These pathogens are among the most critical agents of foodborne illness globally, posing severe risks to public health and food safety (Bhatia et al., 2024). This study addresses this knowledge gap by investigating whether endophytic and rhizosphere-associated bacteria from *S. europaea* L., a halophytic plant adapted to extreme environments (Puccinelli et al., 2024), can serve as natural sources of antimicrobial mVOCs. To test this, we employed a bipartite *in vitro* assay to evaluate antimicrobial activity, in combination with HS-SPME-GC-MS for the identification and characterization of volatiles.

Our results support earlier findings that *B. pumilus* CSR28 possesses antibacterial activity against several HPMOs, such as *S. enterica*, *E. coli*, and *L. monocytogenes* (Chu et al., 2019; Saggese et al., 2022). Those studies identified aliphatic alcohols and peptides as the main antimicrobial compounds. However, we propose a different mechanism in the case of *E. coli*: the elevated % peak area of dimethyl disulfide (DMDS) observed during co-culture suggests that DMDS is a key metabolite responsible for the inhibition. This highlights a potential strain-specific or target-specific shift in the mode of inhibition. Interestingly, no inhibitory mVOCs were detected in cultures with *L. monocytogenes*, suggesting either an absence of effective mVOCs or a resistance mechanism in that species.

One of the most compelling findings of our study was the broad-spectrum inhibitory activity exhibited by *Xanthomonadales* sp. CSE34 against all three tested HPMOs. To our knowledge, no prior reports in the literature have documented this activity, indicating that this species may represent a novel and previously unexplored biocontrol agent against HPMOs. Based on our observations, the inhibitory effect could be attributed to the production of mVOCs such as hexane, methylcyclopentane, and cyclohexane, which may play a key role in its antimicrobial mechanism.

The antimicrobial potential of *S. champavatii* CSR4 remains somewhat ambiguous based on current literature. In our study, however, this strain demonstrated significant inhibitory activity against *E. coli* and *S. enterica*. Previous work supports its effect on *E. coli*, as an extract of *S. champavatii* was found to inhibit certain strains (Ibrahimi et al., 2020), while others reported

no inhibition (Pesic et al., 2013), suggesting that strain-level specificity may influence susceptibility. Notably, no prior studies have reported inhibitory activity of *S. champavatii* against *S. enterica*, making our findings a potential novel contribution. Cyclohexane was detected in both monoculture of *S. champavatii* CSR4 and its co-culture with *L. monocytogenes*, which may imply a potential inhibitory role. However, this compound was also detected in HPMO cultures, which complicates the interpretation of its role in inhibition.

In our study, *B. pseudomycoides* CSE4 exhibited clear inhibitory activity against both *E. coli* and *S. enterica*. Although this species has been previously reported to possess antimicrobial properties, these were largely restricted to Gram-positive bacteria (Basi-Chipalu et al., 2015), and to our knowledge, no prior studies have reported its effects on *E. coli* or *S. enterica*. Notably, DMDS emerged as the predominant mVOC produced by *B. pseudomycoides* CSE4 in both monocultures and co-cultures with *E. coli* and *S. enterica*, suggesting a strong correlation between our bipartite *in vitro* inhibition assays and the HS-SPME-GC-MS mVOCs profiles. Additionally, methylcyclopentane was detected in co-culture with *E. coli*, although this compound was also present in monocultures of the HPMOs, complicating attribution. Intriguingly, while cyclohexane was abundant in HPMO monocultures, it was significantly reduced or absent in co-cultures with *B. pseudomycoides* CSE4, suggesting a potential suppression mechanism that warrants further investigation.

It is not unexpected that certain mVOCs, included those reported in this thesis, are also produced by endophytic or rhizosphere bacteria as a means of antagonism against phytopathogens. Indeed, certain endophytic bacteria classified as plant growth-promoting bacteria (PGPB), such as *Pseudomonas stutzeri* E25 and *Stenotrophomonas maltophilia* CR71, have been shown to produce the antimicrobial mVOC dimethyl disulfide (DMDS), which inhibits the mycelial growth of phytopathogens like *Botrytis cinerea* (Rojas-Solís and Santoyo, 2018). Using 16S rRNA sequencing, researchers have also identified bacteria from the genera *Bacillus* and *Enterobacter* that promote tomato seed germination and seedling growth by reducing *B. cinerea* colonization. These bacteria produce several mVOCs, including 1-octyn-3-ol, 4-ethyl-, β-fenchol, benzene, m-di-tert-butyl, 2-undecanone, 3,3,5-trimethylbicyclo [3.3.0] octan-2,8-dione, and 2-pentadecanone, 6,10,14-trimethyl (Chaouachi et al., 2021). Massawe et al. (2018) identified *B. velezensis* and *B. amyloliquefaciens* as particularly effective antagonists of *Sclerotinia sclerotiorum*. Among the most potent antimicrobial volatiles, 2-undecanone demonstrated a 98% inhibition of mycelial growth. Other volatiles, such as benzothiazole, 1,3-butadiene, and N,N-dimethyldodecylamine, also showed antibiotic activity,

though to a lesser extent. Gao et al. (2017) further identified pyrazine (2,5-dimethyl), benzothiazole, 4-chloro-3-methylphenol, and 2,4-bis(1,1-dimethylethyl)phenol as key antifungal compounds.

Interestingly, we also observed that several mVOCs were emitted in notable quantities from the TSA control medium itself, with nonanal being particularly abundant. This finding is consistent with previous reports indicating that nonanal is a plant-derived compound known for its antimicrobial properties. Studies have shown that nonanal, often found in plant extracts, can exhibit inhibitory activity against various emerging plant pathogens (Oyedeji et al., 2005; Zhang et al., 2017; Li et al., 2021). The detection of such biologically active volatiles in the control medium carries important methodological implications. It suggests that components of the medium—possibly plant-based hydrolysates or additives—may themselves serve as sources of volatiles with potential bioactivity. As such, failure to account for these background emissions could lead to overestimation of the effects attributed to microbial strains or experimental treatments. Therefore, our results reinforce the critical importance of including well-characterized and carefully controlled blanks in experiments investigating mVOC-mediated bioactivities. This ensures that any observed antimicrobial effects are genuinely attributable to the metabolites produced by the organisms under study, rather than to volatiles inherently present in the growth medium.

By integrating microbial inhibition assays with metabolite profiling, this research provided new insight into the antagonistic potential of underexplored microbial strains. The findings may contribute not only to the development of mVOC-based biocontrol strategies in agriculture but also to novel antimicrobial applications in food preservation and public health. To confirm and quantify the antimicrobial potential of the selected mVOCs identified in this study, further investigations are essential using e.g. the disk diffusion method as a standardized and widely accepted approach. This would involve testing each compound individually against the target HPMOs—*E. coli*, *S. enterica*, and *L. monocytogenes*—to evaluate their inhibitory effects under controlled conditions. Importantly, these assays should be conducted at a range of concentrations to assess potential dose-dependent antimicrobial responses and to determine the minimum inhibitory concentrations (MICs) for each mVOC. Such an approach would not only validate the bioactivity suggested by our bipartite *in vitro* and GC-MS results but also help distinguish the specific contributions of each mVOC. Moreover, incorporating synthetic standards of the identified compounds could provide a reliable means of verifying activity, enhancing reproducibility, and enabling comparisons with existing antimicrobial agents. These

further investigations will be crucial for assessing the feasibility of mVOCs as novel biocontrol agents or antimicrobial candidates in food safety and medical applications.

7. Conclusions

The overarching aim of this PhD research was to explore the interactions between *S. europaea* L., a halophyte of growing agronomic and nutritional interest, HPMOs, and the plant endophytic and rhizosphere bacteria under various biological and environmental contexts. Through a combination of microbiological, molecular, and chemical analyses, this work offered new insights into the persistence, suppression, and ecological dynamics of HPMOs in saline plant-soil systems. The findings presented across the included studies highlight several key themes with direct relevance to food safety, biocontrol innovation, and sustainable agriculture in saline environments.

According to hypothesis 1, this thesis examined the role of plant and soil chemistry in modulating HPMOs' abundance. Selective culturing and spectrometric analysis of plant shoots and soils revealed multiple correlations between biochemical composition and HPMOs presence. For instance, higher lignin content in shoots was associated with decreased abundance of *E. coli*, likely due to lignin's structural and chemical recalcitrance. Conversely, lipid-rich tissues supported increased abundance of *E. coli*, suggesting exploitation of these compounds as carbon sources via microbial lipolytic activity. On the soil side, soil salinity and pH were leading controls of HPMOs levels, offering general and fundamental soil parameters for enhancing food safety through soil management practices for saline sites. These results support a model in which chemical and environmental variables act as natural regulators of microbial colonization, with direct applicability to halophyte cultivation strategies.

According to hypothesis 2, this thesis demonstrated that *S. europaea* can support the transient colonization of certain foodborne pathogens, particularly *S. enterica* subsp. *enterica* and *L. monocytogenes*, while resisting colonization by non-pathogenic *E. coli* strain PCM 2057. HPMOs presence declined significantly by the fourth week post-inoculation, yet was accompanied by measurable changes in plant gene expression. Transcriptomic analysis revealed suppression of biosynthetic pathways, including those related to triterpenoid production and phosphoethanolamine N-methyltransferase activity—pathways typically associated with plant defence and membrane function. In contrast, genes linked to reactive oxygen species (ROS) metabolism, especially hydrogen peroxide-related responses, were upregulated, suggesting activation of a hypersensitive-like response. These results confirm that

S. europaea possesses innate immune strategies to cope with HPMOs and that bacteria of this group can manipulate plant transcriptome during colonization.

According to hypothesis 3, this work both identified and selected endophytic and rhizosphere bacteria associated with *S. europaea* that exhibit strong antagonistic effects against foodborne pathogens. Using a bipartite *in vitro* assay coupled with HS-SPME-GC-MS, four bacterial strains—*B. pumilus* CSR28, *Xanthomonadales* sp. CSE34, *S. champavatii* CSR4, and *B. pseudomycoides* CSE4—were found to significantly suppress the growth of *E. coli*, *S. enterica*, and *L. monocytogenes*. Volatile profiling identified DMDS as a key antimicrobial metabolite, with consistent HPMOs' inhibition across multiple assays. These findings provide compelling evidence for the potential of naturally associated microbes and their mVOCs as sustainable biocontrol agents. They also highlighted the untapped reservoir of antimicrobial activity present in halophyte-associated microbiomes, which may be particularly well-suited to function under saline conditions where traditional biological control agents are less effective.

In conclusion, this thesis underscores the complexity and promise of halophyte-HPMOs-microbiome systems. By unravelling these dynamics, we not only gain tools for safer crop production but also enrich our understanding of plant-microbe interactions in extreme environments—insights increasingly relevant in the context of climate change and global food security.

8. Prospects for experimental validation

Future research should aim to:

- characterize the genetic basis of resistance against colonization with HPMOs within *S. europaea* populations, leveraging genomic tools to identify resistant genotypes;
- develop field-scale applications for beneficial microbes and mVOCs, optimizing delivery mechanisms for saline agriculture;
- explore synergistic effects of chemical and biological controls, including the design of tailored cultivation substrates or bio-inoculants;
- assess risks of horizontal gene transfer and unintended ecological impacts of both pathogens and introduced biocontrol strains under field conditions.

References

1. Agake S.I., Plucani do Amaral F., Yamada T., Sekimoto H., Stacey G., Yokoyama T., Ohkama-Ohtsu N. Plant Growth-promoting Effects of Viable and Dead Spores of *Bacillus pumilus* TUAT1 on *Setaria viridis*. Microbes and Environment 2022, 37, 1. https://doi.org/10.1264/jsme2.ME21060
2. Agarwal V.K., Sinclair J.B. Principles of Seed Pathology (2nd ed.). CRC Press 1997. https://doi.org/10.1201/9781482275650
3. Ajilogba C.F., Babalola O.O. GC–MS analysis of volatile organic compounds from *Bambara* groundnut rhizobacteria and their antibacterial properties. World Journal of Microbiology and Biotechnology 2019, 35, 83. https://doi.org/10.1007/s11274-019-2660-7
4. Alexa A., Rahnenfuhrer J. topGO: Enrichment Analysis for Gene Ontology. R package version 2.56.0., 2023. https://rdrr.io/bioc/topGO/
5. Almeida O.A.C., de Araujo N.O., Dias B.H.S., de Sant'Anna Freitas C., Coerini L.F., Ryu C.M., de Castro Oliveira J.V. The power of the smallest: The inhibitory activity of microbial volatile organic compounds against phytopathogens. Frontiers in Microbiology 2023, 13, https://doi.org/10.3389/fmicb.2022.951130
6. Amagliani G., Omiccioli E., Brandi G., Bruce I.J., Magnani M. A multiplex magnetic capture hybridisation and multiplex Real-Time PCR protocol for pathogen detection in seafood. Food Microbiology 2010, 27, 5, 580-585. https://doi.org/10.1016/j.fm.2010.01.007
7. Araus J.L., Rezzouk F.Z., Thushar S., Shahid M., Elouafi I.A., Bort J., Serret M.D. Effect of irrigation salinity and ecotype on the growth, physiological indicators and seed yield and quality of *Salicornia europaea*. Plant Science 2021, 304, 110819. https://doi.org/10.1016/j.plantsci.2021.110819
8. Arcari T., Feger M.L., Guerreiro D.N., Wu J., O'Byrne C.P. Comparative Review of the Responses of *Listeria monocytogenes* and *Escherichia coli* to Low pH Stress. Genes 2020, 11, 1330. https://doi.org/10.3390/genes11111330
9. Augustin J.M., Kuzina V., Andersen S.B., Bak S. Molecular activities, biosynthesis and evolution of triterpenoid saponins. Phytochemistry 2011, 72, 435-457. https://doi.org/10.1016/j.phytochem.2011.01.015
10. Balali G.I., Yar D.D., Afua Dela V.G., Adjei-Kusi P., Microbial Contamination, an Increasing Threat to the Consumption of Fresh Fruits and Vegetables in Today's World. International Journal of Microbiology 2020, 3029295. https://doi.org/10.1155/2020/3029295
11. Basi-Chipalu S., Dischinger J., Josten M., Szekat C., Zweynert A., Sahl H., Bierbaum G. Pseudomycoicidin, a Class II Lantibiotic from *Bacillus pseudomycoides*. Applied and Environmental Microbiology 2015, 81. https://doi.org/10.1128/AEM.00299-15
12. Bhatia V., Nag R., Burgess C.M., Gaffney M., Celayeta J.M.F., Cummins E. Microbial risks associated with Ready-To-Eat Fresh Produce (RTEFP)—A focus on temperate climatic conditions. Postharvest Biology and Technology 2024, 213, 112924. https://doi.org/10.1016/j.postharvbio.2024.112924

13. Bhuiyan N.H., Liu W., Liu G., Selvaraj G., Wei Y., King J. Transcriptional regulation of genes involved in the pathways of biosynthesis and supply of methyl units in response to powdery mildew attack and abiotic stresses in wheat. Plant Molecular Biology 2007, 64, 305–318. https://doi.org/10.1007/s11103-007-9155-x
14. Bigeard J., Colcombet J., Hirt H. Signaling Mechanisms in Pattern-Triggered Immunity (PTI). Molecular Plant 2015, 8, 521–539. https://doi.org/10.1016/j.molp.2014.12.022
15. Bintarti A.F., Sulesky-Grieb A., Stopnisek N., Shade A. Endophytic microbiome variation among single plant seeds. Phytobiomes Journal 2022, 6, 45–55. https://doi.org/10.1094/pbiomes-04-21-0030-r
16. Bobenchik A.M., Augagneur Y., Hao B., Hoch J.C., Mamoun C.B. Phosphoethanolamine methyltransferases in phosphocholine biosynthesis: functions and potential for antiparasite therapy, FEMS Microbiology Reviews 2011, 35, 4, 609–619. https://doi.org/10.1111/j.1574-6976.2011.00267.x
17. Brehm-Stecher B., Young C., Jaykus L.A., Tortorello M.L. Sample preparation: the forgotten beginning. Journal of Food Protection 2009, 72, 1774–1789. https://doi.org/10.4315/0362-028X-72.8.1774
18. Bryant D.M., Johnson K., DiTommaso T., Tickle T., Couger M.B., Payzin-Dogru D., Lee T.J., Leigh N.D., Kuo T.H., Davis F.G., Bateman J., Bryant S., Guzikowski A.R., Tsai S.L., Coyne S., Ye W.W., Freeman R.M. Jr, Peshkin L., Tabin C.J., Regev A., Haas B.J., Whited J.L. A Tissue-Mapped Axolotl De Novo Transcriptome Enables Identification of Limb Regeneration Factors. Cell Reports 2017, 18, 3, 762-776. doi: 10.1016/j.celrep.2016.12.063
19. Caballero-Guerrero B., Garrido-Fernandez A., Fermoso F.G., Rodriguez-Gutierrez G., Fernandez-Prior M.A., Reinhard C., Nystrom L., Benitez-Cabello A., Arroyo-Lopez F. Antimicrobial effects of treated olive mill waste on foodborne pathogens. LWT 2022, 164, 113628. https://doi.org/10.1016/j.lwt.2022.113628
20. Calone R., Mircea D.M., González-Orenga S., Boscaiu M., Lambertini C., Barbanti L., Vicente O. Recovery from Salinity and Drought Stress in the Perennial *Sarcocornia fruticosa* vs. the Annual *Salicornia europaea* and *S. veneta*. Plants 2022, 11, 1058. https://doi.org/10.3390/plants11081058
21. Calone R., Sanoubar R., Noli E., Barbant, L. Assessing *Salicornia europaea* Tolerance to Salinity at Seed Germination Stage. Agriculture 2020, 10, 29. https://doi.org/10.3390/agriculture10020029
22. Cárdenas-Pérez S., Piernik A., Chanona-Pérez J.J., Grigore M.N., Perea-Flores M.J. An overview of the emerging trends of the *Salicornia* L. genus as a sustainable crop. Environmental and Experimental Botany 2021, 191, 104606. https://doi.org/10.1016/j.envexpbot.2021.104606
23. Cárdenas-Pérez S., Rajabi Dehnavi A., Leszczyński K., Lubińska-Mielińska S., Ludwiczak A., Piernik A. *Salicornia europaea* L. Functional Traits Indicate Its Optimum Growth. Plants 2022, 11, 1051. https://doi.org/10.3390/plants11081051
24. Castagna A., Mariottini G., Gabriele M., Longo V., Souid A., Dauvergne X., Magné C., Foggi G., Conte G., Santin M. Ranieri A. Nutritional Composition and Bioactivity of *Salicornia europaea* L. Plants Grown in Monoculture or Intercropped with Tomato Plants

in Salt-Affected Soils. Horticulturae 2022, 8, 828. https://doi.org/10.3390/horticulturae8090828
25. Centers for Disease Control and Prevention. List of Selected Multistate Foodborne Outbreak Investigations, 2021. https://www.cdc.gov/foodsafety/outbreaks/multistate-outbreaks/outbreaks-list.html
26. Cesarino I. Structural features and regulation of lignin deposited upon biotic and abiotic stresses. Current Opinion in Biotechnology 2019, 56, 209-214. https://doi.org/10.1016/j.copbio.2018.12.012
27. Chaouachi M., Marzouk T., Jallouli S., Elkahoui S., Gentzbittel L., Ben C., Djébali N. Activity assessment of tomato endophytic bacteria bioactive compounds for the postharvest biocontrol of *Botrytis cinerea*. Postharvest Biology and Technology 2021, 172, 111389. https://doi.org/10.1016/j.postharvbio.2020.111389
28. Chen W., Taylor M.C., Barrow R.A., Croyal M., Masle J. Loss of Phosphoethanolamine N-Methyltransferases Abolishes Phosphatidylcholine Synthesis and Is Lethal. Plant Physiology 2019, 179, 1, 124–142. https://doi.org/10.1104/pp.18.00694
29. Cheng H., Zhang D., Ren L., Song Z., Li Q., Wu J., Fang W., Huang B., Yan D., Li Y., Wang Q., Cao A. Bio-activation of soil with beneficial microbes after soil fumigation reduces soil-borne pathogens and increases tomato yield. Environmental Pollution 2021, 283, 117160. https://doi.org/10.1016/j.envpol.2021.117160
30. Chu J., Wang Y., Zhao B., Zhang X.M., Liu K., Mao L., Kalamiyets E. Isolation and identification of new antibacterial compounds from *Bacillus pumilus*. Applied Microbiology and Biotechnology 2019, 103, 8375–8381. https://doi.org/10.1007/s00253-019-10083-y
31. Chung J.H., Song G.C., Ryu C.M. Sweet scents from good bacteria: case studies on bacterial volatile compounds for plant growth and immunity. Plant Molecular Biology 2016, 90, 677-687. doi: 10.1007/s11103-015-0344-8
32. Coulombe G., Catford A., Martinez-Perez A., Buenaventura E. Outbreaks of *Escherichia coli* O157:H7 Infections Linked to Romaine Lettuce in Canada from 2008 to 2018: An Analysis of Food Safety Context 2020, 83, 8, 1444-1462. https://doi.org/10.4315/JFP-20-029
33. Daliakopoulos I.N., Tsanis I.K., Koutroulis A., Kourgialas N.N., Varouchakis A.E., Karatzas, Ritsema C.J. The threat of soil salinity: A European scale review. Science of The Total Environment 2016, 573, 727-739. https://doi.org/10.1016/j.scitotenv.2016.08.177
34. Dandie C.E., Ogunniyi A.D., Ferro S., Hall B., Drigo B., Chow C.W.K., Venter H., Myers B., Deo P., Donner E., Lombi E. Disinfection options for irrigation water: Reducing the risk of fresh produce contamination with human pathogens. Critical Reviews in Environmental Science and Technology 2019, 50, 20, 2144–2174. https://doi.org/10.1080/10643389.2019.1704172
35. De Corato U. Disease-suppressive compost enhances natural soil suppressiveness against soil-borne plant pathogens: a critical review. Rhizosphere 2020, 13, 100192. https://doi.org/10.1016/j.rhisph.2020.100192

36. De Oliveira Elias S., Noronha T.B., Tondo E.C. *Salmonella* spp. and *Escherichia coli* O157:H7 prevalence and levels on lettuce: A systematic review and meta-analysis. Food Microbiology 2019, 84, 103217. https://doi.org/10.1016/j.fm.2019.05.001
37. Deering A.J., Jack D.R., Pruitt D.R., Mauer L.J. Movement of *Salmonella* serovar typhimurium and *E. coli* O157:H7 to ripe tomato fruit following various routes of contamination. Microorganisms 2015, 3, 809–825. https://doi.org/10.3390/microorganisms3040809
38. Deering A.J., Mauer L.J., Pruitt R.E. Internalization of *E. coli* O157:H7 and *Salmonella* spp. in plants: A review. Food Research International 2012, 45, 2, 567-575. https://doi.org/10.1016/j.foodres.2011.06.058
39. Diyapoglu A., Oner M., Meng M. Application Potential of Bacterial Volatile Organic Compounds in the Control of Root-Knot Nematodes. Molecules 2022, 27, 4355. https://doi.org/10.3390/molecules27144355
40. Duroux L., Welinder K.G. The Peroxidase Gene Family in Plants: A Phylogenetic Overview. Journal of Molecular Evolution 2003, 57, 397–407. https://doi.org/10.1007/s00239-003-2489-3
41. Effmert U., Kalderás J., Warnke R., Piechulla B. Volatile Mediated Interactions Between Bacteria and Fungi in the Soil. Journal of Chemical Ecology 2012, 38, 665–703. https://doi.org/10.1007/s10886-012-0135-5
42. Food and Agriculture Organization of the United Nations (FAO). International year of plant health – protecting plants, Protecting life 2020. http://www.fao.org/plant-health-2020
43. Foodborne Disease Burden Epidemiology Reference Group 2007-2015. WHO Estimates of the Global Burden of Foodborne Diseases. Geneva: World Health Organization 2015, ISBN 978 92 4 156516 5.
44. Frazee A., Pertea G., Jaffe A., Langmead B., Salzberg S.L., Leek J.T. Ballgown bridges the gap between transcriptome assembly and expression analysis. Nature Biotechnology 2015, 33, 243–246. https://doi.org/10.1038/nbt.3172
45. Friedman M. Antibiotic-resistant bacteria: Prevalence in food and inactivation by food-compatible compounds and plant extracts. Journal of Agricultural and Food Chemistry 2015, 63, 15, 3805–3822. https://pubs.acs.org/doi/10.1021/acs.jafc.5b00778#
46. Furtado B.U., Nagy I., Asp T., Tyburski J., Skorupa M., Golebiewski M., Hulisz P., Hrynkiewicz K. Transcriptome profiling and environmental linkage to salinity across *Salicornia europaea* vegetation. BMC Plant Biology 2019, 19, 427. https://doi.org/10.1186/s12870-019-2032-3
47. Fussy A., Papenbrock J. Molecular analysis of the reactions in *Salicornia europaea* to varying NaCl concentrations at various stages of development to better exploit its potential as a new crop plant. Frontiers in Plant Science 2024. https://doi.org/10.3389/fpls.2024.1454541
48. Gallego-Giraldo L., Posé S., Pattathil S., Peralta A.G., Hahn M.G., Ayre B.G., Sunuwar J., Hernandez J., Patel M., Shah J., Rao X., Knox J.P., Dixon, R.A. Elicitors and defense gene induction in plants with altered lignin compositions. New Phytologist 2018, 219, 1235-1251. https://doi.org/10.1111/nph.15258

49. Gao Z., Zhang B., Liu H., Han J., Zhang Y. Identification of endophytic *Bacillus velezensis* ZSY-1 strain and antifungal activity of its volatile compounds against *Alternaria solani* and *Botrytis cinerea*. Biological Control 2017, 105, 27-39. https://doi.org/10.1016/j.biocontrol.2016.11.007
50. Gareth A.T., Paradell Gil T., Müller C.T., Rogers H.J., Berger C.N. From field to plate: How do bacterial enteric pathogens interact with ready-to-eat fruit and vegetables, causing disease outbreaks? Food Microbiology Volume 2024, 117, 104389. https://doi.org/10.1016/j.fm.2023.104389
51. George A.S., Brandl M.T. Plant Bioactive Compounds as an Intrinsic and Sustainable Tool to Enhance the Microbial Safety of Crops. Microorganisms 2021, 9, 2485. https://doi.org/10.3390/microorganisms9122485
52. Glaize A., Young M., Harden L., Gutierrez-Rodriguez E., Thakur S. The effect of vegetation barriers at reducing the transmission of *Salmonella* and *Escherichia coli* from animal operations to fresh produce. International Journal of Food Microbiology 2021, 109196. https://doi.org/10.1016/j.ijfoodmicro.2021.109196
53. Goberna M., Simón P., Hernández M.T., García C. Prokaryotic communities and potential pathogens in sewage sludge: Response to wastewaster origin, loading rate and treatment technology. Science of the Total Environment 2018, 615, 360–368. https://doi.org/10.1016/j.scitotenv.2017.09.240
54. Grabherr M., Haas B., Yassour M., Levin J.Z., Thompson D.A., Amit I., Adiconis X., Raychowdhury R., Zeng Q., Chen Z., Mauceli E., Hacohen N., Gnirke A., Rhind N., di Palma F., Birren B.W., Nusbaum C., Lindblad-Toh K., Friedman N., Regev A. Full-length transcriptome assembly from RNA-Seq data without a reference genome. Nature Biotechnology 2011, 29, 644–652. https://doi.org/10.1038/nbt.1883
55. Griffin P.M., Tauxe R.V. The Epidemiology of Infections Caused by *Escherichia coli* O157: H7, Other Enterohemorrhagic *E. coli*, and the Associated Hemolytic Uremic Syndrome. Epidemiologic Reviews 1991, 13, 60–98. https://doi.org/10.1093/oxfordjournals.epirev.a036079
56. Gu G., Hu J., Cevallos-Cevallos J.M., Richardson S.M., Bartz J.A., van Bruggen A.H.C. Internal Colonization of *Salmonella enterica* Serovar Typhimurium in Tomato Plants. PLOS ONE 2011, 6, 11, e27340. https://doi.org/10.1371/journal.pone.0027340
57. Guo M., Tian F., Wamboldt Y., Alfano, J.R. The Majority of the Type III Effector Inventory of *Pseudomonas syringae* pv. tomato DC3000 Can Suppress Plant Immunity. Molecular Plant Microbe Interaction 2009, 22, 1069–1080. https://doi.org/10.1094/MPMI-22-9-1069
58. Hassani A., Azapagic A., Shokri N. Global predictions of primary soil salinization under changing climate in the 21st century. Nature Communication 2021, 12, 6663. https://doi.org/10.1038/s41467-021-26907-3
59. Hayashi S., Iwamoto Y., Hirakawa Y., Mori K., Yamada N., Maki T., Yamamoto S., Miyasaka H. Plant-Growth-Promoting Effect by Cell Components of Purple Non-Sulfur Photosynthetic Bacteria. Microorganisms 2022, 10, 771. https://doi.org/10.3390/microorganisms10040771
60. Hoagland D.R., Arnon D.I. The water-culture method for growing plants without soil. California Agricultural Experiment Station Circular 1950, 347, 1–32.

61. Hrynkiewicz K., Patz S., Ruppel S. *Salicornia europaea* L. as an underutilized saline-tolerant plant inhabited by endophytic diazotrophs. Journal of Advanced Research 2019, 19, 49-56. https://doi.org/10.1016/j.jare.2019.05.002
62. https://eu-cap-network.ec.europa.eu/sites/default/files/2024-07/eu-cap-network-good-practice-report-salivitae.pdf
63. https://github.com/FelixKrueger/TrimGalore
64. https://github.com/harvardinformatics/TranscriptomeAssemblyTools/tree/master/utilities
65. Huang L., Li J., Ye H., Li C., Wang H., Liu B., Zhang Y. Molecular characterization of the pentacyclic triterpenoid biosynthetic pathway in *Catharanthus roseus*. Planta 2012, 236, 1571–1581. https://doi.org/10.1007/s00425-012-1712-0
66. Ibrahimi M., Korichi W., Hafidi M., Lemee L., Ouhdouch Y., Loqman S. Marine Actinobacteria: Screening for Predation Leads to the Discovery of Potential New Drugs against Multidrug-Resistant Bacteria. Antibiotics 2020, 9, 91. https://doi.org/10.3390/antibiotics9020091
67. Işık H., Topalcengiz Z., Güner S., Aksoy A. Generic and Shiga toxin-producing *Escherichia coli* (O157:H7) contamination of lettuce and radish microgreens grown in peat moss and perlite. Food Control 2020, 107079. https://doi.org/10.1016/j.foodcont.2019.107079
68. Jacob C., Velásquez A.C., Josh N.A., Settles M., Yang He S., Melotto M, Dual transcriptomic analysis reveals metabolic changes associated with differential persistence of human pathogenic bacteria in leaves of *Arabidopsis* and lettuce. G3 Genes|Genomes|Genetics 2021, 11, 12, jkab331. https://doi.org/10.1093/g3journal/jkab331
69. Janssen J.A.M., Rodwell J.S., Garcia Criado M., Arts G.H.P., Bijlsma R.J., Schaminee J.H.J. European Red List of Habitats: Part 2. Terrestrial and freshwater habitats. European Union 2016. https://doi.org/10.2779/091372
70. Jayaraman D., Valdés-Lòpez O., Kaspar C.W., Ané, J.M. Response of *Medicago truntula* seedlings to colonization by *Salmonella enterica* and *Escherichia coli* O157:H7. PLoS One 2014, 9:e87970. https://doi.org/10.1371/journal.pone.0087970
71. Johnson K.W., Carmichael M.J., McDonald W., Rose N., Pitchford J., Windelspecht M., Karatan E., Bräuer, S.L. Increased Abundance of *Gallionella* spp., *Leptothrix* spp. and Total Bacteria in Response to Enhanced Mn and Fe Concentrations in a Disturbed Southern Appalachian High Elevation Wetland. Geomicrobiology Journal 2011, 29, 2, 124–138. https://doi.org/10.1080/01490451.2011.558557
72. Jovanovic J., Ornelis V.F.M., Madder A., Rajkovic A. *Bacillus cereus* food intoxication and toxicoinfection. Comprehensive Review in Food Science and Food Safety 2021, 20, 3719–3761. https://doi.org/10.1111/1541-4337.12785
73. Kai M., Haustein M., Molina F., Petri A., Scholz B., Piechulla B. Bacterial volatiles and their action potential. Applied Microbiology and Biotechnology 2009, 81, 1001–1012. https://doi.org/10.1007/s00253-008-1760-3
74. Kawasaki S., Fratamico P.M., Kamisaki-Horikoshi N., Okada Y., Takeshita K., Sameshima T., Kawamoto S. Development of the multiplex PCR detection kit for *Salmonella* spp., *Listeria monocytogenes*, and *Escherichia coli* O157:H7. Japan Agricultural Research Quarterly 2011, 45, 77–81. doi: 10.6090/jarq.45.77

75. Khan D., Shaw R., Kabiraj A., Paul A., Bandopadhyay R. Microbial inheritance through seed: a clouded area needs to be enlightened. Archives of Microbiology 2025, 207, 23. https://doi.org/10.1007/s00203-024-04225-8
76. Kim D., Paggi J.M., Park C., Bennett C., Salzberg S.L. Graph-based genome alignment and genotyping with HISAT2 and HISAT-genotype. Nature Biotechnology 2019, 37, 907–915. https://doi.org/10.1038/s41587-019-0201-4
77. Kim S., Lee E.Y., Hillman P.F., Ko J., Yang I., Nam S.J. Chemical Structure and Biological Activities of Secondary Metabolites from *Salicornia europaea* L. Molecules 2021, 26, 2252. https://doi.org/10.3390/molecules26082252
78. Kiselev K.V., Nityagovsky N.N., Aleynova O.A. A Method of DNA Extraction from Plants for Metagenomic Analysis Based on the Example of Grape *Vitis amurensis* Rupr. Applied Biochemisry and Microbiology 2023, 59, 361–367. https://doi.org/10.1134/S0003683823030110
79. Klerks M. K., Franz E., van Gent-Pelzer M., Zijlstra C., van Bruggen A.H.C. Differential interaction of *Salmonella enterica* serovars with lettuce cultivars and plant-microbe factors influencing the colonization efficiency. The ISME Journal 2007, 1, 620–631. https://doi.org/10.1038/ismej.2007.82
80. Koilybayeva M., Shynykul Z., Ustenova G., Waleron K., Jońca J., Mustafina K., Amirkhanova A., Koloskova Y., Bayaliyeva R., Akhayeva T., Alimzhanova M., Turgumbayeva A., Kurmangalieyeva G., Kantureyeva A., Batyrbayeva D., Alibayeva Z. Gas Chromatography–Mass Spectrometry Profiling of Volatile Metabolites Produced by Some *Bacillus* spp. and Evaluation of Their Antibacterial and Antibiotic Activities. Molecules 2023, 28, 7556. https://doi.org/10.3390/molecules28227556
81. Kosikowska P., Pikula M., Langa P., Trzonkowski P., Obuchowski M., Lesner A. Synthesis and Evaluation of Biological Activity of Antimicrobial – Pro-Proliferative Peptide Conjugates. PLOS ONE 2015, 10, 10, e0140377. https://doi.org/10.1371/journal.pone.0140377
82. Kulkova I., Dobrzyński J., Kowalczyk P., Bełżecki G., Kramkowski K. Plant Growth Promotion Using *Bacillus cereus*. International Journal of Molecular Sciences 2023, 24, 9759. https://doi.org/10.3390/ijms24119759
83. Kuźniak E., Urbanek H. The involvement of hydrogen peroxide in plant responses to stresses. Acta Physiologiae Plantarum 2000, 22, 195–203. https://doi.org/10.1007/s11738-000-0076-4
84. Kyere E.O., Palmer J., Wargent J.J., Fletcher G.C., Flint S. Colonisation of lettuce by *Listeria monocytogenes*. International Journal of Food Science & Technology 2019, 54, 1, 14–24. https://doi.org/10.1111/ijfs.13905
85. Lee M.H., Jeon H.S., Chung J.H., Roppolo D., Lee H.J., Cho H.J., Tobimatsu Y., Ralph J., Park O.K. Lignin-based barrier restricts pathogens to the infection site and confers resistance in plants. The EMBO Journal 2019, 38, e101948. https://doi.org/10.15252/embj.2019101948
86. Li F., Xiong X.S., Yang Y.Y., Wang J.J., Wang M.M., Tang J.W., Liu Q.H., Wang L., Gu B. Effects of NaCl Concentrations on Growth Patterns, Phenotypes Associated With

Virulence, and Energy Metabolism in *Escherichia coli* BW25113. Frontiers in Microbiology 2021, 12. https://doi.org/10.3389/fmicb.2021.705326
87. Li Q., Zhu X., Xie Y., Liang J. Antifungal properties and mechanisms of three volatile aldehydes (octanal, nonanal and decanal) on *Aspergillus flavus*. Grain & Oil Science and Technology 2021, 4, 3, 131-140. https://doi.org/10.1016/j.gaost.2021.07.002
88. Li Y., Zwe Y.H., Tham C.A.T., Zou Y., Li W., Li D. Fate and mitigation of *Salmonella* contaminated in lettuce (*Lactuca sativa*) seeds grown in a hydroponic system. Journal of Applied Microbiology 2022, 132, 2, 1449–1456. https://doi.org/10.1111/jam.15295
89. Ling L., Wang Y., Cheng W., Jiang K., Luo H., Pang M., Yue R. Research progress of volatile organic compounds produced by plant endophytic bacteria in control of postharvest diseases of fruits and vegetables. World Journal of Microbiology and Biotechnology 2023, 39, 149. https://doi.org/10.1007/s11274-023-03598-0
90. Litalien A., Zeeb B. Curing the earth: A review of anthropogenic soil salinization and plant-based strategies for sustainable mitigation. Science of The Total Environment 2019, 134235. doi: 10.1016/j.scitotenv.2019.1342
91. Ma J., Zhang M., Xiao X., You J., Wang J., Wang T., Yao Y., Tian C. Global Transcriptome Profiling of *Salicornia europaea* L. Shoots under NaCl Treatment. PLoS ONE 2013, 8, 6, e65877. https://doi.org/10.1371/journal.pone.0065877
92. Ma Q.H., Zhu H.H., Qiao M.Y. Contribution of both lignin content and sinapyl monomer to disease resistance in tobacco. Plant Pathology 2018, 67, 642-650. https://doi.org/10.1111/ppa.12767
93. Mapelli F., Marasco R., Rolli E., Barbato M., Cherif H., Guesmi A., Ouzari I., Daffonchio D., Borin S. Potential for Plant Growth Promotion of Rhizobacteria Associated with *Salicornia* Growing in Tunisian Hypersaline Soils. BioMed Research International 2013, 248078. https://doi.org/10.1155/2013/248078
94. Marangi M., Szymanska S., Eckhardt K.U., Beske F., Jandl G., Hrynkiewicz K., Pétillon J., Baum C., Leinweber P. Abundance of Human Pathogenic Microorganisms in the Halophyte *Salicornia europaea* L.: Influence of the Chemical Composition of Shoots and Soils. Agronomy 2024, 14, 2740. https://doi.org/10.3390/agronomy14112740
95. Massawe V.C., Hanif A., Farzand A., Mburu D.K., Ochola S.O., Wu L., Tahir H.A.S., Gu Q., Wu H., Gao X. Volatile compounds of endophytic *Bacillus* spp. have biocontrol activity against *Sclerotinia sclerotiorum*, Phytopathology 2018, 108, 12, 1373-1385. https://doi.org/10.1094/PHYTO-04-18-0118-R
96. Mendes R., Garbeva P., Raaijmakers J.M. The rhizosphere microbiome: Significance of plant beneficial, plant pathogenic, and human pathogenic microorganisms. FEMS Microbiology Reviews 2013, 37, 5, 634–663. doi: 10.1111/1574-6976.12028
97. Miceli, A., Settanni, L. Influence of agronomic practices and pre-harvest conditions on the attachment and development of *Listeria monocytogenes* in vegetables. Annals of Microbiology 2019, 69, 3, 185–199. https://doi.org/10.1007/s13213-019-1435-6
98. Miles J.M., Sumner S.S., Boyer R.R., Williams R.C., Latimer J.G., McKinney J.M. Internalization of *Salmonella enterica* serovar *Montevideo* into greenhouse tomato plants through contaminated irrigation water or seed stock. Journal Food Protection 2009, 72, 4, 849-852. https://doi.org/10.4315/0362-028X-72.4.849

99. Muñoz-Bertomeu J., Lorences E.P. Changes in xyloglucan endotransglucosylase/hydrolase (XTHs) expression and XET activity during apple fruit infection by *Penicillium expansum* Link. A. Europena Journal of Plant Pathology 2014, 138, 273–282. https://doi.org/10.1007/s10658-013-0327-z
100. Nabti E., Schmid M., Hartmann A. Application of Halotolerant Bacteria to Restore Plant Growth Under Salt Stress. In: Maheshwari D., Saraf M. (eds) Halophiles. Sustainable Development and Biodiversity 2015, 6, Springer. https://doi.org/10.1007/978-3-319-14595-2_9
101. Naz R., Khushhal S., Asif T., Mubeen S., Saranraj P., Sayyed R.Z. Inhibition of Bacterial and Fungal Phytopathogens Through Volatile Organic Compounds Produced by *Pseudomonas sp*. In: Sayyed R.Z., Uarrota V.G. (eds) Secondary Metabolites and Volatiles of PGPR in Plant-Growth Promotion. Springer, 2022. https://doi.org/10.1007/978-3-031-07559-9_6
102. Nelson E.B. The seed microbiome: Origins, interactions, and impacts. Plant and Soil 2018, 422, 7–34. https://doi.org/10.1007/s11104-017-3289-7
103. Neshat M., Abbasi A., Hosseinzadeh A., Sarikhani M.R., Chavan D.D., Rasoulnia A. Plant growth promoting bacteria (PGPR) induce antioxidant tolerance against salinity stress through biochemical and physiological mechanisms. Physiology and Molecular Biology of Plants 2022, 28, 347–361. https://doi.org/10.1007/s12298-022-01128-0
104. Niehaus T.D., Elbadawi-Sidhu M., de Crecy-Lagard V., Fiehn O., Hanson A.D. (2017). Discovery of a widespread prokaryotic 5-oxoprolinase that was hiding in plain sight. Journal of Bioogical Chemistry 2017, 292, 39, 16360–16367. https://doi.org/10.1074/jbc.M117.805028
105. Nielsen U.N., Wall D.H., Six J. Soil biodiversity and the environment. Annual Review Environment Resources 2015, 40, 63-90. https://doi.org/10.1146/annurev-environ-102014-021257
106. Ninkuu V., Yan J., Fu Z., Yang T., Ziemah J., Ullrich M.S., Kuhnert N., Zeng H. Lignin and Its Pathway-Associated Phytoalexins Modulate Plant Defense against Fungi. Journal of Fungi 2023, 9, 52. https://doi.org/10.3390/jof9010052
107. Obayomi O., Bernstein N., Edelstein M., Vonshak A., Ghazayarn L., Ben-Hur M., Tebbe C.C., Gillor O. Importance of soil texture to the fate of pathogens introduced by irrigation with treated wastewater. Science of the Total Environment 2019, 653, 886-896. https://doi.org/10.1016/j.scitotenv.2018.10.378
108. Okur B., Örçen N. Soil salinization and climate change. Climate Change and Soil Interactions 2020, 331–350. https://doi.org/10.1016/B978-0-12-818032-7.00012-6
109. Orzoł A., Głowacka K., Pätsch R., Piernik A., Gallegos-Cerda S.D., Cárdenas-Pérez S. The local environment influences salt tolerance differently in four *Salicornia europaea* L. inland populations. Scientific Reports 2025, 15, 13128. https://doi.org/10.1038/s41598-025-97394-5
110. Oyedeji O.A., Afolayan A.J., Eloff J.N. Comparative study of the essential oil composition and antimicrobial activity of *Leonotis leonurus* and *L. ocymifolia* in the Eastern Cape, South Africa. South African Journal of Botany 2005, 71, 1, 114-116. https://doi.org/10.1016/S0254-6299(15)30160-5

111. Ozturk M., Altay V., Orçen N., Yaprak A.E., Tuğ G.N., Güvensen A. A Little-Known and a Little-Consumed Natural Resource: *Salicornia*. In: Ozturk M., Hakeem K., Ashraf M., Ahmad M. (eds) Global Perspectives on Underutilized Crops. Springer, 2018. https://doi.org/10.1007/978-3-319-77776-4_3
112. Painter J.A., Hoekstra R.M., Ayers T., Tauxe R.V., Braden C.R., Angulo F.J., Griffin P.M. Attribution of foodborne illnesses, hospitalizations, and deaths to food commodities by using outbreak data, United States, 1998-2008. Emerging Infectious Diseases 2013, 19, 3, 407–415. https://doi.org/10.3201/eid1903.111866
113. Paseka R.E., White L.A., Van de Waal D., Strauss A.T., González A.L., Everett R.A., Peace A., Seabloom E.W., Frenken T., Borer E.T. Disease-mediated ecosystem services: pathogens, plants, and people. Trends in Ecology & Evolution 2020, 35, 731-743. https://doi.org/10.1016/j.tree.2020.04.003
114. Passardi F., Cosio C., Penel C., Dunand C. Peroxidases have more functions than a Swiss army knife. Plant Cell Reports 2005, 24, 255–265. https://doi.org/10.1007/s00299-005-0972-6
115. Pertea M., Pertea G., Antonescu C., Chang T.C., Mendell J.T., Salzberg S.L. StringTie enables improved reconstruction of a transcriptome from RNA-seq reads. Nature Biotechnology 2015, 33, 290–295. https://doi.org/10.1038/nbt.3122
116. Pesic A., Baumann H.I., Kleinschmidt K., Ensle P., Wiese J., Süssmuth R.D., Imhoff J.F. Champacyclin, a New Cyclic Octapeptide from *Streptomyces* Strain C42 Isolated from the Baltic Sea. Marine Drugs 2013, 11, 4834-4857. https://doi.org/10.3390/md11124834
117. Polito G., Semenzato G., Del Duca S., Castronovo L.M., Vassallo A., Chioccioli S., Borsetti D., Calabretta V., Puglia A.M., Fani R., Piccionello A.P. Endophytic Bacteria and Essential Oil from *Origanum vulgare* ssp. *vulgare* Share Some VOCs with an Antibacterial Activity. Microorganisms 2022, 10, 1424. https://doi.org/10.3390/microorganisms10071424
118. Poveda J. Beneficial effects of microbial volatile organic compounds (MVOCs) in plants 2021, 168, 104118. https://doi.org/10.1016/j.apsoil.2021.104118
119. Puccinelli M., Marchioni I., Botrini L., Carmassi G., Pardossi A., Pistelli L. Growing *Salicornia europaea* L. with Saline Hydroponic or Aquaculture Wastewater. Horticulturae 2024, 10, 196. https://doi.org/10.3390/horticulturae10020196
120. Schmidt R., Cordovez V., De Boer W., Raaijmakers J., Garbeva P. Volatile affairs in microbial interactions. The ISME Journal 2015, 9, 2329-2335. https://doi.org/10.1038/ismej.2015.42
121. Rafanomezantsoa P., El-Hasan A., Voegele R.T. Potential of *Bacillus halotolerans* in Mitigating Biotic and Abiotic Stresses: A Comprehensive Review. Stresses 2025, 5, 24. https://doi.org/10.3390/stresses5020024
122. Rahmani R., Arbi K.E., Aydi S.S., Hzami A., Tlahig S., Najar R., Debouba M. Biochemical composition and biological activities of *Salicornia europaea* L. from southern Tunisia. Journal of Food Measurement and Characterization 2022, 16, 4833–4846. https://doi.org/10.1007/s11694-022-01574-0

123. Rizzo D.M., Lichtveld M., Mazet J.A.K., Togami E., Miller S.A. Plant health and its effects on food safety and security in a One Health framework: four case studies. One Health Outlook 2021, 3, 6. https://doi.org/10.1186/s42522-021-00038-7
124. Rodríguez C.E., Mitter B., Barret M., Sessitsch A., Compant A. Commentary: Seed bacterial inhabitants and their routes of colonization. Plant and Soil 2018, 422, 129–134. https://doi.org/10.1007/s11104-017-3368-9
125. Rojas-Solís D., Santoyo G. Data on the effect of *Pseudomonas stutzeri* E25 and *Stenotrophomonas maltophilia* CR71 culture supernatants on the mycelial growth of *Botrytis cinerea*. Data in Brief 2018, 17, 234-236, https://doi.org/10.1016/j.dib.2018.01.023
126. Romão I.R., do Carmo Gomes J., Silva D., Vilchez J.I. The seed microbiota from an application perspective: an underexplored frontier in plant–microbe interactions. Crop Health 2025, 3, 12. https://doi.org/10.1007/s44297-025-00051-6
127. Saggese A., De Luca Y., Baccigalupi L., Ricca E. An antimicrobial peptide specifically active against *Listeria monocytogenes* is secreted by *Bacillus pumilus* SF214. BMC Microbiology 2022 22, 3. https://doi.org/10.1186/s12866-021-02422-9
128. Samaddar S., Karp D.S., Schmidt R., Devarajan N., McGarvey J.A., Pires A.F.A., Scow K. Role of soil in the regulation of human and plant pathogens: soils' contributions to people. Philosophical Transactions of Royal Society B 2021, B37620200179 http://doi.org/10.1098/rstb.2020.0179
129. Sarma U.P., Bhetaria P.J., Devi P., Varma A. Aflatoxins: implications on health. Indian Journal of Clinical Biochemistry 2017, 32, 124–133. https://doi.org/10.1007/s12291-017-0649-2
130. Saxena R.K., Edwards D., Varshney R.K. Structural variations in plant genomes. Briefings in Functional Genomics 2014, 13, 4, 296–307. https://doi.org/10.1093/bfgp/elu016
131. Scallan E., Hoekstra R.M., Angulo F.J., Tauxe R.V., Widdowson M.A., Roy S.L., Jones J.L., Griffin P.M. Foodborne Illness Acquired in the United States—Major Pathogens. Emerging Infectious Diseases 2011, 17, 7–15. https://doi.org/10.3201/eid1701.p11101
132. Shahid M., Ahmed T., Noman M., Javed M.T., Javed M.R., Tahir M, Shah S.M. Non-pathogenic *Staphylococcus strains* augmented the maize growth through oxidative stress management and nutrient supply under induced salt stress. Annals of Microbiology 2019, 69, 727–739. https://doi.org/10.1007/s13213-019-01464-9
133. Sidstedt M., Rådström P., Hedman J. PCR inhibition in qPCR, dPCR and MPS—mechanisms and solutions. Analytical and Bioanalytical Chemistry 2020, 412, 2009–2023. https://doi.org/10.1007/s00216-020-02490-2
134. Singh A. Soil salinization management for sustainable development: A review. Journal of Environmental Management 2021, 277, 111383. https://doi.org/10.1016/j.jenvman.2020.111383
135. Singh D., Buhmann A.K., Flowers T.J., Seal C.E., Papenbrock J. *Salicornia* as a crop plant in temperate regions: selection of genetically characterized ecotypes and optimization of their cultivation conditions. AoB Plants 2014, 6, plu071. https://doi.org/10.1093/aobpla/plu071

136. Song L., Florea L. Rcorrector: efficient and accurate error correction for Illumina RNA-seq reads. GigaScience 2015, 4, 1, s13742–015–0089–y. https://doi.org/10.1186/s13742-015-0089-y
137. Steffan J.J., Derby J.A., Brevik E.C. Soil pathogens that may potentially cause pandemics, including SARS coronaviruses. Current Opinion in Environmental Science & Health 2020, 17, 35-40. https://doi.org/10.1016/j.coesh.2020.08.005
138. Szymańska S., Deja-Sikora E., Sikora M., Niedojadło K., Mazur J., Hrynkiewicz K. Colonization of Raphanus sativus by human pathogenic microorganisms. Frontiers in Microbiology 2024, 15, 1296372. doi: 10.3389/fmicb.2024.1296372
139. Szymańska S., Płociniczak T., Piotrowska-Seget Z., Hrynkiewicz K. Endophytic and rhizosphere bacteria associated with the roots of the halophyte *Salicornia europaea* L. – community structure and metabolic potential. Microbiological Research 2016, 192, 37-51. https://doi.org/10.1016/j.micres.2016.05.012
140. Tack D.M., Kisselburgh H.M., Richardson L.C., Geissler A., Griffin P.M., Payne D.C., Gleason B.L. Shiga Toxin-Producing *Escherichia coli* Outbreaks in the United States, 2010–2017. Microorganisms 2021, 9, 1529. https://doi.org/10.3390/microorganisms9071529
141. Tao H., Wang S., Li X., Li X., Cai J., Zhao, Wang J., Zeng J., Qin Y., Xiong X., Cai Y. Biological control of potato common scab and growth promotion of potato by *Bacillus velezensis* Y6. Frontiers in Microbiology 2023, 14. https://doi.org/10.3389/fmicb.2023.1295107
142. Truong H.N., Garmyn D., Gal L., Fournier C., Sevellec Y., Jeandroz S., Piveteau P. Plants as a realized niche for *Listeria monocytogenes*. MicrobiologyOpen 2021, 10, e1255. https://doi.org/10.1002/mbo3.1255
143. Truyens S., Weyens N., Cuypers A., Vangronsveld J. Bacterial seed endophytes: Genera, vertical transmission and interaction with plants. Environmental Microbiology Reports 2015, 7, 1, 40–50. https://doi.org/10.1111/1758-2229.12181
144. Turcios A.E., Braem L., Jonard C., Lemans T., Cybulska I., Papenbrock J. Compositional Changes in Hydroponically Cultivated *Salicornia europaea* at Different Growth Stages. Plants 2023, 12, 2472. https://doi.org/10.3390/plants12132472
145. Tyler H.L., Triplett E.W. Plants as a Habitat for Beneficial and/or Human Pathogenic Bacteria. Annual Review of Phytopathology 2008, 46, 53–73. https://doi.org/10.1146/annurev.phyto.011708.103102
146. Ueda K., Beppu T. Antibiotics in microbial coculture. The Journal of Antibiotics 2017, 70, 361–365. https://doi.org/10.1038/ja.2016.127
147. Ungar, I.A., Benner D.K., McGraw D.C. The Distribution and Growth of *Salicornia Europaea* on an Inland Salt Pan. Ecology 1979, 60, 2, 329–36. https://doi.org/10.2307/1937662
148. Varandas R., Barroso C., Conceição I.L., Egas C. Molecular insights into *Solanum sisymbriifolium*'s resistance against *Globodera pallida* via RNA-seq. BMC Plant Biology 2024, 24, 1005. https://doi.org/10.1186/s12870-024-05694-1
149. Vengosh A. Salinization and Saline Environments. Treatise on Geochemistry 2014, 325–378. doi: 10.1016/b978-0-08-095975-7.00909-8

150. Veselova M.A., Plyuta V.A., Khmel I.A. Volatile compounds of bacterial origin: structure, biosynthesis, and biological activity. Microbiology 2019, 88, 261-274. https://doi.org/10.1134/S0026261719030160
151. Vojkovska H., Kubikova I., Kralik P. Evaluation of DNA extraction methods for PCR-based detection of *Listeria monocytogenes* from vegetables. Letters in Applied Microbiology 2015, 60, 3, 265–272. https://doi.org/10.1111/lam.12367
152. Wang A.H., Yang L., Yao X.Z., Wen X.P. Overexpression of the pitaya phosphoethanolamine N-methyltransferase gene (HpPEAMT) enhanced simulated drought stress in tobacco. Plant Cell, Tissue and Organ Culture 2021, 146, 29–40. https://doi.org/10.1007/s11240-021-02040-3
153. Wang E., Liu X., Si Z., Li X., Bi J., Dong W., Chen M., Wang S., Zhang J., Song A., Fan F. Volatile Organic Compounds from Rice Rhizosphere Bacteria Inhibit Growth of the Pathogen *Rhizoctonia solani*. Agriculture 2021, 11, 368. https://doi.org/10.3390/agriculture11040368
154. Wang J., Raza W., Jiang G., Yi Z., Fields B., Greenrod S., Friman V.P., Jousset A., Shen Q., Wei Z. Bacterial volatile organic compounds attenuate pathogen virulence via evolutionary trade-offs. The ISME Journal 2023, 17, 3, 443–452. https://doi.org/10.1038/s41396-023-01356-6
155. Weisskopf L., Schulz S., Garbeva, P. Microbial volatile organic compounds in intra-kingdom and inter-kingdom interactions. Nature Reviews Microbiology 2021, 19, 391–404. https://doi.org/10.1038/s41579-020-00508-1
156. Weng J.K., Chapple C. The origin and evolution of lignin biosynthesis. New Phytologist 2010, 187, 273–85. doi: 10.1111/j.1469-8137.2010.03327.x
157. Yan J., Su P., Li W., Xiao G., Zhao Y., Ma X., Wang H., Nevo E., Kong L. Genome-wide and evolutionary analysis of the class III peroxidase gene family in wheat and *Aegilops tauschii* reveals that some members are involved in stress responses. BMC Genomics 2019, 20, 666. https://doi.org/10.1186/s12864-019-6006-5
158. Yu Y., Gui Y., Li Z., Jiang C., Guo J., Niu D. Induced Systemic Resistance for Improving Plant Immunity by Beneficial Microbes. Plants 2022, 11, 3, 386. https://doi.org/10.3390/plants11030386
159. Zeng Q., Zhao Y., Shen W., Han D., Yang M. Seed-to-seed: Plant core vertically transmitted microbiota. Journal of Agricultural and Food Chemistry 2023, 71, 49, 19255–19264. https://doi.org/10.1021/acs.jafc.3c07092
160. Zhang G., Bai J., Zhai Y., Jia J., Zhao Q., Wang W., Hu X. Microbial diversity and functions in saline soils: A review from a biogeochemical perspective. Journal of Advanced Research 2024, 59, 129-140. https://doi.org/10.1016/j.jare.2023.06.015
161. Zhang J.H., Sun H.L., Chen S.Y., Zeng L., Wang T.T. Anti-fungal activity, mechanism studies on α-Phellandrene and Nonanal against *Penicillium cyclopium*. Botanical Studies 2017, 58, 13. https://doi.org/10.1186/s40529-017-0168-8
162. Zhao Q., Cao J., Cai X., Wang J., Kong F., Wang D., Wang J. Antagonistic Activity of Volatile Organic Compounds Produced by Acid-Tolerant *Pseudomonas protegens* CLP-6 as Biological Fumigants to Control Tobacco Bacterial Wilt Caused by *Ralstonia*

solanacearum. Applied and Environmental Microbiology 2023, 89:e01892-22. https://doi.org/10.1128/aem.01892-22

163. Zhao Q., Dixon R.A. Altering the cell wall and its impact on plant disease: from forage to bioenergy. Annual Review of Phytopathology 2014, 52, 69–91. https://doi.org/10.1146/annurev-phyto-082712-102237

164. Zheng J., Allard S., Reynolds S., Millner P., Arce G., Blodgett R.J., Brown E.W. Colonization and internalization of *Salmonella enterica* in tomato plants. Applied Environmental Microbiology 2013, 79, 8, 2494–2502. https://doi.org/10.1128/AEM.03704-12

165. Zhou P., Bu Y.X., Xu L., Xu X.W., Shen H.B. Understanding the mechanisms of halotolerance in members of *Pontixanthobacter* and *Allopontixanthobacter* by comparative genome analysis. Frontiers in Microbiology 2023, 14, 1111472. doi: 10.3389/fmicb.2023.1111472

166. Zieniuk B., Bętkowska A. Mixture Design as a Tool for Optimization of Antimicrobial Activity of Selected Essential Oils. Biology and Life Sciences Forum 2021, 6, 98. https://doi.org/10.3390/Foods2021-11018

Appendix I

Publication (P1)

Marangi, M.; Szymanska, S.; Eckhardt, K.-U.; Beske, F.; Jandl, G.; Hrynkiewicz, K.; Pétillon, J.; Baum, C.; Leinweber, P. Abundance of Human Pathogenic Microorganisms in the Halophyte *Salicornia europaea* L.: Influence of the Chemical Composition of Shoots and Soils. *Agronomy* 2024, *14*, 2740. https://doi.org/10.3390/agronomy14112740

agronomy

MDPI

Article

Abundance of Human Pathogenic Microorganisms in the Halophyte *Salicornia europaea* L.: Influence of the Chemical Composition of Shoots and Soils

Matteo Marangi [1,2], Sonia Szymanska [1], Kai-Uwe Eckhardt [2], Felix Beske [2], Gerald Jandl [2], Katarzyna Hrynkiewicz [1], Julien Pétillon [3,4], Christel Baum [2] and Peter Leinweber [2,5,*]

[1] Department of Microbiology, Nicolaus Copernicus University, 87-100 Torun, Poland; matteomarangi@doktorant.umk.pl (M.M.); soniasz@umk.pl (S.S.); hrynk@umk.pl (K.H.)
[2] Soil Science, Faculty of Agricultural and Environmental Sciences, University of Rostock, 18051 Rostock, Germany; kai-uwe.eckhardt@uni-rostock.de (K.-U.E.); felix.beske2@uni-rostock.de (F.B.); gerald.jandl@uni-rostock.de (G.J.); christel.baum@uni-rostock.de (C.B.)
[3] UMR CNRS ECOBIO (Ecosystèmes, Biodiversité, Evolution), University of Rennes, 35042 Rennes, France; julien.petillon@univ-rennes.fr
[4] Institute for Coastal and Marine Research, Nelson Mandela University, Gqeberha 6031, South Africa
[5] Bioeconomy Research Institute, Academy of Agriculture, Vytautas Magnus University, Studentu 11-530, Akademija, LT-53361 Kaunas, Lithuania
* Correspondence: peter.leinweber@uni-rostock.de

Abstract: *Salicornia europaea* L. is a halophilic plant species belonging to Chenopodiaceae, whose shoots are used as a vegetable. Since the shoots can be eaten raw, the objective of the present study was to investigate possible controls on the abundance of human pathogenic microorganisms (HPMOs) in the shoots as a health risk. For this reason, the molecular-chemical composition of shoots, site-specific soil organic matter (bulk and rhizosphere), and soil pH and salinity were analyzed. Plant and soil samples were taken from two test sites with differing salinity levels in France (a young and an old marsh). We hypothesized that the chemical traits of plants and soils could suppress or promote HPMOs and, thus, serve as risk indicators for food quality. The chemical traits of shoots and bulk and rhizosphere soil were measured through thermochemolysis using gas chromatography/mass spectrometry (GC/MS). The densities of cultivable HPMOs (*Salmonella enterica*, *Escherichia coli*, and *Listeria monocytogenes*) were determined in plant shoots, rhizosphere soil, and bulk soil using selective media. Negative correlations between lignin content in the shoots and the abundance of *S. enterica*, as well as between lignin content in bulk soil and the abundance of *E. coli*, are explained by the lignin-based rigidity and its protective effect on the cell wall. In the shoot samples, the content of lipids was positively correlated with the abundance of *E. coli*. The abundance of *E. coli*, *S. enterica*, and *L. monocytogenes* in bulk soil decreased with increasing soil pH, which is linked to increased salinity. Therefore, soil salinity is proposed as a tool to decrease HPMO contamination in *S. europaea* and ensure its food safety.

Keywords: human pathogenic bacteria; lipids; lignin; gas chromatography-mass spectrometry; *Salicornia europaea*

check for updates

Citation: Marangi, M.; Szymanska, S.; Eckhardt, K.-U.; Beske, F.; Jandl, G.; Hrynkiewicz, K.; Pétillon, J.; Baum, C.; Leinweber, P. Abundance of Human Pathogenic Microorganisms in the Halophyte *Salicornia europaea* L.: Influence of the Chemical Composition of Shoots and Soils. *Agronomy* **2024**, *14*, 2740. https://doi.org/10.3390/agronomy14112740

Academic Editor: Carla Gentile

Received: 1 October 2024
Revised: 13 November 2024
Accepted: 18 November 2024
Published: 20 November 2024
Corrected: 29 April 2025

1. Introduction

Salicornia europaea L. (also known as glasswort or sea asparagus) is a halophilic plant species belonging to Chenopodiaceae [1,2]. It prefers temperate and subtropical climates [3,4]. This plant has an important economic value as a healthy food source [5] and is also used as forage and in pharmaceutics and cosmetics [6,7]. It is increasingly grown in open fields and greenhouses for edible or non-edible purposes, and can be irrigated with salt water, sea water, or wastewater with a moderate to high salinity, which cannot be used for other crop species [8]. Increasing soil salinity and scarcity of fresh water, which are the result of climate

change and anthropic activities, make halophytic species an alternative food source for which salt water is used [8]. The most important molecules commonly found in halophytes are phenolic compounds, polysaccharides, and lipids [9]. Lignin is a phenolic polymer that confers rigidity and protection to the cell wall [10,11]. It has been demonstrated that plants under attack by pathogens have a higher lignin content due to increased transcription of genes for lignin biosynthesis [12–14]. Lignin acts as a mechanical barrier that restricts the spread of pathogens, such as pathogenic bacteria, within the extracellular space of the plant tissues. When plants are under attack by pathogens, they induce lignification, a process that strengthens the cell wall's resistance to invasion [12]. Lipids have an important role in conferring resistance to plants against their pathogens [15,16] but are also produced in response to microbial colonization. During pathogen attack, the plant lipid profile is altered, resulting in modifications to plant membrane fluidity and lipid biosynthesis [17]. The genes that encode enzymes involved in lipid metabolism are often upregulated upon infection, leading to synthesis, modification, or re-allocation of lipid-derived molecules, which are crucial for establishing membrane integrity and function during the infection process [18]. The special properties of halophytes can also affect the level of infection by human pathogens of concern (HPMOs—human pathogenic microorganisms), which is especially important when they can be consumed in unprocessed forms, the preparation of which lacks steps to inactivate the pathogens [19]. Among the many enteric pathogens associated with ready-to-eat fresh produce (RTEFP) contamination, *Escherichia coli*, *Salmonella* spp., *Listeria monocytogenes*, and *Bacillus* spp. were the most commonly reported in previously published studies [19]. Certain HPMO bacteria, such as *Salmonella* sp. and *E coli*, use plants as vectors between animal hosts. These pathogens adhere to the life cycle patterns of plant-associated bacteria and can establish themselves in agricultural production areas, which may pose food safety risks, especially considering global warming [20]. HPMOs were found to be able to colonize many parts of different plant species including the epidermis, cortex, vascular tissue, pith, and apoplastic fluid in spinach and peanut [21–24]. Until now, no studies have shown the colonization of *S. europaea* by HPMOs. Furthermore, to the best of our knowledge, the relationships between the composition of plant and soil organic matter (SOM) and the abundance of HPMOs have not yet been investigated for *S. europaea*. Therefore, the aim of the present study is to investigate the chemical composition of plant and soil material and the abundance of HPMOs in order to deduce possible control tools for food safety in this regard. We hypothesize that lignin and lipids might be indicators of a suppressed abundance of HPMOs due to their role in plant protection and partly high resistance to decomposition.

2. Materials and Methods

2.1. Test Sites Description, Environmental Conditions and Sampling

The plant and soil samples were collected at two test sites in France in October 2022, which were selected based on the differing salinity levels between a young and an old marsh. Three plots (1 m × 1 m) were delineated at each site, from which five plants were taken, together with the soil adjacent to their roots (a total of 15 plants per site). The individual plots were located at a distance of 5–10 m from each other. In addition, a bulk soil sample (10 cm × 10 cm × 10 cm; approximately 200 g soil per sample) was taken at each site (a total of five samples per plot). Each sample was stored in a plastic bag and sent immediately by courier at 4 °C to the Department of Microbiology at Nicolaus Copernicus University in Torun (Poland) for further analyses. All root samples were collected in accordance with institutional, national, and international guidelines and legislation with the permission of the General Director for Environmental Protection (DZP-WG.6400.13.2022.EP.1). One test site (F1) was located in the estuary of L'Ilet in the municipality of Plurien (48.634379, −2.415823), and the second site (F2) was located in a salt marsh in the municipality of Beaussais-sur-Mer (48.582263, −2.159779). Both sites have a temperate oceanic climate (sub-type Cfb in the Köppen classification) but differ in their history. F1 is an old, mature salt marsh that developed from a sandy substrate (which is rather unusual for this type of

habitat). It is dominated by *Atriplex portulacoides*, and *Salicornia* stands that occur along the (natural) drainage creeks [25]. F2 is a recently (2020) created young salt marsh, developing on a classical muddy substrate, where pioneer stands of *Salicornia* were found all over the area.

2.2. Thermochemolysis and Pyrolysis-Gas Chromatography/Mass Spectrometry

For thermochemolysis, about 10 mg of plant material and 100 mg of soil, respectively, were inserted into Pasteur pipettes (ISO 7712, 150 mm, [26]) with the tips broken off. Tetramethylammonium hydroxide (TMAH) in water (25%) was added to the sample using a microsyringe (30 µL for plant material and 60 µL for soil). Afterwards, the pipette was connected to a second pipette filled with activated coarse charcoal and a small amount of glass wool at the tip. The whole system was flushed with a nitrogen stream; 5 min after adding TMAH, the sample was heated to 220 °C for 6 min using a hot air gun. After allowing it to cool for 5 min, the sample was scratched into a 4 mL vial and both pipettes were rinsed with 1.5 mL each of a dichlormethane/methanol mixture (4:1). The vial was placed in an ultrasonic water bath of 35 °C for 5 min, after which the suspension was allowed to settle for 55 min. For GC/MS, 1 µL from the upper part of the solution was injected into a Thermo Scientific Trace 1310-GC (Thermo Fisher Scientific, Waltham, MA USA 02451) equipped with a 60 m BP5 column (0.25 mm i.d., 0.25 µm coating) at an injector temperature of 300 °C. The carrier gas, helium 5.0, was set up with a constant flow of 1 mL min^{-1}. Following split injection for up to 45 s (splitless), the split ratio was 1:100 from 45 s up to 90 s and 1:5 from 90 s onward. The temperature program was set as 5 min at 100 °C, and was subsequently heated at a rate of 5 K min^{-1} to 280 °C for a total measurement time of 120 min. The GC was connected to a Thermo Scientific DFS magnetic sector MS (Thermo Fisher Scientific, Waltham, MA, USA, 02451). The conditions for mass spectrometric detection in the electron impact mode were as follows: 4.7 kV accelerating voltage, 70 eV electron energy, 1.2 kV multiplier voltage, m/z 48–600 mass range, 0.5 s (mass decade)$^{-1}$ scan rate, and 0.6 s interscan time. The identified single compounds were summed into the compound classes of carbohydrates, lignin, and lipids. The peak areas of each compound class to the total peak area of the carbohydrates, lignin, and lipids are given in %. Peaks were assigned by comparing spectra with the NIST 2017 database using Thermo Xcalibur version 2.2.

2.3. Abundance of HPMOs in Bulk Soil, Rhizosphere, Shoot and Root of S. europaea

Three plots (A, B, C) with five replicates per plot were considered for each site. Rhizosphere and/or bulk soil (1 g) was transferred into falcon tubes for the next part of the experiment. Separated plant organs (roots and shoots) were surface sterilised with 70% ethanol (3 min), rinsed three times with 2% NaCl (1 min each time), treated with 7.5% H_2O_2 (3 min), and washed three times with 2% NaCl (1 min each time). Then, dried shoots and roots (1 g of fresh biomass) were homogenized in 2% NaCl (1:9 ratio) using a sterile mortar and pestle. Serial dilutions for plant (10^{-1}–10^{-2}) and soil (10^{-1}–10^{-3}) samples were prepared and 100 µL of dilutions were plated in triplicate on selective media for the abundance of HPMOs: *L. monocytogenes* (Chromogenic *Listeria* acc. to Ottaviani and Agostii LAB-AGAR™ Base and Chromogenic *Listeria* Supplement acc. to ISO 11290-1:2017 [27], Biomaxima, Lublin, Poland), *E. coli* (*E. coli* Chromogenic Medium, Biomaxima, Lublin, Poland), *S. enterica* (Chromogenic, *Salmonella* LAB-AGAR™ and *Salmonella* Chromogenic Supplement, EN-ISO 6579 [28], Biomaxima, Lublin, Poland), and *B. cereus* (*B. cereus* Selective LAB—AGAR™ Base and *B. cereus* Supplement, EN ISO 7932:2004 [29], Biomaxima, Lublin, Poland). The plates were incubated for seven (for *S. enterica*, *L. monocytogenes*, *E. coli*) and two days (for *B. cereus*) at 37 °C. The colony forming units (CFU) were counted and calculated per 1 g of dry weight. The CFU g^{-1} was transformed into $\log_{10}$.

2.4. Bulk and Rhizosphere Soil Analysis

The soil samples were air-dried at room temperature and passed through a 2 mm mesh sieve to remove debris. Total carbon (C_t) and total nitrogen (N_t) were determined using Elementar Vario CNS analyser (Elementar Analysensysteme GmbH, Langenselbold, Germany). The calcium carbonate ($CaCO_3$) content of the soil was determined by the volumetric method using a Scheibler apparatus [30]. Total inorganic carbon (TIC) was calculated from the calcium carbonate content. Total organic carbon (TOC) was calculated as the difference between TC and TIC. Bio-available phosphorus (P_{ca}) was determined colorimetrically by the citrate method using a Rayleigh UV-1601 spectrophotometer (Beifen-Ruili Analytical Instrument Co., Ltd., Beijing, China) [31]. The saturated paste extracts were prepared according to the methodology of van Reeuwijk [31]. The pH ($CaCl_2$) was measured potentiometrically using a CP-551 Elmetron pH meter. Electrical conductivity (EC) was determined at 25 °C using the conductometric method with a CPC-401 conductivity meter (Elmetron Ltd., Zabrze, Poland). The concentrations of Mg and Ca were determined by atomic absorption spectrometry (AAS), while the concentrations of K and Na were determined by optical emission spectrometry (OES) using a SOLAAR Unicam 969 (Unicam Ltd., Cambridge, UK) flame spectrometer. The concentration of bicarbonates (HCO_3^-) was determined by titration with 0.1 M HCl [32]. The concentration of sulphate (SO_4^{2-}), chloride (Cl^-), and bromide (Br^-) was determined by ion chromatography using a Thermo Scientific Dionex Aquion system (Thermo Fisher Scientific Inc., Waltham, MA, USA, 02451). Soil texture was measured using 10 g of bulk soil from each test site as follows: Carbonate was dissolved in the soil sample taken from the young marsh by incubation in a 1:3 dilution with 10% HCl for 60 min. This suspension was filtrated, and the filtrate was collected in a tube, to which NH_4^+ oxalate was added. For the organic matter destruction, 10 mL bi-distilled water (H_2O_{bidest}) and about 300 to 500 mL H_2O_2 (30%) were added to the remaining soil under heat (ca 95 °C) for approximately 2 weeks (until no reaction was visible). The resulting dry samples were then transferred to new vessels. For sedimentation preparation, the remaining soil was weighed, and 25 mL pyrophosphate (0.1 M) was added to the samples, mixing the solution thoroughly. Disaggregation was carried out in a supersonic bath (15 min in H_2O_{bidest}). For the final step, sedimentation, the samples were transferred to a 1 L cylinder, with H_2O_{bidest} added, and placed in a Sedimat instrument (Sedimentation device; Sedimat 4–12 Umwelt-Geräte-Technik GmbH (Hallbergmoos, Germany). Sedimentation took place in a 25 °C water bath for one night. The instrument automatically separated the silt and clay fractions and transferred them to vessels of known mass, where the samples were dried and weighed. The remaining soil in the cylinder was transferred to a sieve (0.063 mm mesh size) to determine the sand fraction. Finally, the total texture fraction composition was calculated.

2.5. Statistical Analyses

The results showing the abundance of HPMOs in the selective media, the % peak area of lipids and lignin from GC/MS, and the log pH values of bulk soil and rhizosphere soil samples were analysed by evaluating the Pearson coefficient of correlation (r) and the significance of correlation ($p < 0.05$) in R 5.2-0 (RStudio, Hmisc package). Statistical analyses of carbohydrate, lignin, and lipid content in shoots, bulk soil, and rhizosphere soil were performed using R (RStudio, agricolae package) in order to mark the significance: the raw data were normally distributed in all variants (Shapiro–Wilk test, $p > 0.05$); the equality of variance was performed according to Levene test ($p > 0.05$); the significance was evaluated using one-way ANOVA analyses and the Tukey test ($p < 0.05$). Correlation graphs were calculated in R version 4.4.0 with package corrr 0.4.4.

3. Results

At the old marsh site, the bulk soil and the rhizosphere soil were slightly alkaline (pH 7.4–7.8) with the exception of rhizosphere soil at plot A (neutral, pH 6.6–7.3). At the young marsh site, the bulk soil was slightly alkaline (pH 7.4–7.8) while the rhizosphere soil

was moderately alkaline (pH 7.9–8.4) (Table 1). With regard to electrical conductivity at the old marsh site, the bulk soil was moderately saline (8 < EC < 16 mS cm^{-1}) and the rhizosphere soil was strongly saline (EC ≥ 16), with the exception of plot C (moderately saline, 8 < EC < 16). At the young marsh site, the bulk soil was strongly saline (EC ≥ 16) and the rhizosphere soil was moderately saline (8 < EC < 16).

Table 1. Physicochemical parameters of the bulk and rhizosphere soils (RS) at an old, mature salt marsh (OM) and a recently (2020) created salt marsh (YM) in France (mean values and standard deviations values are presented). Significant differences ($p < 0.05$, one-way ANOVA with Newman–Keuls post hoc comparisons) between sites (OM, YM)) are marked by different letters. The following parameters are included: C_{org}—organic carbon, N_t—total nitrogen, the C:N ratio, the calcium carbonate ($CaCO_3$) content, the P_{citr}—concentration, the pH values, the electroconductivity (EC), the chloride—(Cl^-), sulfate—(SO_4^{2-}), hydrogen carbonate—(HCO_3^-), bromide—(Br^-), calcium-, magnesium, sodium, and potassium concentrations.

	Old Marsh Soil	Old Marsh RS	Young Marsh Soil	Young Marsh RS
C_{org} (%)	1.8 ± 1.6 a	1.2 ± 2 a	2.8 ± 0.6 a	3.7 ± 0.2 a
N_t (%)	0.2 ± 0.1 ab	0.2 ± 0.1 b	0.4 ± 0 ab	0.4 ± 0 a
C:N	7.2 ± 3.1 a	4.3 ± 5.4 a	7.6 ± 0.7 a	8.5 ± 0.6 a
$CaCO_3$ (%)	6.9 ± 2.1 c	13.2 ± 3.8 c	27.5 ± 0.7 b	35.4 ± 2.8 a
P_{citr} (mg kg^{-1})	257 ± 72.8 b	147.4 ± 12.6 b	413.8 ± 79.5 a	285.8 ± 12.6 ab
pH	7.6 ± 0.1 ab	7.5 ± 0.3 ab	7.5 ± 0.1 b	8.1 ± 0.1 a
EC (mS cm^{-1})	10.4 ± 1.6 b	15.6 ± 6.3 ab	24.4 ± 2.3 a	14.1 ± 1.6 b
Cl^- (mg L^{-1})	2933.8 ± 488.8 b	4910.5 ± 2385.9 ab	7745.1 ± 1067.1 a	4435.5 ± 820.6 ab
SO_4^{2-} (mg L^{-1})	440.5 ± 74.1 b	638.6 ± 286.6 b	2409.4 ± 271.7 a	721.5 ± 116.3 b
HCO_3^- (mg L^{-1})	252.6 ± 58 b	462.6 ± 74.2 a	439.6 ± 42 a	427.4 ± 69 a
Br^- (mg L^{-1})	9.7 ± 2.5 b	18.5 ± 8.2 ab	22.9 ± 2.4 a	13 ± 2.2 ab
Ca (mg L^{-1})	63.8 ± 26.8 b	73.8 ± 33.5 b	547.7 ± 76.3 a	156 ± 20 b
Mg (mg L^{-1})	95.9 ± 36.6 b	131.2 ± 70.6 b	549.7 ± 61.6 a	233.9 ± 35.4 b
Na (mg L^{-1})	964.6 ± 351.1 b	1418.5 ± 681 b	3753.5 ± 359.7 a	1795.4 ± 293.8 b
K (mg L^{-1})	71.4 ± 65.6 a	74.9 ± 29.5 a	160.3 ± 29.2 a	154.8 ± 1.4 a

The soil texture at the OM site was loamy sand/clayey sand while that at the YM site was loamy silt/clayey silt (Table 2).

Table 2. Proportions of particle-size fractions (%) and classification of the bulk soil texture at an old, mature salt marsh (Old marsh) and a recently (2020) created salt marsh (Young marsh) in France.

Particle-Size Fraction	Old Marsh	Young Marsh
Clay	13.9	18.7
Fine silt	2.9	3.2
Medium silt	4.6	12.6
Coarse silt	17.9	41.9
Fine sand	60.7	23.6
Texture class	Loamy sand/clayey sand	Loamy silt/clayey silt

Statistical analyses of carbohydrate, lipid, and lignin content in shoots, bulk soil, and rhizosphere soil for the two sites (old marsh and young marsh) (Table S4) in France revealed no statistically significant differences in carbohydrate content across all sample types and locations (Figure 1a). However, lignin content analysis (Figure 1b) yielded significant differences ($p < 0.05$) between shoots and rhizosphere soil at both test sites. Notably, the rhizosphere soil consistently exhibited the highest lignin content, while shoots had markedly lower levels. Furthermore, a significant difference ($p < 0.05$) in lipid content was observed between bulk soil samples from the two test sites (Figure 1c). Specifically, the bulk soil at the young marsh site contained a higher concentration of lipids compared to the old marsh site.

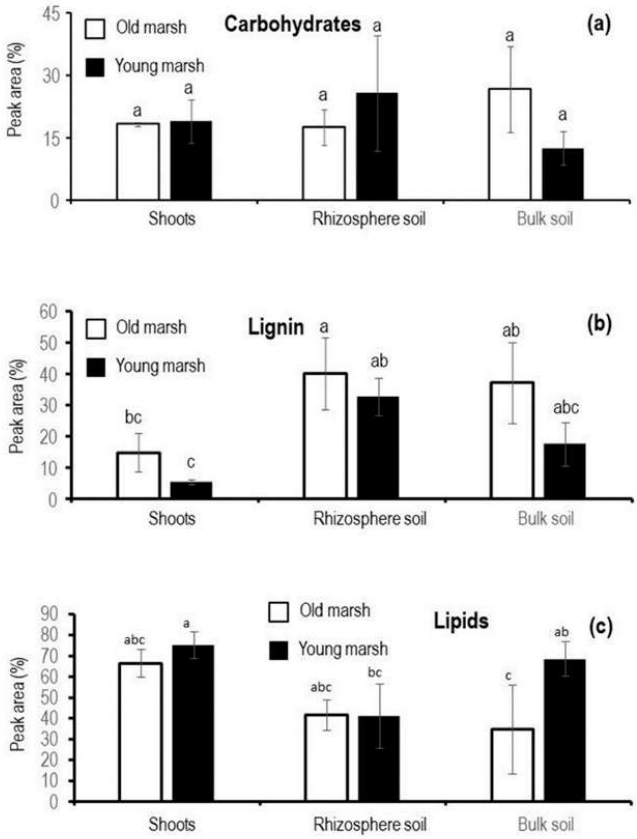

Figure 1. Relative abundance (% peak area) of (**a**) carbohydrates, (**b**) lignin, and (**c**) lipids in shoots, rhizosphere soil, and bulk soil as mean values with standard deviation at an old, mature salt marsh (Old marsh) and a recently (2020) created salt marsh (Young marsh) in France. Different letters indicate significance of differences between samples.

In shoots (Table S1), the abundance of *S. enterica* was negatively correlated with the content of lignin (p = 0.0130; r = −0.82) (Figure 2a), while the abundance of *E. coli* was positively correlated with the content of lipids (p = 0.0304; r = 0.75) (Figure 2b).

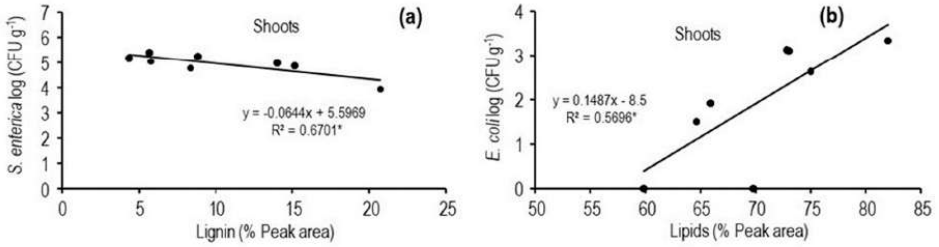

Figure 2. Correlation between (**a**) the log (CFU g^{-1}) of *S. enterica* and the lignin (% Peak area) content in shoots of *S. europaea*; and (**b**) between the log (CFU g^{-1}) of *E. coli* and the lipid (% Peak area) content in shoots of *S. europaea*. * means significance level of correlation coefficient is 0.05

In the data set from bulk soil samples (Table S3), lignin content (% peak area) was negatively correlated (p = 0.0494; r = −0.81) with the abundance of *E. coli* log (CFU g^{-1}) (Figure 3a). Furthermore, pH values and the abundance of *E. coli* (p = 0.0306; r = −0.85) (Figure 3b) and of *L. monocytogenes* (p = 0.0013; r = −0.97) (Figure 3c) and *S. enterica* (p = 0.0283; r = −0.86) (Figure 3e) were negatively correlated. In the rhizosphere soil (Table S2) we found a positive correlation (p = 0.0356; r = 0.84) between the colonisation density of *L. monocytogenes* and the pH (Figure 3d). The correlation network graph (Figure 3f) visualizes that there were strong and weak relationships between the data determined for the bulk and rhizosphere soil samples.

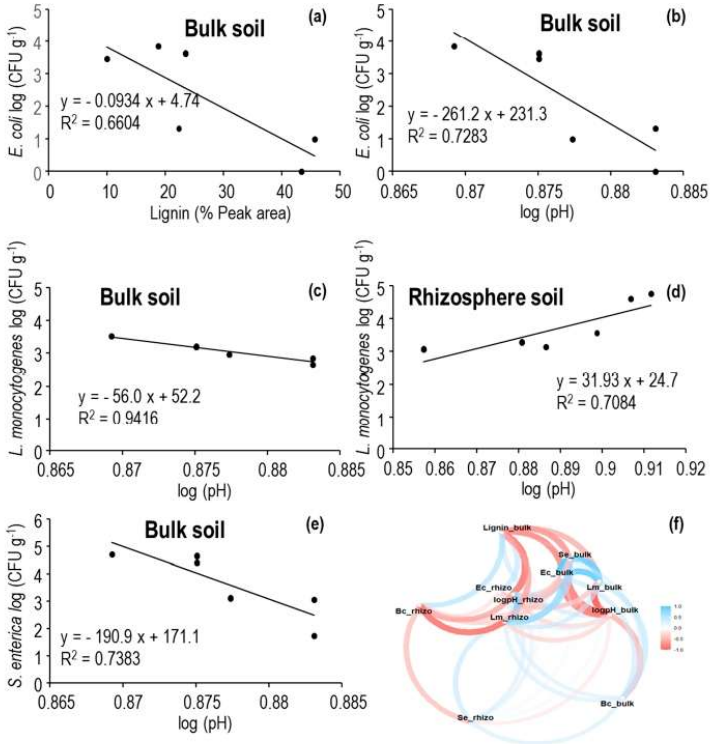

Figure 3. Correlation between the lignin content (% peak area) and the abundance of *E. coli* log (CFU g^{-1}) (**a**), between the pH and *E. coli* log (CFU g^{-1}) (**b**), between the pH value and *L. monocytogenes* log (CFU g^{-1}) (**c**), and between the pH value and *S. enterica* log (CFU g^{-1}) (**e**), and in the rhizosphere soil, between the colonisation density of *L. monocytogenes* log (CFU g^{-1}) and the pH (**d**), and visualization of interdependencies between these data in a correlation network graph (**f**).

4. Discussion

The abundance of HPMOs is affected by environmental conditions and the specific controls for defined bacterial species were investigated in the present study. The results of the present study focus on soil characteristics and microbial dynamics in old marsh and young marsh sites in France, as well as on their potential implications for HPMOs. According to our results (Figure 1), the lignin content found in shoots was lower than in the rhizosphere soil, suggesting both that *S. europaea* has a low lignin content and that the rhizosphere soil is a complex system where the activity of the plant roots plays a crucial role. This is confirmed by the same significant difference at both sites analysed in France. The low lignin content in *S. europaea* (Figure 1) confirms results reported by other studies where *S. europaea* was compared to other halophilic plants [33,34]. Until now, no studies

have shown the colonization of *S. europaea* by HPMOs. Furthermore, to the best of our knowledge, the relationships between the composition of plant and soil organic matter (SOM) and the abundance of HPMOs have not yet been investigated for *S. europaea*. The negative correlation between lignin content and the abundance of *S. enterica* in shoots of *S. europaea* and between the abundance of *E. coli* and lignin content in bulk soil suggest that lignin or associated compounds may have antimicrobial properties against these pathogens. Indeed, polyphenols in lignin can damage bacterial cell walls, causing lysis and leakage of internal fluids [35]. While lignin's role in plant defence against plant pathogens is documented as explained in detail below, the impact of lignin on HPMOs within plant tissues has still not been tested. Lignin has been reported to confer resistance to both abiotic and biotic stress [36]. Among these, the growth of plant pathogens was inhibited in plants with high lignin presence [37]. Interestingly, the attack of plant pathogens stimulates the plants to produce more lignin to reinforce their cell walls and block the traffic of the plant pathogens [12,38]. In halophilic plants like *S. europaea*, lignin plays a crucial role in strengthening the cell wall in response to salt stress [39,40]. It has been demonstrated that *Bacillus subtilis*, under specific saline conditions, increased the quantity of lignin in common bean roots, strengthening the cell walls, which was connected to a better plant growth and reduction of oxidative damages [41]. The transcriptomic profile of *Eutrema salsugineum*, another halophilic plant, revealed that salt stress led to the over-expression of lignin-biosynthesis genes, suggesting that enhanced lignin accumulation could have an active role in response to a salt environment [42]. Quantitative trait loci (QTLs) analyses revealed that crown rust resistance mapped onto LG3 and LG7 loci; coincidentally, those mapped genes were connected to cell wall development, including lignin biosynthesis [43]. Interestingly, the importance of lignin is not only linked with stronger immune systems for plants, but also with healthy diet for humans, since lignin derivatives can reduce blood cholesterol, obesity, and diabetes [44]. Moreover, we found a positive correlation between the lipids content and abundance of *E. coli* in the plant material (Figure 3). We assume that the majority of lipids originate from the plant; however, a potential contribution from the bacterial biomass to the total lipid content cannot be ruled out. The above correlation might be based on adequate changes in the plant membrane composition and in its fluidity [15]. Lipids, including phospholipids and sphingolipids, are not only involved in plant development and membrane fluidity, but can also confer salt tolerance in *S. europaea* [45]. One particular lipid molecule—phosphatidylserine—protects cells from biotic and abiotic stress, including pathogens and salinity, respectively [46,47]. Cuticular lipids serve as messenger molecules during pathogen attack [48,49]. A significant contribution of plant bacteria to total lipid content has been reported [50]. Human pathogenic bacteria, such as *E. coli*, *Salmonella* spp., and *L. monocytogenes*, have demonstrated remarkable adaptability in colonizing plant surfaces and, in some cases, internalizing within plant tissues [51]. The presence of these pathogens in fresh produce has been a persistent concern for public health, leading to numerous foodborne illness outbreaks worldwide. However, to the best of our knowledge, no studies have shown if and how the above bacteria interact with *S. europaea*. Understanding the factors that generally influence the abundance of these bacteria in plants is crucial for developing effective strategies to enhance food safety. Moreover, saline soils are less likely to be colonized by HPMOs, as salt has been previously identified as an inhibitory factor for these pathogenic bacteria [52–54]. Increased NaCl concentrations typically inhibit the growth of *E. coli* and its virulence-related traits, including biofilm formation, oxidative resistance, and motility [52]. A 5% NaCl concentration significantly decreased the growth of *S. enterica*, whereas the lowest concentration that affected the growth of *L. monocytogenes* was 7% NaCl [53,54]. However, we must also consider situations where HPMOs might promote plant growth, e.g., by improving the nitrogen nutrition of plants [55]. It is possible that the presence of HPMOs will increase as changes in global climate raise the temperature of soils close to body temperature, which is the optimal temperature for HMPO growth [55]. Thus, in summary, the relationships between plant and soil chemistry and their microbial colonization are fundamental controls

for food quality and will become even more important due to global climate change. The ongoing challenge will be to divide causal and successive changes in chemical plant traits in response to colonization by HPMOs in subsequent inoculation experiments.

5. Conclusions

The new insights into the relationships between the molecular-chemical composition of *S. europaea* L. shoots and soils and the abundance of HPMOs confirm that the methodological approach using selective media and mass spectrometric analyses of plant and soil materials was suitable and can be recommended in forthcoming studies. Our findings suggest that plants' chemical composition and environmental factors play crucial roles in controlling HPMO populations, with potential implications for food safety. the key findings from our research are as follows: (i) lignin content indicates a protective role of lignin against some HPMOs; (ii) the negative correlation of *E. coli* abundance with lignin content in bulk soil indicates a possible direct suppressing effect of soil organic matter composition, as bacteria cannot use lignin as a carbon source; (iii) the positive correlation of lipid content in shoots with the abundance of *E. coli* points to the use of lipids as a carbon source due to their lipolytic enzymes; (iv) the higher soil pH values and salinity associated with lower contamination levels by *E. coli*, *S. enterica*, and *L. monocytogenes* in bulk soil underscore the potential of these fundamental soil parameters as simple natural tools for enhancing food safety in *S. europaea* cultivation. Further research is recommended to explore the mechanisms behind these correlations and to investigate potential applications in agricultural practices. This knowledge could lead to improved cultivation methods and risk assessment strategies for *S. europaea* and potentially other halophilic crops, contributing to safer food production in saline environments.

Supplementary Materials: The following supporting information can be downloaded at: https://www.mdpi.com/article/10.3390/agronomy14112740/s1, Table S1: $\log_{10}$ CFU g^{-1} of *Escherichia coli*, *Salmonella enterica*, *Listeria monocytogenes* and *Bacillus cereus* with % peak area of carbohydrate, lignin, and lipid content in shoots of *S. europaea*; Table S2: $\log_{10}$ CFU g^{-1} of *Escherichia coli*, *Salmonella enterica*, *Listeria monocytogenes* and *Bacillus cereus* with % peak area of carbohydrate, lignin, and lipid content and log pH in rhizosphere soil; Table S3: $\log_{10}$ CFU g^{-1} of *Escherichia coli*, *Salmonella enterica*, *Listeria monocytogenes* and *Bacillus cereus* with % peak area of carbohydrate, lignin and lipid content and log pH in bulk soil; Table S4: Carbohydrate, lignin, and lipid content at two sites in France.

Author Contributions: Conceptualization, K.H., S.S. and C.B.; methodology, S.S. and K.-U.E.; formal analysis, M.M., K.-U.E., F.B. and J.P.; investigation, M.M., C.B., K.H., S.S. and K.-U.E.; writing—original draft preparation, M.M.; writing—review and editing, M.M., K.H., C.B., J.P., G.J., P.L., K.-U.E., F.B. and S.S.; supervision, K.H., C.B., S.S., K.-U.E., G.J. and P.L.; funding acquisition, K.H. and C.B. All authors have read and agreed to the published version of the manuscript.

Funding: The study was financially supported by the National Science Centre (NSC. Poland) OPUS 2019/33/B/NZ9/02803.

Data Availability Statement: The data presented in this study are available on request from the corresponding author.

Acknowledgments: The authors would like to thank Adam Michalski, Michał Dąbrowski, and Adam Solarczyk from the Laboratory for Environmental Analysis, Faculty of Earth Sciences and Spatial Management, Nicolaus Copernicus University in Toruń, for their support in laboratory analysis; Aurélien Ridel and Frédéric Bioret for their help in fieldwork and *Salicornia* identification, respectively.

Conflicts of Interest: The authors declare no conflicts of interest.

References

1. Singh, D.; Buhmann, A.K.; Flowers, T.J.; Seal, C.E.; Papenbrock, J. *Salicornia* as a crop plant in temperate regions: Selection of genetically characterized ecotypes and optimization of their cultivation conditions. *AoBP* **2014**, *6*, plu071. [CrossRef] [PubMed]
2. Kim, S.; Lee, E.-Y.; Hillman, P.F.; Ko, J.; Yang, I.; Nam, S.-J. Chemical Structure and Biological Activities of Secondary Metabolites from *Salicornia europaea* L. *Molecules* **2021**, *26*, 2252. [CrossRef] [PubMed]

3. Santos, J.; Al-Azzawi, M.; Aronson, J.; Flowers, T.J. eHALOPH a database of salt-tolerant plants: Helping put halophytes to work. *Plant Cell Physiol.* **2016**, *57*, e10. [CrossRef] [PubMed]
4. Cárdenas-Pérez, S.; Rajabi Dehnavi, A.; Leszczyński, K.; Lubińska-Mielińska, S.; Ludwiczak, A.; Piernik, A. *Salicornia europaea* L. Functional Traits Indicate Its Optimum Growth. *Plants* **2022**, *11*, 1051. [CrossRef] [PubMed]
5. Antunes, M.D.; Gago, C.; Guerreiro, A.; Sousa, A.R.; Julião, M.; Miguel, M.G.; Faleiro, M.L.; Panagopoulos, T. Nutritional Characterization and Storage Ability of *Salicornia ramosissima* and *Sarcocornia perennis* for Fresh Vegetable Salads. *Horticulturae* **2021**, *7*, 6. [CrossRef]
6. Rhee, M.H.; Park, H.-J.; Cho, J.Y. *Salicornia herbacea*: Botanical chemical and pharmacological review of halophyte marsh plant. *J. Med. Plant Res.* **2009**, *3*, 548–555.
7. Cárdenas-Pérez, S.; Piernik, A.; Chanona-Pérez, J.J.; Grigore, M.N.; Perea-Flores, M.J. An overview of the emerging trends of the *Salicornia* L. genus as a sustainable crop. *Environ. Exp. Bot.* **2021**, *191*, 104606. [CrossRef]
8. Puccinelli, M.; Marchioni, I.; Botrini, L.; Carmassi, G.; Pardossi, A.; Pistelli, L. Growing Salicornia europaea L. with Saline Hydro-ponic or Aquaculture Wastewater. *Horticulturae* **2024**, *10*, 196. [CrossRef]
9. Ferreira, M.J.; Pinto, D.C.G.A.; Cunha, Â.; Silva, H. Halophytes as Medicinal Plants against Human Infectious Diseases. *Appl. Sci.* **2022**, *12*, 7493. [CrossRef]
10. Cesarino, I.; Simões, M.S.; dos Santos Brito, M.; Fanelli, A.; da Franca Silva, T.; Romanel, E. Building the wall: Recent advances in understanding lignin metabolism in grasses. *Acta Physiol. Plant.* **2016**, *38*, 269. [CrossRef]
11. Cesarino, I. Structural features and regulation of lignin deposited upon biotic and abiotic stresses. *Curr. Opin. Biotechnol.* **2019**, *56*, 209–214. [CrossRef] [PubMed]
12. Lee, M.H.; Jeon, H.S.; Kim, S.H.; Chung, J.H.; Roppolo, D.; Lee, H.J.; Cho, H.J.; Tobimatsu, Y.; Ralph, J.; Park, O.K. Lignin-based barrier restricts pathogens to the infection site and confers resistance in plants. *EMBO J.* **2019**, *38*, e101948. [CrossRef] [PubMed]
13. Bhuiyan, N.H.; Selvaraj, G.; Wei, Y.; King, J. Gene expression profiling and silencing reveal that monolignol biosynthesis plays a critical role in penetration defence in wheat against powdery mildew invasion. *J. Exp. Bot.* **2008**, *60*, 509–521. [CrossRef] [PubMed]
14. Miedes, E.; Vanholme, R.; Boerjan, W.; Molina, A. The role of the secondary cell wall in plant resistance to pathogens. *Front. Plant Sci.* **2014**, *5*, 358. [CrossRef]
15. Cavaco, A.R.; Matos, A.R.; Figueiredo, A. Speaking the language of lipids: The cross-talk between plants and pathogens in defence and disease. *Cell. Mol. Life Sci.* **2021**, *78*, 4399–4415. [CrossRef]
16. Walley, J.W.; Kliebenstein, D.J.; Bostock, R.M.; Dehesh, K. Fatty acids and early detection of pathogens. *Curr. Opin. Plant Biol.* **2013**, *16*, 520–526. [CrossRef]
17. Ludovici, M.; Ialongo, C.; Reverberi, M.; Beccaccioli, M.; Scarpari, M.; Scala, V. Quantitative profiling of oxylipins through comprehensive LC-MS/MS analysis of *Fusarium verticillioides* and maize kernels. *Food Addit. Contam. Part A* **2014**, *31*, 2026–2033. [CrossRef]
18. Siebers, M.; Brands, M.; Wewer, V.; Duan, Y.; Hölzl, G.; Dörmann, P. Lipids in plant–microbe interactions. *Biochim. Biophys. Acta* **2016**, *1861 Pt B*, 1379–1395. [CrossRef]
19. Bhatia, V.; Nag, R.; Burgess, C.M.; Gaffney, M.; Celayeta, J.M.F.; Cummins, E. Microbial risks associated with Ready-To-Eat Fresh Produce (RTEFP)—A focus on temperate climatic conditions. *Postharvest Biol. Technol.* **2024**, *213*, 112924. [CrossRef]
20. Barak, J.D.; Schroeder, B.K. Interrelationships of food safety and plant pathology: The life cycle of human pathogens on plants. *Annu. Rev. Phytopathol.* **2012**, *50*, 241–266. [CrossRef]
21. Warriner, K.; Spaniolas, S.; Dickinson, M.; Wright, C.; Waites, W.M. Internalization of bioluminescent *Escherichia coli* and Salmonella Montevideo in growing bean sprouts. *J. Appl. Microbiol.* **2003**, *95*, 719–727. [CrossRef] [PubMed]
22. Deering, A.J.; Pruitt, R.E.; Mauer, L.J.; Reuhs, B.L. Identification of the Cellular Location of Internalized *Escherichia coli* O157:H7 in Mung Bean Vigna radiata using Immunocytochemical Techniques. *J. Food Prot.* **2011**, *74*, 1224–1230. [CrossRef] [PubMed]
23. Deering, A.J.; Mauer, L.J.; Pruitt, R.E. Internalization of *E. coli* O157:H7 and *Salmonella* spp. in plants: A review. *Food Res. Int.* **2012**, *45*, 567–575. [CrossRef]
24. McCoy Sanders, J.; Alarcon, V.; Marquis, G.; Tabb, A.; Van Kessel, J.A.; Sonnier, J.; Haley, B.J.; Baek, I.; Qin, J.; Kim, M.; et al. Inactivation of *Escherichia Coli*, *Salmonella Enterica*, and *Listeria Monocytogenes* Using the Contamination Sanitization Inspection and Disinfection (CSI-D) Device. *Heliyon* **2024**, *10*, e30490. [CrossRef] [PubMed]
25. Géhu, J.-M.; Bioret, F. *Étude Synécologique et Phytocoenotique des Communautés à Salicornes des Vases Salées du Littoral Breton*; Bulletin de la Société Botanique duy Centre-Ouest NS: Bouguenais, France, 1992; Volume 23, pp. 347–419.
26. *ISO 7712:1983*; Laboratory Glassware—Disposable Pasteur Pipettes. ISO: Geneva, Switzerland, 1983.
27. *ISO 11290*; Microbiology of the Food Chain—Horizontal Method for the Detection and Enumeration of *Listeria monocytogenes* and of *Listeria* spp. ISO: Geneva, Switzerland, 2017.
28. *EN-ISO 6579-1*; Microbiology of the Food Chain—Horizontal Method for Detection, Enumeration and Serotyping of *Salmonella*—Part 1: Detection of *Salmonella* spp. ISO: Geneva, Switzerland, 2017.
29. *EN ISO 7932*; Microbiology of Food and Feed—Horizontal Method for the Enumeration of Presumptive *B. cereus*—Colony Count Method at 30 °C. ISO: Geneva, Switzerland, 2004.
30. Pansu, M.; Gautheyrou, J. *Handbook of Soil Analysis. Organic and Inorganic Methods*; Springer: Berlin/Heidelberg, Germany, 2006; pp. 596–599.
31. Van Reeuwijk, L.P. *Technical Paper 09: Procedures for Soil Analysis*, 6th ed.; ISRIC: Wageningen, The Netherlands, 2002.

32. Pokojska, U. *Przewodnik Metodyczny do Analizy Wód*; UMK: Toruń, Poland, 1999; pp. 25–27.
33. Hulkko, L.S.S.; Turcios, A.E.; Kohnen, S.; Chaturvedi, T.; Papenbrock, J.; Thomsen, M.H. Cultivation and characterisation of *Salicornia europaea*, *Tripolium pannonicum* and *Crithmum maritimum* biomass for green biorefinery applications. *Sci. Rep.* **2022**, *12*, 20507. [CrossRef]
34. Cybulska, I.; Chaturvedi, T.; Brudecki, G.P.; Kádár, Z.; Meyer, A.S.; Baldwin, R.; Thomsen, M.H. Chemical characterization and hydrothermal pretreatment of *Salicornia bigelovii* straw for enhanced enzymatic hydrolysis and bioethanol potential. *Bioresour. Technol.* **2014**, *153*, 165–172. [CrossRef]
35. Sholahuddin, S.; Arinawati, D.Y.; Nathan, V.K.; Asada, C.; Nakamura, Y. Antioxidant and antimicrobial activities of lignin-derived products from all steam-exploded palm oil mill lignocellulosic biomass waste. *Chem. Biol. Technol. Agric.* **2024**, *11*, 5. [CrossRef]
36. Sattler, S.; Funnell-Harris, D. Modifying lignin to improve bioenergy feedstocks: Strengthening the barrier against pathogens? *Front. Plant Sci.* **2013**, *4*, 70. [CrossRef]
37. Bonello, P.; Storer, A.J.; Gordon, T.R.; Wood, D.L.; Heller, W. Systemic effects of *Heterobasidion annosum* on ferulic acid glucoside and lignin of presymptomatic ponderosa pine phloem. and potential effects on bark-beetle-associated fungi. *J. Chem. Ecol.* **2003**, *29*, 1167–1182. [CrossRef]
38. Menden, B.; Kohlhoff, M.; Moerschbacher, B.M. Wheat cells accumulate a syringyl-rich lignin during the hypersensitive resistance response. *Phytochemistry* **2007**, *68*, 513–520. [CrossRef]
39. Le Gall, H.; Philippe, F.; Domon, J.-M.; Gillet, F.; Pelloux, J.; Rayon, C. Cell Wall Metabolism in Response to Abiotic Stress. *Plants* **2015**, *4*, 112–166. [CrossRef] [PubMed]
40. Villarreal, M.R.; Navarro, D.A.; Ponce, N.M.A.; Rojas, A.M.; Stortz, C.A. Perennial halophyte *Salicornia neei* Lag.: Cell wall composition and functional properties of its biopolymers. *Food Chem.* **2021**, *350*, 128659. [CrossRef] [PubMed]
41. Lastochkina, O.; Aliniaeifard, S.; Garshina, D.; Garipova, S.; Pusenkova, L.; Allagulova, C.; Fedorova, K.; Baymiev, A.; Koryakov, I.; Sobhani, M. Seed priming with endophytic *Bacillus subtilis* strain-specifically improves growth of *Phaseolus vulgaris* plants under normal and salinity conditions and exerts anti-stress effect through induced lignin deposition in roots and decreased oxidative and osmotic damages. *J. Plant Physiol.* **2021**, *263*, 153462. [PubMed]
42. Li, C.; Qi, Y.; Zhao, C.; Wang, X.; Zhang, Q. Transcriptome Profiling of the Salt Stress Response in the Leaves and Roots of Halophytic *Eutrema salsugineum*. *Front. Genet.* **2021**, *12*, 770742. [CrossRef]
43. Dracatos, P.M.; Cogan, N.O.; Dobrowolski, M.P.; Sawbridge, T.I.; Spangenberg, G.C.; Smith, K.F.; Forster, J.W. Discovery and genetic mapping of single nucleotide polymorphisms in candidate genes for pathogen defence response in perennial ryegrass (*Lolium perenne* L.). *Theor. Appl. Genet.* **2008**, *117*, 203–219. [CrossRef]
44. Ishida, H.; Suzuno, H.; Sugiyama, N.; Innami, S.; Tadokoro, T.; Maekawa, A. Nutritive evaluation on chemical components of leaves. stalks and stems of sweet potatoes (*Ipomoea batatas poir*). *Food Chem.* **2000**, *68*, 359–367. [CrossRef]
45. Yang, L.; Bai, Y.; Yang, J.; Gao, Y.; Shi, P.; Hou, C.; Wang, Y.; Gu, X.; Liu, W. Transcriptomic and lipidomic analysis reveals the salt-adapted in Salicornia europaea. *Res. Sq.* **2023**. [CrossRef]
46. Lv, S.; Tai, F.; Guo, J.; Jiang, P.; Lin, K.; Wang, D.; Zhang, X.; Li, Y. Phosphatidylserine Synthase from *Salicornia europaea* Is Involved in Plant Salt Tolerance by Regulating Plasma Membrane Stability. *Plant Cell Physiol.* **2021**, *62*, 66–79. [CrossRef]
47. Chen, Y.; Cao, C.; Guo, Z.; Zhang, Q.; Li, S.; Zhang, X.; Gong, J.; Shen, Y. Herbivore exposure alters ion fluxes and improves salt tolerance in a desert shrub. *Plant Cell Environ.* **2020**, *43*, 400–419. [CrossRef]
48. Kolattukudy, P.E.; Rogers, L.M.; Li, D.; Hwang, C.S.; Flaishman, M.A. Surface signaling in pathogenesis. *Proc. Natl. Acad. Sci. USA* **1995**, *92*, 4080–4087. [CrossRef]
49. Reina-Pinto, J.J.; Yephremov, A. Surface lipids and plant defenses. *Plant Physiol. Biochem.* **2009**, *47*, 540–549. [CrossRef] [PubMed]
50. Sohlenkamp, C.; Geiger, O. Bacterial membrane lipids: Diversity in structures and pathways. *FEMS Microbiol. Rev.* **2016**, *40*, 133–159. [CrossRef] [PubMed]
51. Lim, J.A.; Lee, D.H.; Heu, S. The interaction of human enteric pathogens with plants. *Plant Pathol. J.* **2014**, *30*, 109–116. [CrossRef] [PubMed]
52. Li, F.; Xiong, X.-S.; Yang, Y.-Y.; Wang, J.-J.; Wang, M.-M.; Tang, J.-W.; Liu, Q.-H.; Wang, L.; Gu, B. Effects of NaCl Concentrations on Growth Patterns, Phenotypes Associated with Virulence, and Energy Metabolism in *Escherichia coli* BW25113. *Front. Microbiol.* **2021**, *12*, 705326.
53. Thayer, D.W.; Muller, W.S.; Buchanan, R.L.; Phillips, J.G. Effect of NaCl, pH, Temperature, and Atmosphere on Growth of Salmonella Typhimurium in Glucose-Mineral Salts Medium. *Appl. Environ. Microbiol.* **1987**, *53*, 13111315.
54. Wiktorczyk-Kapischke, N.; Skowron, K.; Wałecka-Zacharska, E.; Grudlewska-Buda, K.; Wnuk, K.; Buszko, K.; Gospodarek-Komkowska, E. Assessment of the Influence of Selected Stress Factors on the Growth and Survival of *Listeria Monocytogenes*. *BMC Microbiol.* **2023**, *23*, 27.
55. Tyler, H.L.; Triplett, E.W. Plants as a Habitat for Beneficial and/or Human Pathogenic Bacteria. *Annu. Rev. Phytopathol.* **2008**, *46*, 53–73.

agronomy

MDPI

Correction

Correction: Marangi et al. Abundance of Human Pathogenic Microorganisms in the Halophyte *Salicornia europaea* L.: Influence of the Chemical Composition of Shoots and Soils. *Agronomy* 2024, *14*, 2740

Matteo Marangi [1,2], Sonia Szymanska [1], Kai-Uwe Eckhardt [2], Felix Beske [2], Gerald Jandl [2], Katarzyna Hrynkiewicz [1], Julien Pétillon [3,4], Christel Baum [2] and Peter Leinweber [2,5,*]

1 Department of Microbiology, Nicolaus Copernicus University, 87-100 Torun, Poland; matteomarangi@doktorant.umk.pl (M.M.); soniasz@umk.pl (S.S.); hrynk@umk.pl (K.H.)
2 Soil Science, Faculty of Agricultural and Environmental Sciences, University of Rostock, 18051 Rostock, Germany; kai-uwe.eckhardt@uni-rostock.de (K.-U.E.); felix.beske2@uni-rostock.de (F.B.); gerald.jandl@uni-rostock.de (G.J.); christel.baum@uni-rostock.de (C.B.)
3 UMR CNRS ECOBIO (Ecosystèmes, Biodiversité, Evolution), University of Rennes, 35042 Rennes, France; julien.petillon@univ-rennes.fr
4 Institute for Coastal and Marine Research, Nelson Mandela University, Gqeberha 6031, South Africa
5 Bioeconomy Research Institute, Academy of Agriculture, Vytautas Magnus University, Studentu 11-530, Akademija, LT-53361 Kaunas, Lithuania
* Correspondence: peter.leinweber@uni-rostock.de

Addition of References Citations

In the original publication [1], references number 30–32 were not cited. The citation has now been inserted in Section 2.4 "Bulk and Rhizosphere Soil Analysis", the first paragraph, and should read as follows:

The soil samples were air-dried at room temperature and passed through a 2 mm mesh sieve to remove debris. Total carbon (C_t) and total nitrogen (N_t) were determined using Elementar Vario CNS analyser (Elementar Analysensysteme GmbH, Langenselbold, Germany). The calcium carbonate ($CaCO_3$) content of the soil was determined by the volumetric method using a Scheibler apparatus [30]. Total inorganic carbon (TIC) was calculated from the calcium carbonate content. Total organic carbon (TOC) was calculated as the difference between TC and TIC. Bio-available phosphorus (P_{ca}) was determined colorimetrically by the citrate method using a Rayleigh UV-1601 spectrophotometer (Beifen-Ruili Analytical Instrument Co., Ltd., Beijing, China) [31]. The saturated paste extracts were prepared according to the methodology of van Reeuwijk [31]. The pH ($CaCl_2$) was measured potentiometrically using a CP-551 Elmetron pH meter. Electrical conductivity (EC) was determined at 25 °C using the conductometric method with a CPC-401 conductivity meter (Elmetron Ltd., Zabrze, Poland). The concentrations of Mg and Ca were determined by atomic absorption spectrometry (AAS), while the concentrations of K and Na were determined by optical emission spectrometry (OES) using a SOLAAR Unicam 969 (Unicam Ltd., Cambridge, UK) flame spectrometer. The concentration of bicarbonates (HCO_3^-) was determined by titration with 0.1 M HCl [32].

In addition, references citations [29,30] should be changed into [33,34] in Section 4. With this correction, the order of some references in Section 4 has been adjusted accordingly. References 52–55 should also be added as outlined below.

check for updates

Received: 17 March 2025
Accepted: 31 March 2025
Published: 29 April 2025

Citation: Marangi, M.; Szymanska, S.; Eckhardt, K.-U.; Beske, F.; Jandl, G.; Hrynkiewicz, K.; Pétillon, J.; Baum, C.; Leinweber, P. Correction: Marangi et al. Abundance of Human Pathogenic Microorganisms in the Halophyte *Salicornia europaea* L.: Influence of the Chemical Composition of Shoots and Soils. *Agronomy* 2024, *14*, 2740. *Agronomy* **2025**, *15*, 1080. https://doi.org/10.3390/agronomy15051080

Addition of References

52. Li, F.; Xiong, X.-S.; Yang, Y.-Y.; Wang, J.-J.; Wang, M.-M.; Tang, J.-W.; Liu, Q.-H.; Wang, L.; Gu, B. Effects of NaCl Concentrations on Growth Patterns, Phenotypes Associated with Virulence, and Energy Metabolism in *Escherichia coli* BW25113. *Front. Microbiol.* **2021**, *12*, 705326.
53. Thayer, D.W.; Muller, W.S.; Buchanan, R.L.; Phillips, J.G. Effect of NaCl, pH, Temperature, and Atmosphere on Growth of Salmonella Typhimurium in Glucose-Mineral Salts Medium. *Appl. Environ. Microbiol.* **1987**, *53*, 13111315.
54. Wiktorczyk-Kapischke, N.; Skowron, K.; Wałecka-Zacharska, E.; Grudlewska-Buda, K.; Wnuk, K.; Buszko, K.; Gospodarek-Komkowska, E. Assessment of the Influence of Selected Stress Factors on the Growth and Survival of *Listeria Monocytogenes*. *BMC Microbiol.* **2023**, *23*, 27.
55. Tyler, H.L.; Triplett, E.W. Plants as a Habitat for Beneficial and/or Human Pathogenic Bacteria. *Annu. Rev. Phytopathol.* **2008**, *46*, 53–73.

The authors state that the scientific conclusions are unaffected. This correction was approved by the Academic Editor. The original publication has also been updated.

Reference

1. Marangi, M.; Szymanska, S.; Eckhardt, K.-U.; Beske, F.; Jandl, G.; Hrynkiewicz, K.; Pétillon, J.; Baum, C.; Leinweber, P. Abundance of Human Pathogenic Microorganisms in the Halophyte *Salicornia europaea* L.: Influence of the Chemical Composition of Shoots and Soils. *Agronomy* **2024**, *14*, 2740. [CrossRef]

Appendix II

Table 1. Sequences of probes used for rRNA depletion from total RNA.

Probe name	Sequence	Target rRNA
mit1	GAGCCTCTTTTCTTTCTGCCTAGCTCCC	Mitochondrial 16S rRNA
mit2	ACGCACCCGTTCGCCACTTTGTTCTC	Mitochondrial 16S rRNA
mit3	GTCCTGTCATGATCGCGCACTCAACG	Mitochondrial 16S rRNA
mit4	CGACTTTCACTTTCAACCCGATTCACCG	Mitochondrial 16S rRNA
mit5	GATCCGTGTAGACCAAGGGCGAACAC	Mitochondrial 16S rRNA
mit6	GGCTCCTTGGCTCACTTCGGTTGC	Mitochondrial 16S rRNA
mit7	CCATTGTAGCACGTGTGTGGCCCAG	Mitochondrial 16S rRNA
chl1	GGATTCCTCCTTTTGCTTCTCAGCCT	Chloroplast 16S rRNA
chl2	GATAGTTTCCACCGCCTGTCCAGGG	Chloroplast 16S rRNA
chl3	ACAACACTGCACGGGTCGATACGCACAG C	Chloroplast 16S rRNA
chl4	CTGTTCAGGGTTCCAAACTCAACGT	Chloroplast 16S rRNA
chl5	GAACTGAGGACGGGTTTTTGGGGTTAG	Chloroplast 16S rRNA
chl6	GTCACTAGCCCTGCCTCCGGCATCC	Chloroplast 16S rRNA
nuc1	GAGCCATTCGCAGTTTTACAGTCTGA	Nuclear 18S rRNA
nuc2	CCTCCAATGGATCCTCGTTAAGGGAT	Nuclear 18S rRNA
nuc3	CCCATGCTAATGTATACAGAGCGTAGGC	Nuclear 18S rRNA
nuc4	AGTTTCAGCCTTGCGACCATACTCCC	Nuclear 18S rRNA
nuc5	CTAAGAACGGCCATGCACCACCACC	Nuclear 18S rRNA
nuc6	CCGTGGCCTAAAAGGCCATAGTCCCTC	Nuclear 18S rRNA
nuc7	TCACCGGACCATTCAATGGGTAGGAG	Nuclear 18S rRNA
nuc8	CCCTCGCGGTACTTGTTCGCTATCGG	Nuclear 28S rRNA
nuc9	GACTCGCACACATGTCAGACTCCTTG	Nuclear 28S rRNA
nuc10	CATCCCGCATCGCCAGTTCTGCTTAC	Nuclear 28S

		rRNA
nuc11	GCAAGTGCCGTTCACATGGAACCTTTCC	Nuclear 28S rRNA
nuc12	GGATTCCCCTTGTCCGTACCAGTTCTGA	Nuclear 28S rRNA
nuc13	AACTCCCCACCTGACAATGTCCTCCG	Nuclear 28S rRNA
nuc14	TCTAAACCCAGCTCACGTTCCCTATTGGT	Nuclear 28S rRNA

Appendix III

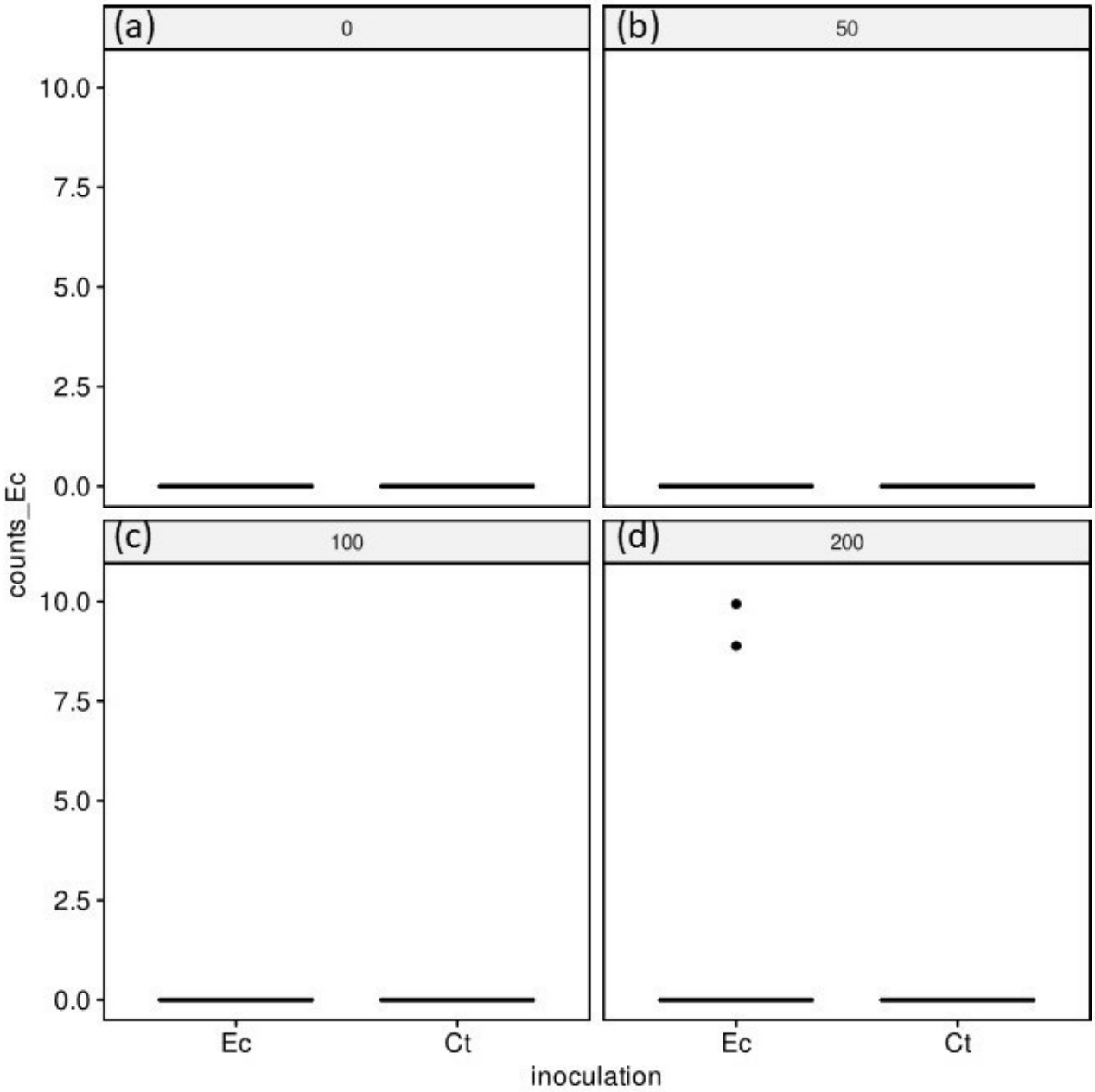

Figure 1. *E. coli* counts (gene copy number ng^{-1}) were measured through qPCR analyses in the shoots of *S. europaea* at varying salinity levels: 0 mM (a), 50 mM (b), 100 mM (c), and 200 mM NaCl (d). The results were compared between *E. coli*-treated plants (Ec) and non-inoculated controls (Control = Ct). Statistical significance was determined at $p < 0.05$.

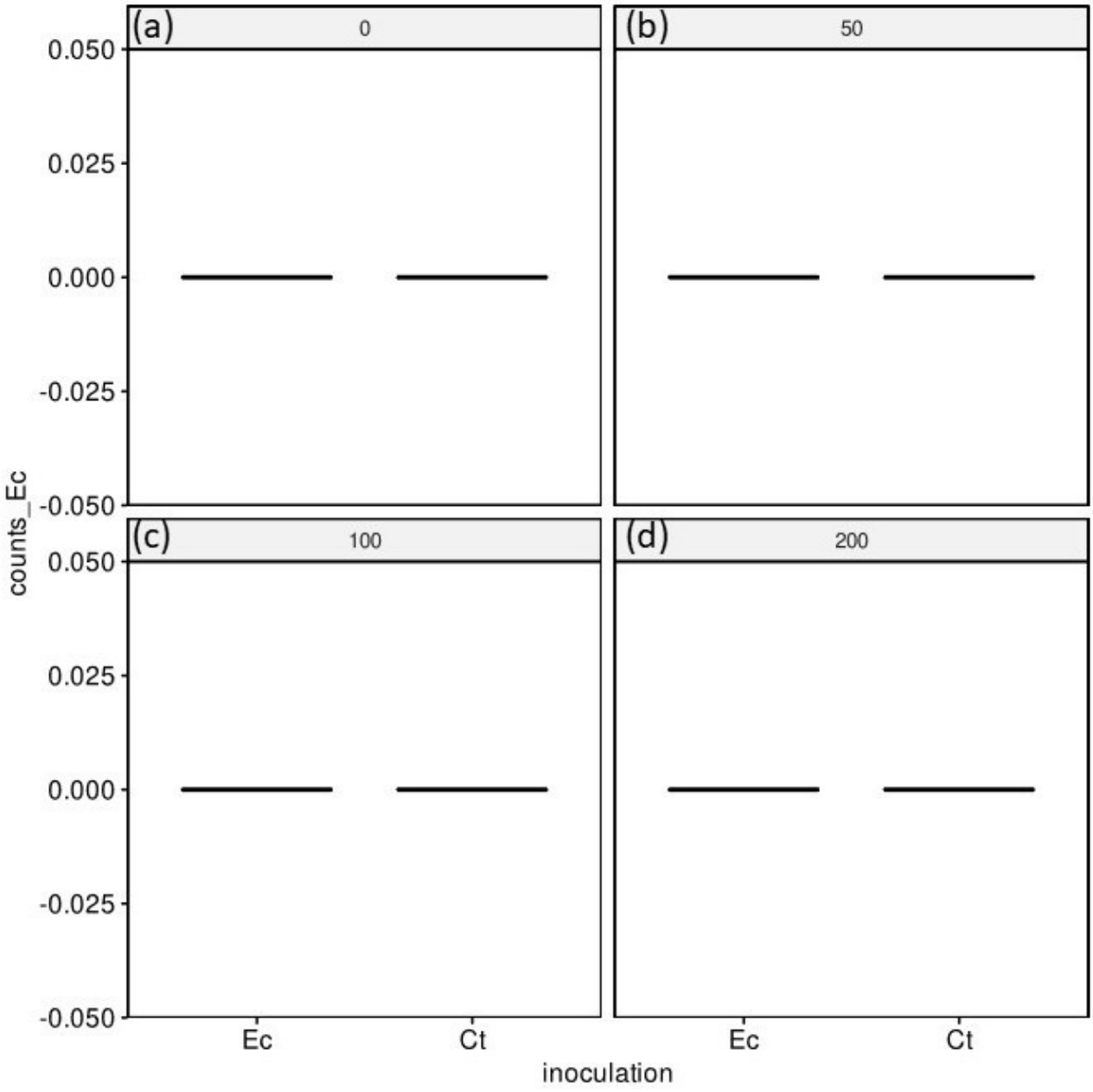

Figure 2. *E. coli* counts (gene copy number ng^{-1}) were measured through qPCR analyses in the roots of *S. europaea* at varying salinity levels: 0 mM (a), 50 mM (b), 100 mM (c), and 200 mM NaCl (d). The results were compared between *E. coli*-treated plants (Ec) and non-inoculated controls (Control = Ct). Statistical significance was determined at $p < 0.05$.

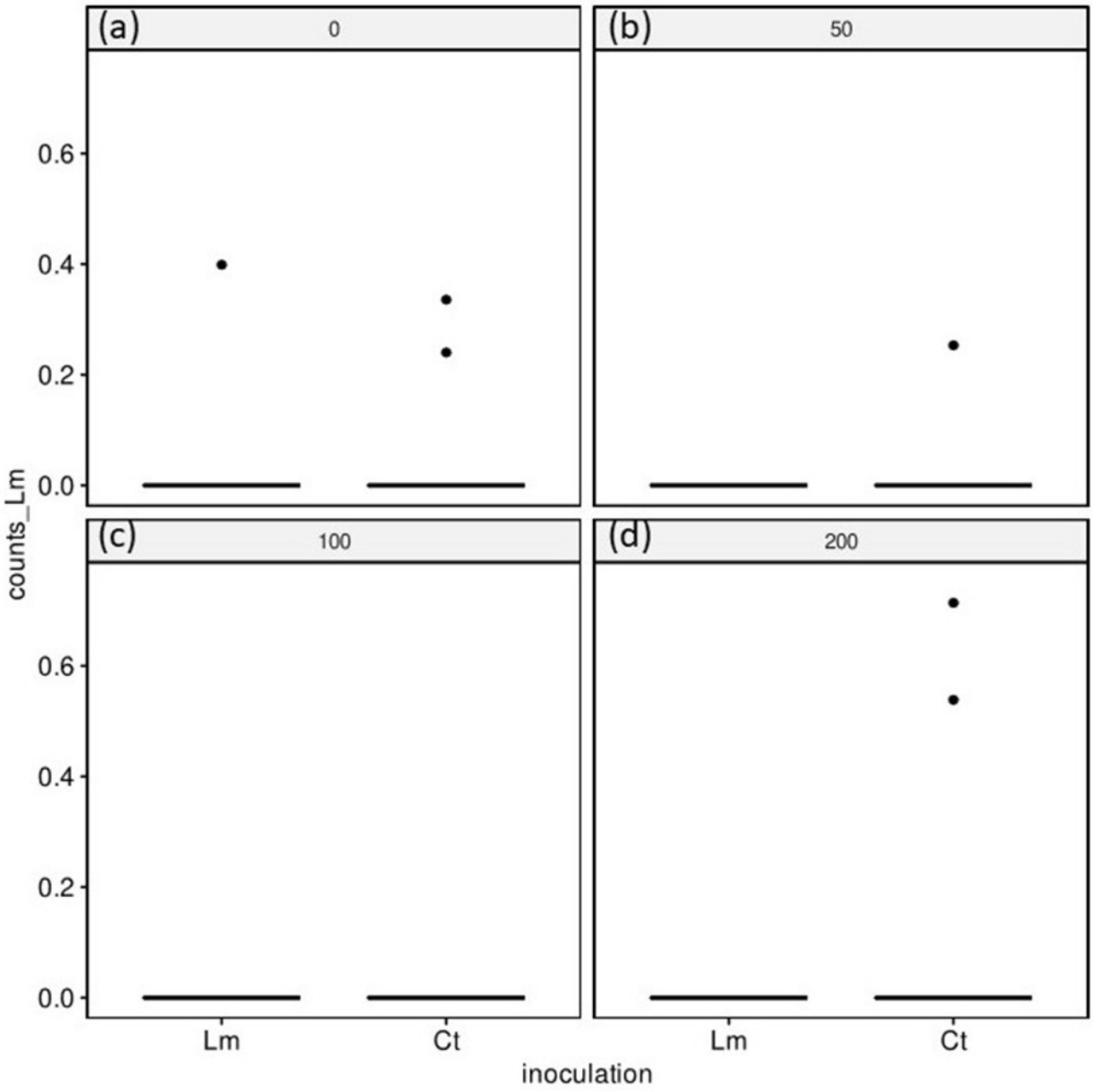

Figure 3. *L. monocytogenes* counts (gene copy number ng^{-1}) were measured through qPCR analyses in the shoots of *S. europaea* at varying salinity levels: 0 mM (a), 50 mM (b), 100 mM (c), and 200 mM NaCl (d). The results were compared between *L. monocytogenes*-treated plants (Lm) and non-inoculated controls (Control = Ct). Statistical significance was determined at $p < 0.05$.

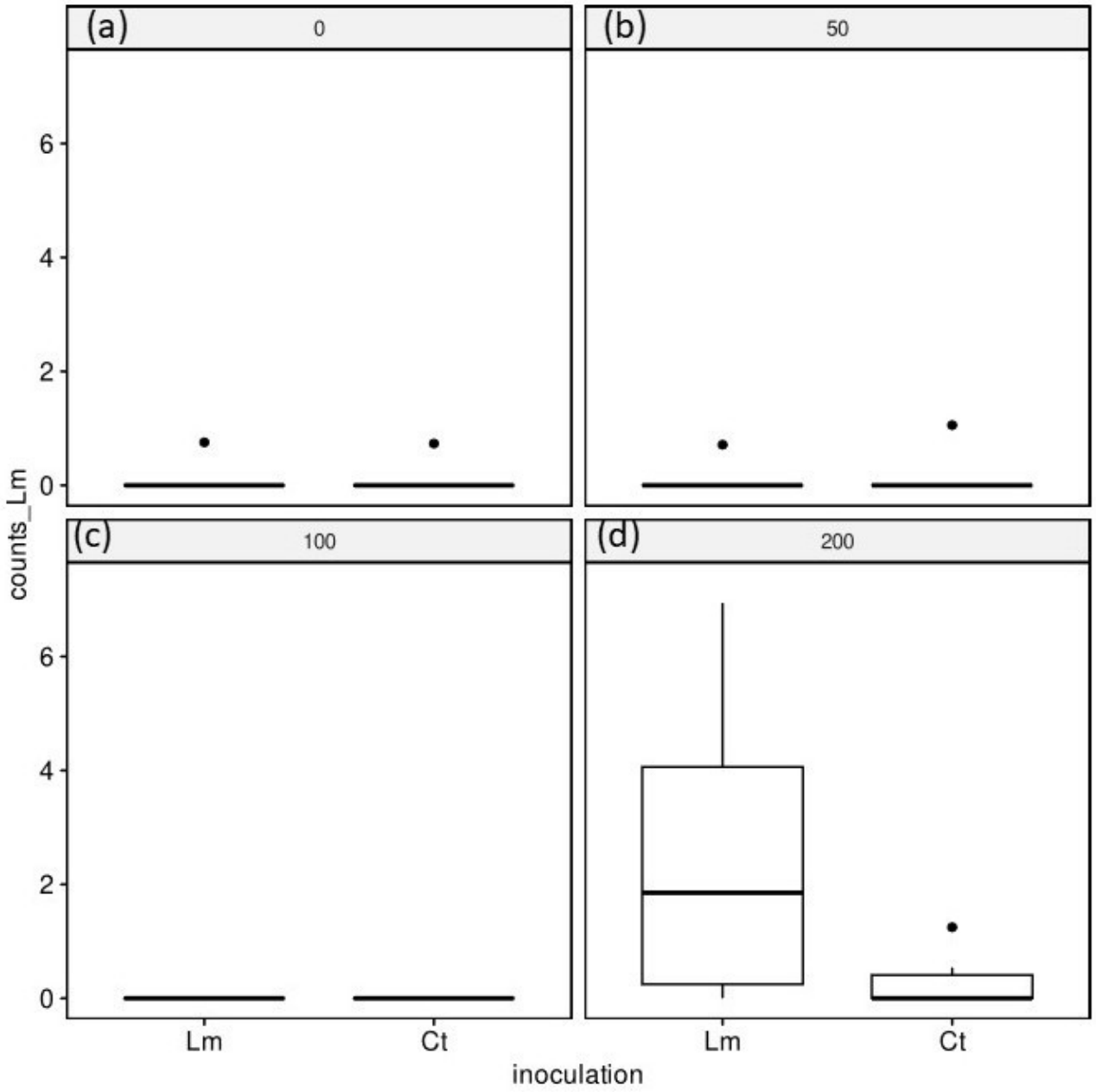

Figure 4. *L. monocytogenes* counts (gene copy number ng^{-1}) were measured through qPCR analyses in the roots of *S. europaea* at varying salinity levels: 0 mM (a), 50 mM (b), 100 mM (c), and 200 mM NaCl (d). The results were compared between *L. monocytogenes*-treated plants (Lm) and non-inoculated controls (Control = Ct). Statistical significance was determined at $p < 0.05$.

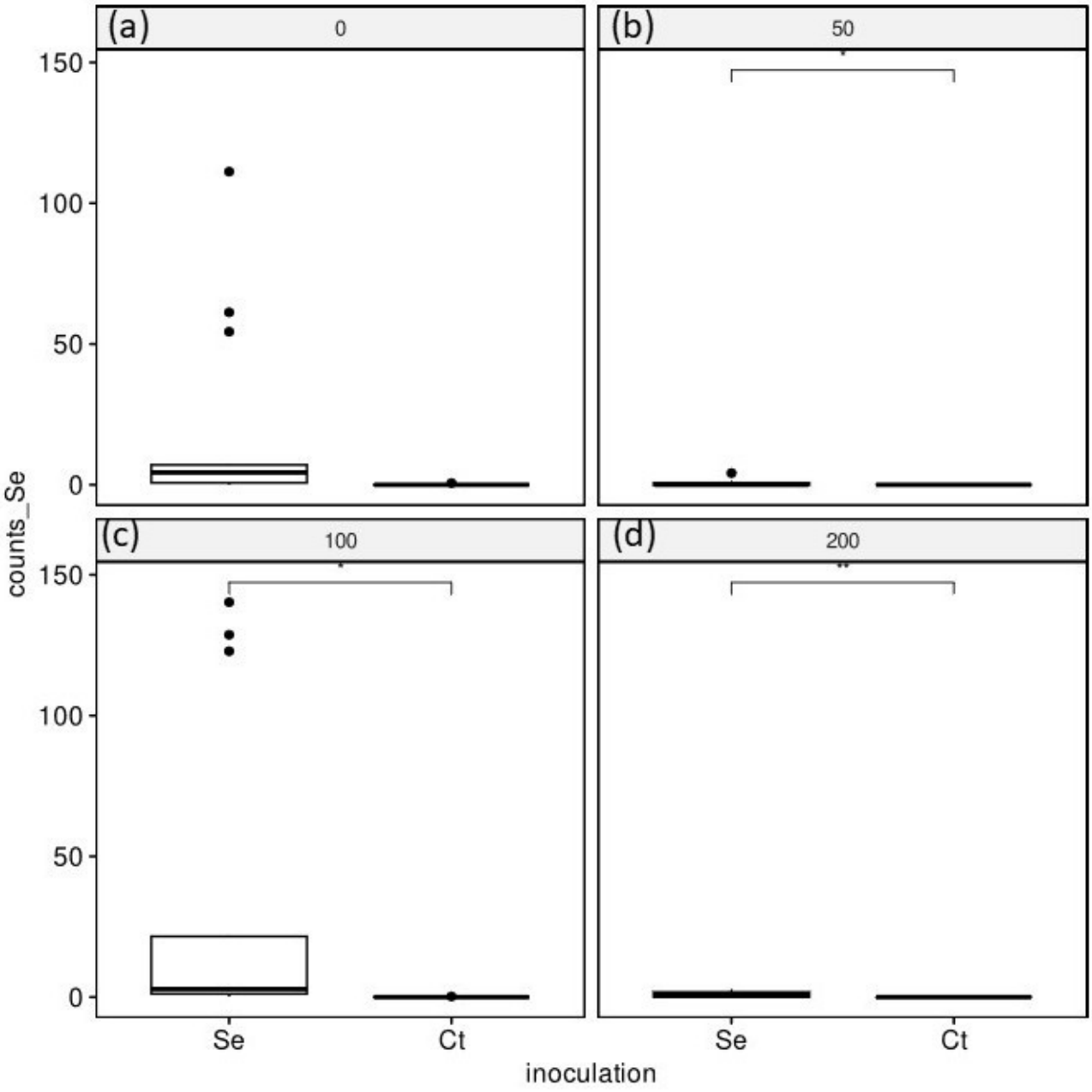

Figure 5. *S. enterica* counts (gene copy number ng^{-1}) were measured through qPCR analyses in the shoots of *S. europaea* at varying salinity levels: 0 mM (a), 50 mM (b), 100 mM (c), and 200 mM NaCl (d). The results were compared between *S. enterica*-treated plants (Se) and non-inoculated controls (Control = Ct). Statistical significance was determined at $p < 0.05$.

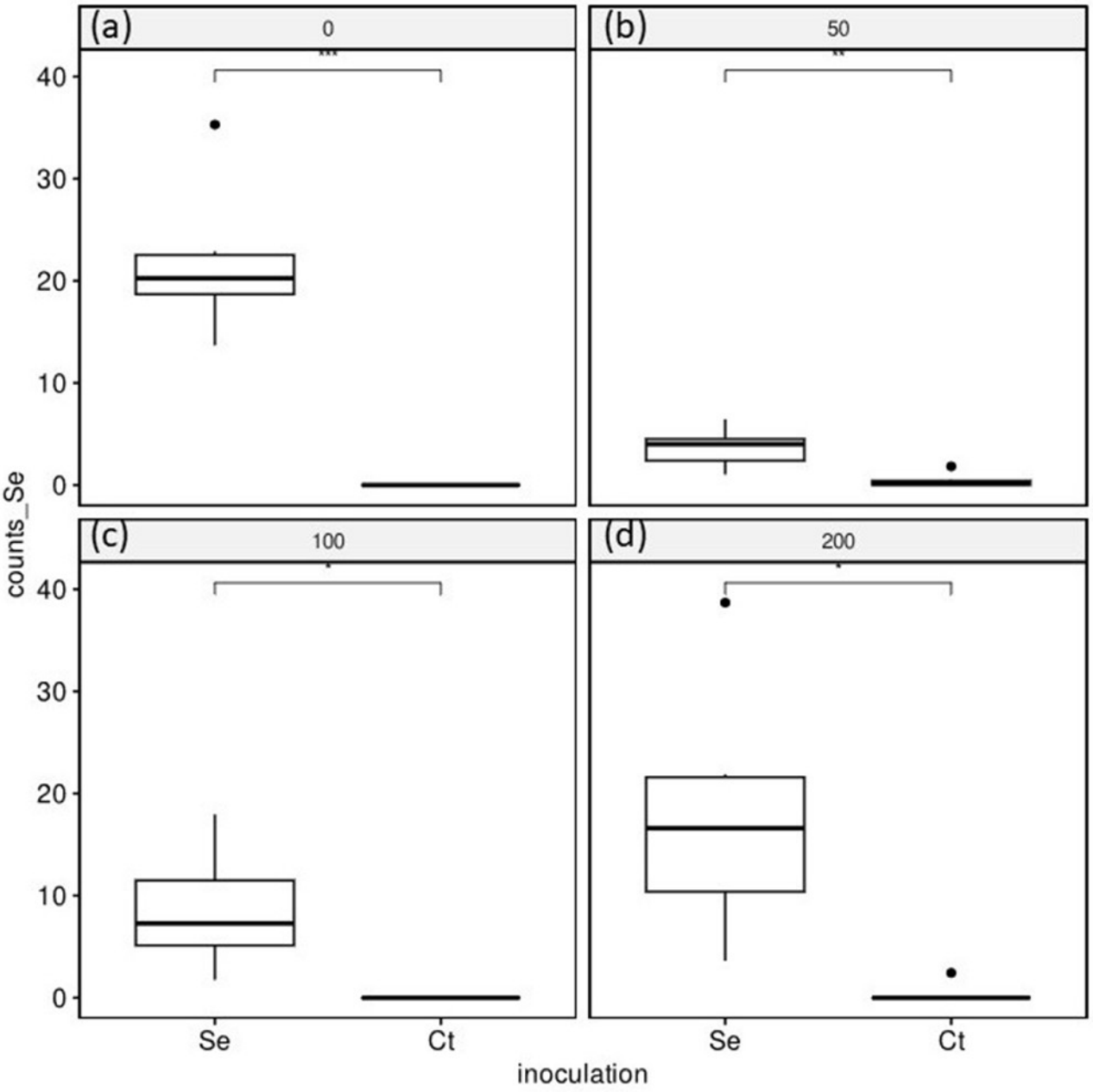

Figure 6. *S. enterica* counts (gene copy number ng^{-1}) were measured through qPCR analyses in the roots of *S. europaea* at varying salinity levels: 0 mM (a), 50 mM (b), 100 mM (c), and 200 mM NaCl (d). The results were compared between *S. enterica*-treated plants (Se) and non-inoculated controls (Control = Ct). Statistical significance was determined at $p < 0.05$.

Author information

Matteo Marangi is an Italian early-career scientist currently defending his PhD in Biological Sciences through a joint-degree program between the Nicolaus Copernicus University (Poland) and the University of Rostock (Germany). His doctoral work, conducted within the Departments of Microbiology & Soil Science, investigates the potential of *Salicornia europaea* to reduce colonization of plants by human pathogenic microorganisms. This research contributes to the Emerging interdisciplinary Field of Microbiology, Soil Science, Food Quality, and Agricultural Genetics (OBSIDIAN), reflecting Matteo's focus on plant microbiomes and food safety.

Matteo began his academic career with a BSc in Agricultural Science and Technology from the University of Turin (2016), where he studied molecular identification of *Xylella fastidiosa* subspecies. He then earned a MSc in Plant Biotechnology (2019) at the same university, completing his thesis at Wageningen University & Research on the epidemiology of *Xylella fastidiosa* using molecular diagnostics such as real-time PCR and LAMP.

Matteo has held research fellowships, scholarships, and internships that have strengthened his expertise in plant pathology, molecular biology, and microbiology. His diverse research experience spans multiple institutions and topics, including drafting protocols for qPCR analyses, serological and molecular diagnostics of *Xylella fastidiosa*, gene annotation for stress resistance in the artichoke genome, and molecular detection of fungal viruses.

Matteo's research output includes a significant publication in *Agronomy* (Q1, 2024) on the abundance of human pathogenic microorganisms in *Salicornia europaea* and the influence of chemical composition of shoots and soils. His active participation in international scientific conferences demonstrates his engagement with the global research community. Highlights include oral presentations at Plants 2025 (Barcelona, 2025) and SolPHe (Reims, 2025), and poster presentations at the Copernican Seminar (Torun, 2024) and the European Culture Collections' Organisation meeting (Bari, 2024). Additionally, Matteo has contributed as a member of the organizing committee for the 5th International Conference OBSIDIAN (Torun, 2025).

In addition to his research, Matteo holds the Cambridge English Certificate (C1), has received a competitive grant for conference participation, and was awarded a six-month internship at the University of Rostock funded by the Polish National Agency for Academic Exchange. He has also completed professional development courses in oral presentations, bacterial genomics, and plant health diagnosis.

With his multidisciplinary background and international experience, Matteo Marangi is a promising scientist advancing plant microbiology and agricultural biotechnology. His works on halophyte endophytes, and human and plant pathogens offers valuable insights for improving plant health and food safety in sustainable agriculture.